BUILDING NEW *IN VIVO* MODELS OF HUMAN PROSTATE CANCER PROGRESSION BY MANIPULATION OF CYCLIN D1 AND PTEN

By

Yue He

Dissertation

Submitted to the Faculty of the

Graduate School of Vanderbilt University

in partial fulfillment of the requirements

for the degree of

DOCTOR OF PHILOSOPHY

in

Cancer Biology

December, 2007

Nashville, Tennessee

Approved,

Robert J. Matusik

Simon W. Hayward

Neil A. Bhowmick

Sarki A. Abdulkadir

To my parents for their infinite support and unconditional love

ACKNOWLEDGEMENTS

This thesis was finished with the help and support of many people who are gratefully acknowledged here. I would like to thank my mentor, Dr. Simon Hayward for his support, encouragement and guidance during the past four years. Thanks him for giving me this great opportunity to work in his lab and undertake my Ph.D. in an outstanding environment. Thanks him for giving me freedom to design experiments and keep me the right direction.

I would like to thank each member of the Hayward lab for their help and support for my work, particularly Dr. Ming Jiang for his comments and great suggestions, Dr. Omar Franco for his help with experiments and his friendship, to Dr. Karin Williams for her valuable advice. My special thanks to Mrs. Suzanne Fernandez for her love and care in my life.

I would like to extend my gratitude to my committee members, Dr. Robert Matusik, Dr. Neil Bhowmick and Dr. Sarki Abdulkadia for their valuable suggestions and guidance.

I am also grateful to everybody in the Vanderbilt Prostate Cancer Center for their help, comments and friendship.

I would like to acknowledge Dr. Peter Nelson in Fred Hutchinson Research Institute for his support of my work.

Finally to my parents, Zhongchi He and Weiyu Li for their love and encouragement. I could not finish my Ph. D. without your motivation and inspiration.

TABLE OF CONTENTS

LIST OF TABLES

LIST OF FIGURES

Figure Page

ABBREVIATIONS

ACS: American Cancer Society

AR: Androgen Receptor

BPH: Benign Prostate Hyperplasia

CAF: Carcinoma Associated Fibroblast

CAT scan: Computed Axial Tomography scan

CCS: Cosmic Calf Serum

DHT: Dihedrotestosterone

DRE: Digital Rectal Examination

DT: Dunning prostatic adenocarcinoma

EGF: Epithelial cell-derived Growth Factor

FBS: Fetal Bovine Serum

FDR: False Discovery Rate

FGF: Fibroblast Growth Factor

HGF: Hepatocyte Growth Factor

HIFU: High Intensity Focused Ultrasound

IGF: Insulin-like Growth Factor

KGF: Keratinocyte Growth Factor

LOH: Loss Of Heterozygosity

MRI: Magnetic Resonance Imaging

NPF: Normal Prostate Fibroblast

PEDB: Prostate Expression Data Base

PI: Propidium Iodide

PIA: Proliferative Inflammatory Atrophy

PIN: Prostatic Intraepithelial Neoplasia

PIP-3: Phosphatidylinositol 3,4,5-trisphosphate

PRCA: Human Prostate Cancer Progression

PrE: Prostatic Epithelial cell

PSA: Prostate specific antigen

PSMA: Prostate Specific Membrane Antigen

RITA: Radiofrequency Interstitial Tumor Ablation

rUGM: rat Urogenital Mesenchyme

SAM: Significance Analysis of Microarrays

SCID: Severe Combined Immunodeficient

SD: Standard Deviation

TGF-β1: Transforming Growth Factor β1

Tfm: Testicular Feminized

TRUS: Transrectal Ultrasound

UGE: Urogenital Sinus Epithelium

UGM: Urogenital Sinus Mesenchyme

CHAPTER I

INTRODUCTION

Prostate overview

The prostate is a male accessory reproductive gland commonly described as being about the size and shape of a walnut. The prostate is located below the bladder surrounding the urethra (Aumuller, 1989). The seminal vesicles, are diverticula of the Wolffian ducts and are attached to the prostate, between the rectum and the bladder (Josso, 1981).

During ejaculation the prostate expels a proteolytic solution into the urethra. The fluid secreted by the prostate gland is rich in acid phosphatase, citric acid, the protease fibrinolysin, kallikreins (such as prostate specific antigen [PSA]), the enzyme amylase, fibronectin, phospholipids, cholesterol, zinc, calcium and many proteins with unknown function (Aumuller and Seitz, 1990). The proteins in the prostatic fluid modify the vaginal environment to support sperm survival in the female reproductive tract (Aumuller and Seitz, 1990). The anatomy

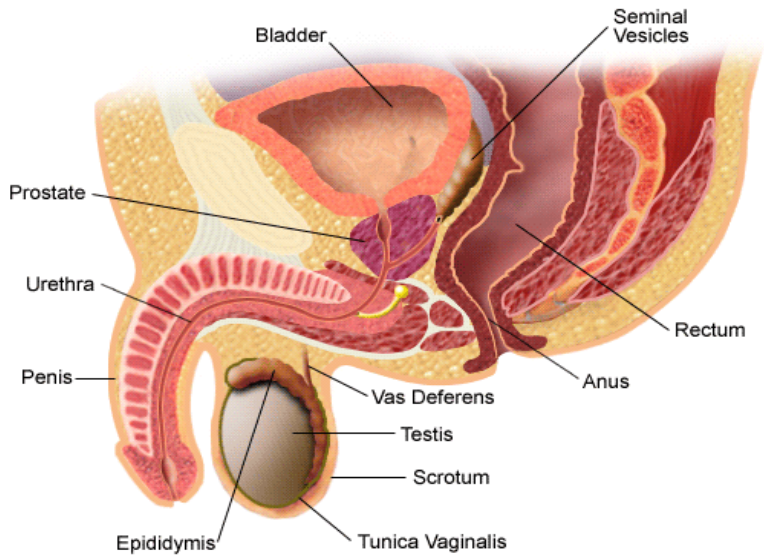

Figure 1-1. Sagittal view of the lower urogenital tract (Krongrad and Drollen, 1993).

of the human male reproductive tract is shown in Figure 1-1. The human prostate gland is located beneath the bladder and surrounds the first 3 cm of the urethra as it leaves the urinary bladder. The prostate is covered by a thin vascularized fibrous sheath surrounding a fibromuscular layer continuous with the smooth muscle surrounding the bladder. The fibromuscular layer extends within the organ and divide the gland into different zones (Kumar and Majumder, 1995; McNeal, 1980).

Prostate structure

The mouse prostate comprises four pairs of lobes named after their spacial orientation. These are: the anterior (AP), the ventral (VP), the dorsal (DP) and the lateral prostates (LP) (Figure 1-2). The DP and LP lobes are commonly referred to the dorsolateral prostate (DLP) due to their close position. The AP is also commonly referred to as the coagulating gland. The first discussion of the developmental organization of the human prostate was provided by Osward Lowsley in 1912 (Lowsley, 1912). Lowsley's work was based on studies of fetal glands. He described five groups of periurethral embryonic tubules lobes: (a) middle (prespermatic

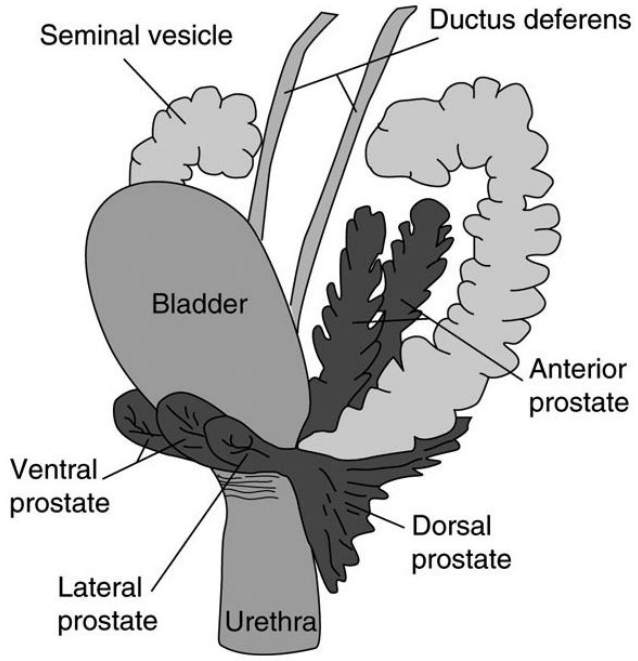

Figure 1-2. schematic diagram of the adult mouse genitourinary tract (lateral view). (Sugimura et al., 1986b)

and posturethral), (b) right lateral, (c) left lateral, (d) posterior (postspermatic and posturethral), and (e) ventral (anterior to the urethra). Several years after Lowsley's observation of the prostate, L. M. Franks challenged Lowsley's concept of prostatic lobes, finding no evidence of lobe boundaries (Franks, 1954a). Franks proposed that carcinoma could be found anywhere within the lobes. Frank's model has been criticized for a lack of anatomical precision. McNeal reported histological heterogeneity of the prostate gland with sub-division into prostatic zones (McNeal, 1980; McNeal, 1983). Currently, the overwhelming majority of pathologists and urologists follow McNeal's model and do not adhere to a lobar architecture in respect to human prostate (McNeal, 1984).

McNeal Prostate

In contrast to mouse prostate, which is comprised of four lobes, the concept of 5-lobed human prostate as proposed by Lowsley has been replaced by that of zonal architecture derived from McNeal.The human prostate is composed of 4 glandular zones which were described by McNeal. The prostate includes the peripheral zone, transition zone, periurethral zone and central zone. Each zone has their own ductal system (McNeal, 1980) (Figure 1-3). The peripheral zone is

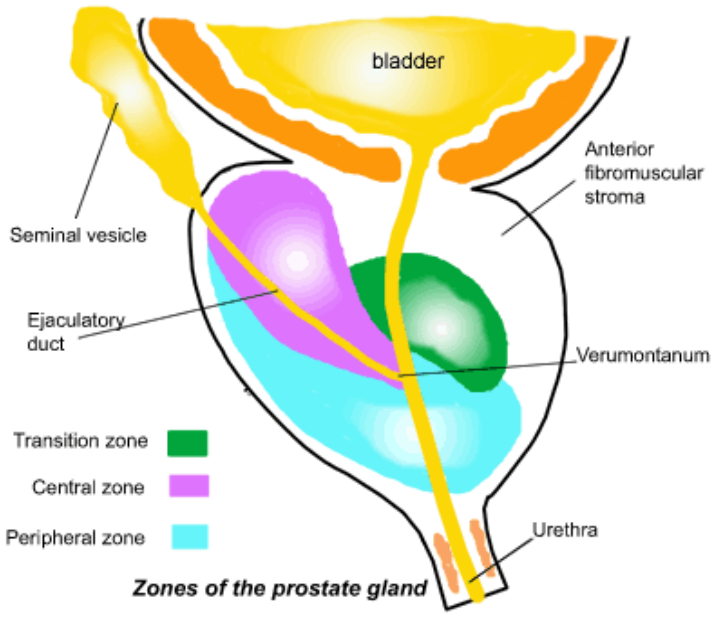

Figure 1-3. Zones of human prostate.

closest to the rectum and is the back part of the prostate gland,. It composes almost 75% of the normal prostate gland. Approximately 70% of prostate carcinomas arise in this zone (McNeal, 1969). The randomly oriented muscle fibers formed the stroma. The central zone composes 25% of the normal prostate and approximately 5-10% of prostate carcinomas arise from this zone (McNeal, 1969). Approximately 5-10% of the normal prostate gland is transition zone. In the transition zone, the stroma is more compact than peripheral zone, and the glandular architecture is similar to the peripheral zone. The transition zone is the place where benign prostatic hyperplasia (BPH) originates and approximately 20% of prostate carcinomas arise from this zone (McNeal, 1978).

Prostate development

During the seventh week of human fetal development, the male and female urogenital systems are anatomically indistinguishable. Both the male and female embryos have a pair of undifferentiated gonads and two sets of ducts: the paramesonephric (Mullerian) ducts and the mesonephric (Wolffian) ducts. In males, gonads differentiate into the testes, which produce testosterone and Mullerian inhibiting substance (Jost, 1947). The Wolffian ducts are stabilized by testosterone and its metabolites, while in males Mullerian ducts regress because of the presence of Mullerian inhibiting substance except the extreme ends (Jost, 1947). The lower end of the Mullerian tubercle is involved in the subsequent formation of the prostate utricle. Testosterone is required for late-stage Wolffian duct differentiation. These ducts differentiate into epididymis, ductus deferens, ejaculatory duct and seminal vesicles. (Anderson and Liao, 1968; Imperato-McGinley et al., 1985; Imperato-McGinley

et al., 1974; Walsh et al., 1983; Walsh et al., 1974). The urogenital sinus is also a component of the ambisexual stage in both male and females. In males, it develops into bladder, urethra, prostate, bulbourethral (in humans, Cowper's) glands, and periurethral glands under the influence of DHT (5α-dihydrotestosterone), which is a potent mitogenic hormone (Anderson and Liao, 1968; Bruchovsky and Wilson, 1968; Imperato-McGinley et al., 1974). The female urogenital sinus can form prostate in response to androgens. It was determined by growing embryonic female urogenital sinuses from 13 to 18 day old embryonic mice and vaginas from 1 to 30 day old mice as grafts to male mouse hosts. All embryonic urogenital sinuses as well as vaginas from 1 day old mice were responsive to androgens and formed prostate, however, vaginas from mice 5 or more days old never formed prostate (Cunha, 1975). It was found that the developmental response of the age-dependent loss in responsiveness of the intact vagina to androgens results from an age-dependent loss in the ability of vaginal stroma to participate in prostatic morphogenesis. These data emphasize the importance of stromal factors during prostatic morphogenesis (Cunha, 1975).

Stromal-epithelial interaction in prostate development

The stroma encompasses all of the non-epithelial components of an organ. For most organs, stroma is mainly composed of fibroblasts, smooth muscle cells, blood vessels, nerves and fat cell etc. The predominant cells in adult prostates are smooth muscle cells.

The prostate develops from the embryonic urogenital sinus as a result of interactions of urogenital sinus epithelium (UGE) and urogenital sinus mesenchyme (UGM). Prostate development is controlled by steroid hormones that induce and maintain a complex cross talk between the stromal and epithelial cells (Cunha et al., 1992). The result of this intercellular communication depends upon the context and differentiation status of the cell type being stimulated (Hayward and Cunha, 2000; Hayward et al., 1998). In developing fetal prostate, DHT binds to the androgen receptors on mesenchymal cells to send signals to adjacent epithelium, inducing epithelial ductal brunching morphogenesis; expression of epithelial androgen receptors; regulation of epithelial cell proliferation; and specification of the expression of prostatic lobe-specific secretory proteins (Chung and Cunha, 1983; Cunha et al., 1987; Hayashi et al., 1993; Sugimura et al., 1986a; Takeda et al., 1990). Concurrently, the developing prostatic epithelium induces the differentiation and morphological patterning of smooth muscle in the UGM (Hayward et al., 1998; Hayward et al., 1997). In the healthy adult prostate, both epithelial and stromal compartments are highly differentiated. While under steady state concentration of androgen, the highly differentiated stroma is in close contact with highly differentiated and functional epithelium to maintain prostate homeostasis. The normal prostatic epithelial growth is regulated by reciprocal smooth muscle-epithelial cell interactions which are mediated by the local synthesis and action of paracrine signaling molecules (Hayward et al., 1997).

Abnormalities in smooth muscle-to-epithelial signaling may either actively promote carcinogenesis or permit the progression to neoplasia through the loss of restriction of normal homeostatic controls (Grossfeld et al., 1998; Hayward et al., 1998). Thus, the process of prostatic carcinogenesis may include aberrations in the interactions of the prostatic epithelium, with its smooth muscle microenvironment resulting in reciprocal de-differentiation of both the emerging carcinoma cells and the prostatic smooth muscle.

Prostate disease. There are a number of diseases of the prostate, which can be divided into cancerous prostate problems, and non-cancerous prostate problems. The clinical conditions of non-cancerous prostate disease include the following:

(1) Prostatism. A disease caused by urethra compression or obstruction, due most commonly to benign prostatic hyperplasia of the prostate gland. Symptoms include urination difficulties and, occasionally, urine retention. Prostatism can interfere with bladder urine flow rate (Hamilton et al., 2006).

(2) Prostatitis. A disease resulting from inflammation of the prostate gland. 25 percent of men who have genital and urinary problems may have prostatitis (De Marzo et al., 2007). Prostatitis is composed of four disorders:

(a) Acute bacterial prostatitis: the least common type of prostatitis and easy to diagnose and treat. Symptoms include fever, pain, increased white blood cells and

bacteria in the urine. Since the symptoms are caused by bacteria, an appropriate antibiotic is the treatment of choice for this type of prostatitis (Hua and Schaeffer, 2004).

(b) Chronic bacterial prostatitis: uncommon and often associated with defects in the prostate. Therefore, effective treatment includes removing the defect and treating with appropriate antibiotics (Hua and Schaeffer, 2004).

(c) Chronic prostatitis/chronic pelvic pain syndrome is the most common but least understood type of prostatitis (Rivero et al., 2007). It can be either inflammatory or noninflammatory. Men of any age can have this problem and the symptoms can appear sporadically. Antibiotics may not be the suitable choice because there is no solid evidence of bacteria infection in either types.

(d) The fourth type of prostatitis is asymptomatic inflammatory prostatitis. There are infected cells in the semen but may not cause any symptoms (Simardi et al., 2004). It can be associated with infertility or prostate cancer .

(3) Benign prostatic hyperplasia (Also called BPH or benign prostatic hypertrophy). An enlarged prostate is a sign of this disease. BPH is the most common prostate problem. Although it is not cancer, BPH symptoms are often similar to those of prostate cancer. It can cause discomfort and urinary problems. BPH represents an overgrowth of epithelial nodules and stroma tissue in the transition zone of the prostate. At cellular level, basal cell hyperplasia and increased stromal mass are commonly seen in BPH (Bostwick et al., 1992). Advanced age and circulating androgens are the two well-established risk factors for BPH (Isaacs and Coffey, 1989). Autopsy data indicated that the presence of

microscopic BPH (histologically) in 80% of males at 71-80 and 90% at 81-90, however the incidence of microscopic BPH is greater the clinically detectable disease (Berry et al., 1984). Enlargements of prostate cause increasing pressure within the bladder causing frequently contractions even only a small amount of urine is present. Eventually, the bladder loses the ability to empty itself, causing many problems.

The prostate is regulated by sex-steroid hormone levels. Androgens and estrogens are important for prostate cell growth. Estrogen is generated through stromal aromatization of androgen and the ratio of estrogen/androgen increases in BPH patients (Roberts et al., 2004; Shibata et al., 2000). As men age, lower concentration of testosterone and higher concentration of estrogen are found in the blood.. Studies have suggested that BPH may occur because the higher amount of estrogen increases smooth muscle cell proliferation and differentiation (Zhang et al., 1997). Anti-estrogens such as aromatase inhibitors (testolactone) which prevents conversion of androgen to estrogen have been used in the treatment of BPH patients (Royuela et al., 2001).

The conversion of the main androgenic steroid testosterone to dihydrotestosterone (DHT) is catalyzed by the 5α-reductase isoenzymes Types 1 and 2. DHT is required for secretory epithelial cells function. 5α-reductase Type 1 is most prevalent in the liver and the skin, with minimal amounts found in the prostate, whereas Type 2 is most prevalent in the prostate . In the prostate, DHT is generated by 5α-reductase type 2. Higher 5α-reductase activity has been demonstrated in BPH as compared to in normal tissue (Silver et al., 1994).

Clinically, finasteride (a 5α-reductase type 2 inhibitor) has been used to treat BPH patients (Bautista et al., 2003; Sandhu and Te, 2004).

Many growth factors (including: fibroblast growth factor [FGF] family members, insulin like factors [IGF], transforming growth factor α [TGF-α], transforming growth factor βs [TGF-β], and epidermal growth factor [EGF]), mediate epithelial-stromal interaction to sustain prostate homeostasis. Increased FGF2 levels have been found in early stages of BPH patients (Mori et al., 1990). Transforming growth factor β1 (TGF-β1) expression and secretion have also been shown to increase in BPH patients (Mori et al., 1990). Low concentrations of TGF-β1 increase cell proliferation, but high concentrations inhibit stromal cell growth (Kassen et al., 1996). TGF-β1 treatment could generate a reactive stroma composed of myofibroblasts and fibroblasts which express extra cellular matrix components and stromal cell markers, such as α-smooth muscle actin, calponin and tenascin (Peehl et al., 1997; Tuxhorn et al., 2002). Elevation of a variety of factors influences extracellular matrix production and secretion, which is similar to the stroma of BPH patients (Untergasser et al., 2005).

(4) PIN (Prostatic Intraepithelial Neoplasia). PIN has been identified as the most likely precursor lesion for prostatic carcinoma. The term was introduced in 1987 by Bostwick and Brawer (Bostwick and Brawer, 1987; Mikuz, 1997). PIN indicates the progressive abnormalities of phenotype and genotype that are similar to cancer rather than normal prostatic epithelium. PIN is strongly predictive of adenocarcinoma (Webber et al., 1995).

Two grades of PIN:low-grade PIN (LGPIN), and high-grade PIN (HGPIN)), has been used for diagnosis. However, many pathologists no longer report the presence of LGPIN and note only the histologic findings associated with HGPIN.

(5) Prostate cancer. Early stage prostate cancer is not lethal, but can progress to become a systemic malignancy. Cancer grows in the interior of the prostate gland, but can spread to surrounding tissues near the prostate, such as the seminal vesicles and bladder and can metastasize to distant organs of the body prominently including bones, liver and lymph nodes (Coffey and Pienta, 1987). Early stage of prostate cancer can be treated successfully, but metastasized tumors are often lethal. Prostate cancer is the most common type of non-skin cancer in men in the United States and is the second leading cause of cancer death in men. It was estimated that 27,050 men in the United States will die of prostate cancer in 2007 (American Cancer Society, 2007). African American men have the highest incidence of prostate cancer, and Asian and Native American men have the lowest incidence. Rates for Asian and African men increase dramatically when

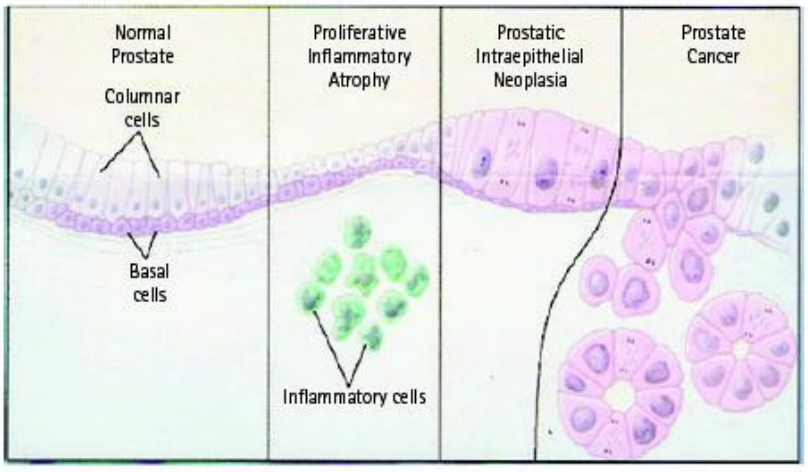

Figure 1-4. Role of inflammation in prostate carcinogenesis. (Nelson et al., 2004). Copyright @Massuchusetts Medical Society. 2003

they emigrate to the United States, suggesting an environmental (probably diet related) connection.

It has been suggested that inflammation may contribute to the risk of developing prostate cancer (Goldstraw et al., 2007). Although there is no conclusive data supporting a role for inflammation in the pathogenesis of prostate cancer, there are accumulating data in favor of this idea. Inflammatory cytokines and genotoxic reactive oxygen radicals produced by microbial infections can increase cell proliferation and promote tumorigenesis (Dennis et al., 2002). Some pathologists have proposed inflammation as a factor in the etiology of prostate cancer (De Marzo et al., 2007). Chronic inflammation is commonly found in the peripheral zone of the prostate adjacent to foci of PIN or prostate cancer. The lesions are thought to form as a consequence of the regenerative proliferation of epithelium in response to injury caused by inflammatory oxidants (Hsieh-Li et al., 1995). The suggested pathway is shown in Figure 1-4.

Gleason Score

The Gleason score was established in 1966 by pathologist Dr. Donald Gleason, and has been widely used to diagnose prostate cancer (Gleason, 1977). He gathered biopsy information from nearly 3000 prostate cancer patients and developed a histopathologic scoring system. The score is based on the glandular histological patterning and cytological appearance. The Gleason score is used to help evaluate the prognosis of men with prostate cancer. Together with other parameters, it is used to predict prognosis and identify the best

treatment strategy for prostate cancer.

In a biopsy specimen the pathologist takes the two most prominent patterns or scores (scores ranges from 1 to 5) . The scores are added to obtain the final Gleason score. The Gleason score ranges from two to ten. A Gleason score of two is associated with the best prognosis and a score of ten with the worst. For example, a prostate biopsy specimen may be diagnosed by two scores, one is two and the other number is three. The final Gleason score in this case would be five. Gleason scores are associated with the following features (Figure 1-5):

Grade 1. The cancerous prostate closely resembles normal prostate tissue. The glands are small, well-formed, and closely packed.

Grade 2. The tissue still has well-formed glands, but they are larger and have more stroma tissue between them.

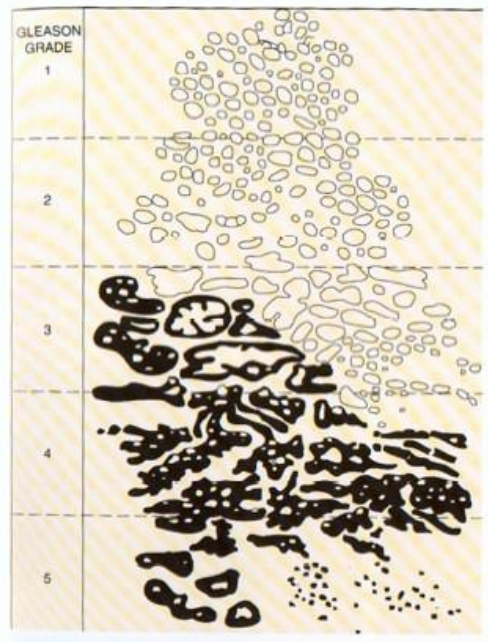

Figure 1-5 Gleason score system (Gleason D, 1974)

Grade 3. The tissue still has recognizable glands, but the cells are darker. Some of the cells are beginning to infiltrate the surrounding tissue.

Grade 4. The tissue has few recognizable glands. Many cells are invading the surrounding tissue.

Grade 5. The tissue does not have recognizable glands. There are often just sheets of cells throughout the surrounding tissue.

Risk factors for prostate cancer. The major risk factors for prostate cancer include genetic, dietary, and environmental factors that affect male hormones (such as DHT production) and make men more susceptible to this cancer.

(1) Age. Age is the most important epidemiological risk factor for prostate cancer (Greenlee et al., 2001). As the population ages, new cases of prostate cancer will increase significantly. It is estimated that by age 70, about 65% of men have at least microscopic evidence of prostate cancers. There is a positive correlation between time and prostate cancer progression.

(2) Family History. It has been suggested that heredity may play a role in prostate cancer. Men with a family history of prostate cancer may have a higher risk of having this disease (Damber, 1998; Gann, 2002; Lesko et al., 1996).

(3) Ethnicity. African American men have the highest risk for prostate cancer, more than 50% higher than the risk for Caucasian American males (Bloom et al., 2006; Gann, 2002; Powell, 2007). Asian men have a lower risk for prostate cancer, but their risk increases if they move to North America (Lee et al., 2007). Therefore, environmental or dietary factors might be associated with the risk of developing prostate cancer.

(4) Dietary Factors. A high-fat diet may increase the risk of prostate cancer. Researchers theorize that fat increases production of the hormone testosterone, which may promote the

growth of prostate cancer cells. Specific fat subtypes may influence cancer cell growth. A higher ratio of omega-3 fat acid/omega-6 fat acid can suppress prostate cancer cell growth (Kobayashi et al., 2006). Because prostate cancer is rare in many parts of Africa, it has been postulated that dietary factors may play a role in African American men and may put them at higher risk. HAs (heterocyclic amines), a group of carcinogens known as PhIP (2-amino-1-methyl-6-phenylimidazo[4,5-b]pyridine), is found in grilled beef, pork, chicken, lamb, and fish. It has been indicated that PhIP relates to prostate cancer incidence (Tang et al., 2007).

(5) Exposure to Chemicals. The relationship between prostate cancer and chemical exposure is controversial. Men whose work involves heavy labor and those exposed to certain metals and chemicals, including cadmium, dimethyl formamide, and acrylonitrile, may be at higher risk for prostate cancer (O'Berg et al., 1985; Walrath et al., 1989). Some studies have indicated that farmers might be also be at higher risk (Parker et al., 1999).

(6) Infection and Inflammation. Genetic factors that affect the body's response to viruses can also associate with inherited prostate cancer. Some association has been seen between prostate cancer and bacterial or viral infections, such as herpesvirus, human papillomavirus, and cytomegalovirus. It was suggested that men with genetic susceptibilities could develop a chronic inflammatory condition in the prostate by viral infection and possibly initiate cancerous changes. It proposed that exposure to environmental factors such as infectious agents and dietary carcinogens, and hormonal

imbalances could lead to prostate injury and develop chronic inflammation and regenerative 'risk factor' lesions, referred to as proliferative inflammatory atrophy (PIA), which could progress to PIN (prostatic intraepithelial neoplasia) and eventually invasive carcinoma (De Marzo et al., 2007). However, some recent studies have shown that there is no link between viral infections and prostate cancer development (Bergh et al., 2007).

(7) Smoking. Cigarette smoking may increase the risk of prostate cancer by affecting circulating hormone levels or through exposure to carcinogens (Plaskon et al., 2003). A few hypothetical mechanisms were proposed to enhance the risk of prostate cancer. It has been suggested that smoking can increase the circulating levels of bioavailable testosterone and lower levels of bioavailable estradiol in men (Ferrini and Barrett-Connor, 1998). There are significant positive correlations between cigarettes smoked/day and serum total androstenedione as well as total and free testosterone in men (Dai et al., 1988). Data from a population based case-control study suggest that smoking is a risk factor of prostate cancer Current smokers appear to be at moderately increased risk for this disease compared with non-smokers (Plaskon et al., 2003).

Procedures used to evaluate prostate problems

Blood and urine laboratory tests are necessary for men during their annual physical examinations. Evaluation of the prostate gland is also recommended by the National Cancer Institute and the American Cancer Society.

(1) DRE (digital rectal examination). A digital rectal examination is performed to

examine abnormalities of the prostate (Sneyd et al., 2003; Villers et al., 2003). Enlargement of the prostate gland can be found in BPH patients. An irregular or hard lump may indicate the presence of a tumor. However, the digital rectal exam is not the best method of detecting prostate cancer because not all abnormalities in the prostate can be found through the rectum without performing histological examination of the prostate tissue.

(2) Blood prostate-specific antigen (PSA) test. PSA was discovered in 1970 by Ablin, and PSA testing has been widely used and is the most important method to detect prostate cancer (Ablin, 1997). PSA is a kallikrein serine protease that is secreted by prostate epithelial cells diffuses into the bloodstream in areas of tissue damage caused by, for example, inflammation or cancer. Morphological and histological changes of the prostate lead to leakage of PSA into blood. PSA levels higher than 4.0 ng/ml may indicate prostate disease (infection, enlargement of the prostate gland or prostate cancer). PSA testing is commonly recommended for men over 50. A PSA blood test can be done alone or in conjunction with DRE to improve the odds of detecting prostate cancer (Webber et al., 1995). PSA is the only serum marker recommended by American Cancer Society to screen for prostate cancer, and the value is limited because of its lack of specificity and sensitivity. The cutoff upper limit of 4.0 ng/ml is still under debate. There is strong evidence that a PSA cutpoint of 4.0 ng/ml actually misses the majority of prostate cancers, up to 15% of which may be potentially aggressive cancers (Thompson et al., 2005).

(3) Prostate-specific membrane antigen (PSMA) test. PSMA is an integral glycoprotein,

and was shown to be overexpressed in prostate tumor epithelial cells and serum of cancer patients. Studies have suggested that PSMA correlates with Gleason score and stage of prostate cancer. Despite its expression by subsets of various types of malignancies, such as urothelial carcinomas of the bladder, PSMA is still considered to be relatively sensitive and highly specific for prostate cancer (Mhawech-Fauceglia et al., 2007).

Other molecular markers such as prostate stem cell antigen, early prostate cancer antigen, hepsin, enhancer of zeste homolog gene 2, human glandular kallikrein 2, transforming growth factor-β1, chromogranin A have been suggested as potential promising biomarkers for prostate cancer.

If the DRE or PSA levels are unusual, ultrasound can also be performed to examine prostate cancer candidates. (Franco et al., 2000)

(4) Transrectal ultrasound (TRUS). Prostate enlargement, cancer nodules, and tumor invasion to the seminal vesicles can all be found by ultrasound. TRUS can also be used for guidance of needle biopsies of the prostate gland (Mikuz, 1997).

(5) Computed axial tomography scan (CAT scan). The combination of x-rays and computer technology can produce horizontally and vertically cross-sectional images , of the prostate. Abnormalities within the prostate gland can be found by CT scan, but additional tests such as PSA test should be used in combination to diagnose prostate cancer

(Golimbu et al., 1981).

(6) Magnetic resonance imaging (MRI). This technique uses a combination of large magnets, radiofrequencies, and a computer to produce detailed images of organs and structures within the body (Vilanova and Barcelo, 2007). Prostate abnormalities can found by MRI.

(7) Biopsy. A procedure in which tissue samples are removed from the prostate, and are examined under a microscope. A pathologist can examine the slide to determine if cancer is present within the prostate. Cancer cells have large nuclei, increase nuclei/cytoplasm ratio compared with normal cells. False-negative results might occur and some patients will need rebiopsy (Hori et al., 2006). Combination of endorectal MRI and magnetic resonance spectroscopy imaging (MRSI) might be a useful tool to decrease rebiopsy rate (Amsellem-Ouazana et al., 2005).

Treatment of prostate cancer

(1) Surgery. Radical prostatectomy is the most common therapy for early stage prostate cancer. The ideal responsive candidate can live 10 to 20 years after surgery. Radical prostatectomy is a major surgery performed to remove the entire prostate gland and the surrounding tissues such as the seminal vesicles. Lymph nodes can also be sampled for biopsy to examine if the cancer has metastasized or not. The goal is to remove the cancer

entirely and prevent its spread to other parts of the body. The risks after surgery include impotence, heart attack, stroke, blood clots, infection or bleeding like other surgeries.

(2) Radiation therapy. Radiation therapy has been used in the treatment of prostate cancer for several decades (Zagars and Pollack, 1995). Prostate cancer is a radiation-sensitive neoplasm that demonstrates a classic sigmoid dose response curve to X-rays. Higher volume tumors need higher radiation doses. Tissues such as bladder and rectum are at risk when radiation is performed.

(3) Hormone therapy. Hormone therapy blocks action of hormone and stops cancer cells from growing. Luteinizing hormone-releasing hormone agonists are potent inhibitor of gonadotropin secretion. Following an initial stimulation of gonadotropins, chronic administration of leuprolide acetate results in suppression of testicular steroidogenesis. Administration of luteinizing hormone-releasing hormone agonists has resulted in inhibition of the growth of certain hormone dependent tumors (such as prostatic tumors). Examples are leuprolide, goserelin, and buserelin. Antiandrogens exerts its action by inhibiting androgen uptake and/or by inhibiting nuclear binding of androgen to the androgen receptors on prostatic cells. Such as flutamide and nilutamide.

Studies are still being carried on to find the ideal therapy for localized prostate cancer. Currently, the two most common therapies used in the United States to treat prostate cancer remain radical prostatectomy and radiation therapy (Frank et al., 2007; Rossi,

2006). The newer focal therapy consists of cryoablation techniques and heat energy–based treatments [high intensity focused ultrasound (HIFU), radiofrequency interstitial tumor ablation (RITA), and thermal brachytherapy] (Zhao et al., 2006). Radioactive seeds were first used by Dr. Anthoy D'Amico at Harvard Medical School to treat early stages of prostate cancer. Magnetic resonance imaging (MRI) was used to place 100 radioactive seeds into tumors inside prostate to destroy cancer cells. For some patients, it may be superior to the usual methods of surgical removal of the gland.

Animal models of prostate cancer

(1) Transgenic models**.** There are a limited number of promoters which were used to introduce transgenes to prostate epithelial cells. The probasin promoter is one of them. It includes the minimal promoter, long promoter and composite promoter containing multiple androgen response elements.

TRAMP and LADY mouse models are two well-known animal models used to investigate prostate cancer progression (Masumori et al., 2001; Matusik et al., 2001). The TRAMP model uses the minimal rat probasin promoter to forcibly express the SV40 early genes (T/t antigen:Tag) specifically targeted to the terminally differentiated tall columnar epithelial cells of the mouse prostate. Male TRAMP mice develop progressive prostate disease that histologically and pathologically mimics human disease with metastatic spread to distant sites. The LADY mouse model uses a long probasin promoter to express large T antigen. It elicited a higher level of expression in the mouse prostate that was developmentally and

differentially regulated by androgen. The LADY model is advantageous in that expression is high but the disease progression is less aggressive with no metastasis (Abate-Shen and Shen, 2002). Although both the TRAMP and LADY models offer many advantages, they both differ from the human disease in their rapid onset and frequent occurrence of neuroendocrine tumor (Abate-Shen and Shen, 2002). The C3(1)-Tag mice also develop progressive prostate cancer, but tumors can be found in other tissues as well, which limits its use to prostate cancer research. Cryptdin-2-T and Gg-SV40 T also develop progressive prostate cancer, however the promoters used to drive SV40 large T antigen are not prostate specific.

Other genes such as c-myc (Zhang et al., 2000), Ras and Fgf8b (Song et al., 2002) have been suggested to play a role in prostate cancer progression. These genes have been used in mouse models. However, in the majority of these models, only a relatively mild phenotype, such as hyperplasia or PIN, instead of adenocarcinoma was seen (Abate-Shen and Shen, 2002).

(2) Knockout models. Deletion of a gene of interest is another way to generate mouse models (Sharma and Schreiber-Agus, 1999). PTEN heterozygous knockout mice, Nkx3.1 null and p27 null mice have displayed prostate phenotypes (Lei et al., 2006). The loss of these genes has been suggested to play a role in the development of human prostate cancer, and this theory is supported by observations in the knockout mice. Similar to transgenic mouse models, the resulting phenotypes in these knock out mice were hyperplasias as well.

Because of embryonic lethality of specific ablation, conditional knock out mice were generated by applying the PSA promoter to drive prostate-specific Cre expression. The targeted gene was inactivated by PSA-Cre targeted deletion of the floxed region resulting in the expression of a truncated protein lacking the gene function. It was found that targeted biallelic inactivation of Pten in the mouse Prostate leads to prostate cancer (Ma et al., 2005b).

(3) Canine models. Dogs are the only species besides humans that develop spontaneous prostate cancer with high frequency (Waters and Bostwick, 1997; Waters et al., 1997). Dogs also display a high frequency of metastasis, especially to the bone (Rosol et al., 2003). Compared to other animal models, the use of dog models is limited, because the high expense to maintain dog colonies and the progression of cancer is slow and thus time consuming (Waters et al., 1998).

(4) Rat models. Several Lobund-Wistar, Dunning, and Noble rat models have been used extensively to study prostate cancer progression. Rats are one of the few species that spontaneously develop prostate adenocarcinomas. The Dunning rat model is the most common model and is widely used for nutritional studies (Dunning, 1963). Lobund Wistar was shown to have an increased incidence of prostate cancers in the anterior prostate (Pollard, 1992; Pollard, 1998). Noble rat have been used to study hormone-induced prostatic carcinogenesis and it was shown that IGF-1 and VEGF may be the critical regulators in mediating epithelial-stromal interactions in sex hormone-induced prostate carcinogenesis (Wang and Wong, 1998). However, these models are limited by long tumor

latencies, and lack of spontaneous metastases (Bostwick, 2000).

Human models

(1) Xenografts and orthotopic models. Cell lines, such as CWR22, LAPC and LNCaP cells, which were isolated from primary tumors or metastasized tissues can be injected subcutaneously or orthotopically in the severe combined immune deficiency (SCID) mice or nude mice (van Weerden and Romijn, 2000). They represent a range of malignant potential and also display differential responses to androgens. However, the cells are already transformed therefore limit their use to the study of prostate cancer initiation.

(2) Tissue recombination and xenograft. The tissue recombination technique was studied in detail in the Cunha lab. To date this technique is one of the best models to study stromal-epithelial interactions. Epithelial cells are combined with stromal cells in a collagen gel, and grafted under kidney capsule of SCID or nude mice. Genes of interest can either be overexpressed or knocked down in a tissue specific manner. Based on the size and histology of the graft, the function of the gene can be examined. There are limited human models of prostate cancer progression. This technique can provide new insights to prostate cancer research (Hayward et al., 1998; Hayward, 2002)

Virtues of BPH-1 cells and its derivatives

Prostate cancer research has been hindered by a lack of well established, characterized, immortalized benign prostatic epithelial cells lines that express markers of normal

prostatic epithelial cells. Such cells can used to study multistep carcinogenesis, cancer progression and study potential therapeutic agents to inhibit prostate cancer growth. BPH-1 cell line is one of such cell line has been widely used in prostate cancer research. It is by far the only line which start off benign an can by pushed into malignant phenotypes by either genetic modification or hormone treatment.

(1) BPH-1 cell lines. BPH-1 cell line was established and characterized in 1995 by Dr. Simon W. Hayward (Hayward et al., 1995). Prostate tissues were isolated from a 68 yr-old BPH patient undergoing transurethral resection of the prostate for urinary obstruction. The stromal fraction was separated from prostatic epithelial organoids by repeated unit gravity sedimentation. Epithelial cells from the organoid were immortalized by infection with the Zippneo SV virus carrying the large SV40 T antigen, which was used in establishment of LAZY mice. Resistant colonies were selected using 800 μg/ml Geneticin in the culture medium and then expanded. Morphology of BPH-1 cells showed an even cobblestone appearance typical of epithelial cells which was similar to primary cultured prostatic epithelial cells. The expression profile of cytokeratin was consistent with luminal epithelial cells. BPH-1 cells respond to a number of different growth factors, such as EGF family and TGF-β, EGF and TGF-α stimulate BPH-1 cells proliferation, but TGF-β1 and TGF-β2 inhibit cell proliferation. Based on the fact that androgen receptor (AR) is induced by the urogenital sinus mesenchyme during development (Cunha et al., 1980; Neubauer et al., 1983), the loss of AR expression in this cell line may be due to lack of inductive stromal signal. Grafting or injecting BPH-1 cells to male nude mice

could not demonstrate any tumorigenic response up to1 year (Ricke et al., 2006). However small clumps of cells could still be found in the grafts which demonstrated that cells were still viable in the host animals. This phenomenon indicated that BPH-1 is a benign prostatic epithelial cell which can be used as a parental cell line to generate derivative cell lines in order to study genes function. Modification of expression levels of oncogenes and tumor suppressors in BPH-1 cells can be utilized to study functions of those genes in prostate cancer progression.

(2) BPH-1^{CAFTD} lines. Majority of human prostatic cancers arise as adenocarcinomas which are derived from the epithelial cells that form the glands and ducts of the prostate. As the carcinoma evolves, alterations in gene expression also occur in the adjacent stroma. These "changes" may enhance the invasive potential of the epithelial tumor (Ao et al., 2007; Grossfeld et al., 1998). BPH-1 cells can be induced to undergo malignant changes either by association with tumorigenic stromal microenvironment or by treatment with hormonal carcinogens (Olumi et al., 1999; Wang et al., 2001). It has been shown that carcinoma associated fibroblast (CAF) direct tumor progression in initiated human prostatic epithelium, while normal prostatic fibroblasts were incapable of stimulating such progression (Olumi et al., 1999).

BPH-1 cells are considered to be initiated since they are SV-40 immortalized, therefore they are susceptible to further genetic changes to progress to a malignancy. The epithelial cells derived from these tumors (BPH1^{CAFTD}) are tumorigenic without the stimulation of

stromal cells when re-grafted to mice. The data demonstrated for the first time that genetically initiated, non-tumorigenic epithelial cells can undergo a permanent malignant change with previous exposure to CAFs. Tissue from BPH-1 + CAF recombinants were put into culture and resistant epithelial cells were selected by G418. Four sublines were isolated from these tumors which were subsequently designated as BPH-1 ^{CAFTD}-1, -3, -5 and –7. These lines were then regrafted to SCID mice and further cell selection was performed from which BPH-1 ^{CAFTD}-2, -4, -6 and –8 were derived (Hayward et al., 2001). All eight derivatives are tumorigenic in SCID mice. Tumors recapitulate small acinar prostatic carcinoma or squamous carcinoma. Although different CAF populations were used to recombine with BPH-1 cells to generate the 4 BPH-1^{CAFTD} derivatives, all BPH-1^{CAFTD} lines share recurrent chromosomal rearrangements. This finding indicated that common genetic changes can be induced by stromal environment through paracrine interactions.

(3) BPH-1^{TETD}. Previous data demonstrated that the non-tumorigenic BPH-1 cells can be induced to be form tumors under the influence of testosterone and estrogen (T+E2) as a result of paracrine signaling transduction (Wang et al., 2001). The cell lineages (BPH-1^{TETD}-A and BPH-1^{TETD} –B) derived from the hormonally induced tumors are also tumorigenic like BPH-1^{CAFTD} lines. It demonstrated that stromal cells are required for this hormonally induced carcinogenesis (Hayward et al., 2001). The malignant potential of the isolated epithelial cells from the hormone induced tumors demonstrated BPH-1 cells are

permanently transformed under the influence of T + E2. BPH-1^{TETD} lines shared similar chromosome amplifications seen in BPH-1^{CAFTD} strains.

BPH-1 and its derivatives have been widely used to study prostate carcinogenesis and evaluate stromal-epithelial interactions during carcinogenesis. These models allow for genetic manipulation of epithelium and stroma. The commonalities of these models, other conventional human models (RWPE, RC165N) and human prostate cancer progression (PRCA) are outlined Tables 1, 2, 3 which tabulate the abundant preliminary data using immunohistochemical, PCR, rtPCR, Western analysis, immunoprecipitation, gene expression array, SNP array and proteomic techniques (Data provided by Dr. William Ricke). The vast number of similarities between these models and human PRCA validates and justifies the use of these models in the study of PRCA-progression. Moreover, this model is well suited to address stromal-epithelial interactions during PRCA-progression.

Table 1. A comparison of human cell lines to human primary prostate epithelial cells grown *in vitro*.

Criteria Cells→	RWPE-1	RC165N	BPH-1	BPH-1$^{C}_{AFTD}$	Primary human	References
Keratins-8,18	+	+	+	+	+	PD (Bello et al., 1997; Gu et al., 2005; Gu et al., 2006; Hayward et al., 1995)
Keratin-14	-	NT	-	-	+	(Bello et al., 1997; Gu et al., 2005; Gu et al., 2006; Hayward et al., 1995)
chromogranin-A	NT	NT	-		-	UF
AR mRNA	+	+	+	-	+	PD (Hayward et al., 1995; Lau et al., 2000)
AR protein	+	+	-	-	-	PD (Bello et al., 1997; Gu et al., 2005; Gu et al., 2006)
PSA mRNA	+	-	-	-	-	UF (Bello et al., 1997; Gu et al., 2005; Gu et al., 2006; Hayward et al., 1995)
pS2	NT	NT	-	NT	-	(Lau et al., 2000)
AR and glandular epithelium induction by stroma	NT	NT	+	NT	+	PD, UF (Cunha et al., 1983; Lang et al., 2001a; Lang et al., 2001b; Wang et al., 2001)
PSA induction by stroma	NT	NT	NT	NT	+	(Cunha et al., 1983; Lang et al., 2001a; Lang et al., 2001b)
E-cadherin	NT	NT	+	+	+	UF (Bello et al., 1997; Gu et al., 2006; Hayward et al., 1995)
in vitro: proliferation, forms mono-layers, cobblestone morphology	+	+	+	+	+	(Bello et al., 1997; Gu et al., 2006; Hayward et al., 1995)
Nontumorigenic *in vivo*	+	+	+	-	+	(Bello et al., 1997; Gu et al., 2005; Gu et al., 2006; Hayward et al., 1995)
Immortalization	HPV	hTert	SV-40 Tag	SV-40 Tag	-	(Bello et al., 1997; Gu et al., 2005; Gu et al., 2006; Hayward et al., 1995)

Zinc content	NT	NT	+*	NT	+	(Feng et al., 2002)
TGFβ□ □ inhibited	+	NT	+	-	+	(Ao et al., 2006; Bello et al., 1997; Gu et al., 2005; Gu et al., 2006; Hayward et al., 1995)
EGF, FGF-2, -7 stimulated growth	+	NT	+	NT	+	(Bello et al., 1997; Gu et al., 2005; Gu et al., 2006; Hayward et al., 1995)
Race	cs	aa	cs	cs	n/a	(Bello et al., 1997; Gu et al., 2005; Gu et al., 2006; Hayward et al., 1995)

*Zinc content is consistent with luminal epithelial levels and not cancer or benign prostate hyperplasia. NT=not tested; PD=preliminary data; UF=unpublished findings; cs=Caucasian; aa=African American

Table 2. Functional similarities between UGM+BPH-1 models and human PRCA

Function	UGM+BPH-1 model	Human Prostate
E_2-administration induces squamous metaplasia	+	+
Anti-androgens stimulate squamous metaplasia	+	+
Anti-androgens decrease growth of tumorigenic cells	+	+
Progression states: non-tumorigenic tumorigenic state	+	+
Progression states: tumorigenic into metastatic state	+	+
Androgen-ablation decreased benign epithelial growth	+	+
Androgen-ablation induced benign epithelial apoptosis	+	+
Androgen-ablation decreased tumorigenic growth	+	+
Androgen-ablation induced carcinoma apoptosis	+	+
Isolated human benign, tumorigenic, metastatic cells	+	+

NT=not tested; PD=preliminary data; UF=unpublished findings

Table 3. Comparisons of UGM+BPH-1 TRs vs human PRCA-progression

Markers	molecule	Benign UGM+BPH-1 untreated		Tumorigenic UGM+BPH-1+[T+E_2]		Parallels human
Cell types		stroma	epithelium	stroma	epithelium	
luminal cell	Keratin-8,18	-	+	-	+	yes
basal cell	Keratin-14/p63	-	+	-	+/-	yes
muscular	□a-actin	+	-	+	-	yes
fibroblastic	vimentin	+/-	-	+	+	yes
vasculature□	Cd31	+	-	+	-	yes
Steroid	AR	+	+	+	-	yes
	ER-□□	-	+	-	-	yes
	ER-□	+	-	+	-	yes
AR regulated genes	PSA	-	NT	-	NT	NT
	Nkx3.1□	-	+	-	-	yes
Progression markers						yes
	Akt	-	-	-	+	
	E-cadherin	-	+	-	-	yes
	MMP-9	low	low	low	+	yes
	aromatase	low	low	+	+	yes
	T□ R-II	NT	+	NT	-	yes
	SSeCKS	NT	high	NT	low	yes
Epigenetics	GSTpi□	-	+	-	-	yes
Cellular progression: □		Orderly	Benign	Reactive	Tumor/Mets	yes
Genetics: LOH □	3p,8p, 13p,q,17p				Tumor/Mets	yes
Proteomics-2	B23,G3PDH,	NT	low	NT	high	yes

Table 3 continued. Preliminary data from Dr. William Ricke comparing UGM+BPH-1 TRs vs human PRCA-progression

Markers	molecule	tumorigenic CAF+BPH-1 untreated		Parallels human
Cell types		stroma	epithelium	
luminal cell	Keratin-8,18	-	+	yes
basal cell	Keratin-14/p63	-	+	yes
muscular stroma	a-actin	+	-	yes
fibroblastic stroma	vimentin	+	-	yes
vasculature	Cd31	NT	-	yes
Steroid receptors	AR	+	+	yes
	ER-	-	+	yes
	ER-	+	-	yes
AR regulated genes	PSA	+	NT	yes
	Nkx3.1	?	+	yes
Progression markers	Akt	+	+	yes
	E-cadherin	-	+low	yes
	MMP-9	NT	NT	yes
	aromatase	NT	low	
	T R-II	_+	+	yes
	SSeCKS	NT	NT	
Epigenetics	GSTpi	NT	NT	
Cellular progression: benign, tumorigenic, and metastatic		Reactive	Tumor/Met	
Genetics: LOH	3p,8p, 13p,q,17p			yes
		NT	+	
Proteomics-2D/MS	B23,G3PDH,Lmn	NT	low	yes

NT= not tested; = factor is also a PRCA-progression marker; LOH=loss of heterozygosity; vasculature, muscular stroma, fibroblastic stroma are all localized in a manner consistent with human PRCA-progression. Detection of markers were performed by immunohistochemistry, gene expression arrays, rtPCR, SNP arrays, Mass Spec, Western blotting, and 2D gel electrophoresis.

Stroma in prostate carcinogenesis

The process of prostatic carcinogenesis includes aberrations in the interactions of the prostatic epithelium and its local microenvironment. These changes result in reciprocal de-differentiation of both the emerging carcinoma cells and the prostatic smooth muscle. The vast majority of human prostatic cancers arise as adenocarcinomas, which are derived from the epithelial cells that form the glands and ducts of the prostate. As the carcinoma evolves, phenotypic changes and alterations in gene expression also occur in the adjacent stroma. These “changes” may enhance the invasive potential of the epithelial tumor (Grossfeld et al., 1998; Joesting et al., 2005). Chung and co-workers reported that co-inoculation of tumorigenic Nbf-1 fibroblasts with human PC-3 cells accelerated tumor growth (Chung, 1991; Chung, 1995; Chung et al., 1981). It was shown that CAFs were capable of stimulating carcinogenesis and inducing the progression of an initiated epithelium (the SV-40 immortalized BPH-1 cell line), while normal prostatic fibroblasts were incapable of stimulating such progression (Olumi et al., 1999). The mechanistic basis by which stromal-epithelial interactions enhance the process of carcinogenesis is still poorly understood. Many signaling pathways and molecules play important roles in controlling proliferation, differentiation and function in both epithelial and stromal cells. The cells in the tumor microenvironment supporting and nurturing the developing tumor include stromal fibroblasts, infiltrating immune cells, as well as blood and lymphatic vascular networks (Mueller and Fusenig, 2004). Tissue reaction to wound healing represents circumstances in which "reactive" fibroblasts with unique phenotypic characteristics have been described (Grinnell, 1994). These lesions were characterized by

the appearance of myofibroblasts. Myofibroblasts are abundant during wound contraction, and gradually disappear during the later stages of scar formation (Grinnell, 1994; Schmitt-Graff et al., 1994). These cells may arise according to specific physiological needs as a result of modified signals from the microenvironment (Schmitt-Graff et al., 1994). Similar to that seen in myofibroblasts associated with wound healing, there is abnormal expression of smooth muscle actin, metalloproteinases and the production of extracellular matrix proteins (Basset et al., 1990; Chiquet-Ehrismann et al., 1986; Knudson and Knudson, 1993) These differences may enhance the invasive potential of initiated epithelial cells and modulate the phenotype of nearby epithelial cells. A detailed understanding of the changes occurring within tumor stroma and to the signaling mechanisms acting between stroma and epithelium will allow for the rational design of therapies aimed at inhibiting prostate tumor growth.

Stroma as a therapeutic target in prostate cancer

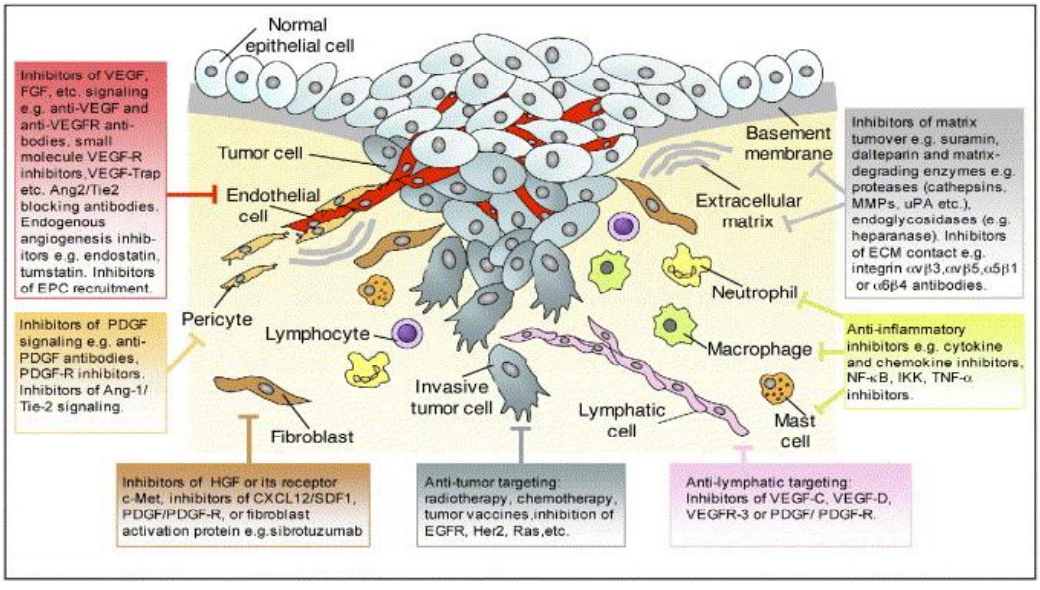

Figure 1-6. Therapeutic strategies that have been designed or suggested to target different cells in the tumor microenvironment (Joyce, 2005)

Traditional therapy for all epithelial malignancies, including prostate cancer, has been targeted at the epithelial cell which represents a moving target for treatment, in the sense that as the disease progresses these cells acquire progressively severe genetic changes. The stroma may provide a more stable target at which to direct treatment. The supporting players of cancer in the tumor microenvironment include stromal fibroblasts, infiltrating immune cells, the blood and lymphatic vascular networks and the extracellular matrix (Joyce, 2005) (Figure 1-6). CAF-induced tumorigenesis of BPH-1 cells is an epigenetic effect that drives initiated BPH-1 cells to be tumorigenic CAFs have been used to study stromal-epithelial interactions in prostate cancer progression (Ao et al., 2007). There is also a growing evidence that DNA methylation and histone modifications play essential roles in prostate cancer initiation and progression (Li et al., 2005).

A detailed understanding of the signaling mechanisms between stroma and epithelium will allow for the rational design of therapies aimed at inhibiting prostate tumor growth. Specific growth factors may play an important role in the stroma-epithelial interactions. The FGF family contains members that have been studied in regard to prostatic growth and branching morphogenesis. It has been shown that FGF7 and FGF10 play important roles during prostatic development (Thomson et al., 1997). FGF-7 is capable of imitating some of the effects of testosterone (Thomson et al., 1997). FGF10 (also known as keratinocyte growth factor-2) shows a high degree of sequence homology and shares a same receptor with FGF7 (Ropiquet et al., 2000). It functions as a mesenchymal paracrine regulator of epithelial growth in the prostate and seminal vesical, is not regulated by

androgens (Thomson and Cunha, 1999). The IGF family is also includes important mediators, which may potentially influence prostatic growth and carcinogenesis. We have found that TGF-ß expression is elevated in CAFs versus normal prostatic fibroblasts (NPFs). Also stromal-derived TGF- β can regulate expression of receptors for other growth promoting factors expressed by CAFs. These data indicated that the TGF-beta pathway may be important for stromal cells to promote adjacent epithelial tumor progression. Recent experiments in mice suggest that TGF-β is one of the fibroblast-supplied factors involved in suppression of epithelial transformation and loss of TGF-β response in fibroblasts resulted in intraepithelial neoplasia in prostate through the activation of paracrine hepatocyte growth factor (HGF) pathway (Bhowmick et al., 2004a; Bhowmick et al., 2004b).

Senescence and prostate cancer

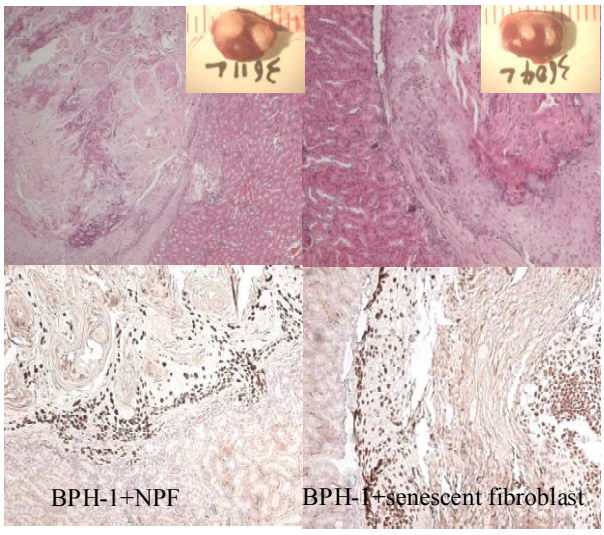

Figure 1-7. BPH-1 invaded to host kidney after *in vivo* incubation with senescent fibroblasts.

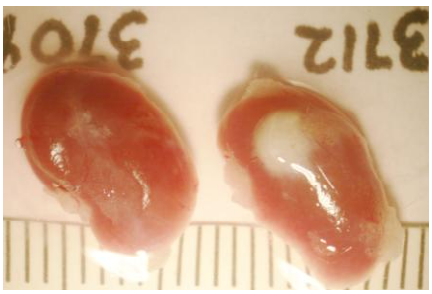

Figure 1-8. Graft size of BPH ^{senescent} and BPH-1^{NPF}.

The greatest risk factor of developing carcinoma of the prostate is advanced age. Cancer is a disease

of uncontrolled cell proliferation caused by upregulation of oncogenic signaling and downregulation of tumor suppressor signaling. To counteract the uncontrolled growth, cells can undergo apoptosis or senescence. However, it has been proposed that in some conditions senescence may actually promote tumor progression, possibly by secreting matrix metalloproteases, growth factors and cytokines. Senescent fibroblasts were shown to promote tumorigenesis by immortalizing pre-malignant epithelial cells (Bavik et al., 2006). Evidence suggested that mutations in epithelial cells alone may not be sufficient for the development of cancer. Malignant transformation also requires changes in the microenvironment in which the initiated cells can progress to full malignancy. Cellular senescence is the phenomenon where normal diploid differentiated cells lose the ability to divide. The senescence response can limit the proliferation of normal cells by telomere shortening. However, it was suggested that senescent cells acquire multiple phenotypic changes, by compromising tissue structure and function. The response may benefit organism in early life by preventing cancer, but could be detrimental later in life as senescent cells accumulate by secreting factors that damage tissue homeostasis. Dr. Peter Nelson's group in Fred Hutchinson Research Institute showed that senescent fibroblasts modulate neoplastic epithelial cell proliferation through paracrine mechanisms (Bavik et al., 2006). Their data showed that senescent fibroblasts can stimulate benign BPH-1 cells growth *in vitro* by culturing BPH-1 cells with senescent fibroblasts conditional media. Their results suggested that a significant component of the senescent fibroblasts' proliferative influence toward epithelium is mediated through soluble factors. The host environment is increasingly viewed as an important active player for tumor growth and

carcinogenesis. From our *in vivo* experiments, BPH-1 cells invaded the kidney after incubation with senescent fibroblasts under the renal capsule of SCID mice for two months (Figure 1-7). The isolated epithelial cells from BPH-1 + senescent fibroblast and BPH-1+NPF (which were designated as BPH-1^{NPF}), showed clear difference in cell proliferation rate. The size of the grafts when re-grafted to kidney capsule alone showed clear difference (Figure 1-8). The size of BPH-$1^{senescent}$ graft was bigger than that of BPH-1^{NPF}. This phenomenon indicated after incubation with senescent fibroblasts the isolated BPH-$1^{senescent}$ cells can grow independently under the kidney capsule.

The somatic mutation theory of cancer suggests that carcinomas result from a single somatic cell that accumulates multiple DNA mutations or chromosomal alterations over time. The concept of a reactive stroma implies that the microenvironment is altered in response to epithelial change. The reactive stroma theory suggests that stromal alterations are operative as primary or permissive events allowing for or magnifying a reactive phenotype. It was suggested that age-dependent stromal processes operate as a tissue-modifying field effect. A number of senescence induced mitogenic factors including HGF, IGF and amphiregulin (AREG) exert important effects on pre-neoplastic lesions.

PTEN signaling pathway

PTEN is one of the most frequently inactivated tumor suppressor genes in many human tumors, including prostate cancer. The PTEN tumor suppressor gene is located at 10q23, a region which has often shown deletions in prostate cancer (DeMarzo et al., 2003; Visakorpi, 1999; Visakorpi, 2003). The PTEN gene encodes a dual specificity

phosphatase that regulates signal transduction pathways. It mainly functions as a lipid phosphatase and targets phosphatidylinositol 3,4,5-trisphosphate (PIP-3) (Maehama and Dixon, 1998). By dephosphorylating PIP-3, PTEN can downregulate the Akt/PKB signaling pathway thus promoting cell survival and inhibiting apoptosis.

Importance of PTEN in prostate cancer and new thoughts

The essential nature of PTEN function is evident from the early embryonic lethality of homozygous mutants. *Pten* heterozygous mutant mice develop cancers or dysplasias of multiple tissues including prostate (Di Cristofano et al., 2001; Di Cristofano et al., 1998; Suzuki et al., 1998). Loss of function of Nkx3.1 and PTEN cooperate in prostate cancer progression (Abate-Shen et al., 2003). In humans, PTEN undergoes Loss Of Heterozygosity (LOH) at relatively advanced stages in many cancers (Di Cristofano et al., 1998; Kim et al., 2002), suggesting that genes within this region are important for progression. The function of PTEN in initiating prostate cancer progression and in response to stroma has not been identified.

Cyclin D1 in prostate tumorigenesis

Cyclin D1 encodes the regulatory subunit of a holoenzyme that phosphorylates and inactivates the retinoblastoma protein and promotes progression through G1 to S phase of the cell cycle (Fu et al., 2004; Petty et al., 2003). Overexpression of cyclin D1 plays important roles in the development of a subset of human cancers including breast cancer, colon cancer and melanoma (Fu et al., 2004; Polsky and Cordon-Cardo, 2003). In human cancers, overexpression of cyclin D1 is one of the most commonly observed alterations

(Fu et al., 2004). Increased cyclin D1 abundance occurs relatively early during tumorigenesis. However, the role of cyclin D1 in prostate cancer has not been previously studied in detail. Studies have shown that mouse prostate epithelial cells have elevated cyclin D1 expression as they enter the cell cycle (Day et al., 2002). Some studies have suggested that human prostate carcinoma cell lines frequently express relatively high levels of cyclin D1 protein, even though this gene is not amplified in these cell lines (Day et al., 2002). This situation is analogous to that seen in a subset of human breast cancer cell lines and tumors. The functional effects of the increased expression of cyclin D1 in prostate carcinoma cells remain to be determined. Immunostaining studies indicated that primary prostate carcinoma samples displayed moderate or strong expression of cyclin D1 protein. Overexpression of cyclin D1 can increase tumorigenicity of LNCaP cell lines (Chen et al., 1998). It has been reported that cyclin D1 overexpression might be related to the evolution of androgen-independent disease in prostate cancer (Chen et al., 1998). However, several studies have also suggested that amplification and/or overexpression of cyclin D1 is not a common event in either primary and tumor-derived prostate cell lines (Chen et al., 1998). This calls into question the relevance of the *in vitro* studies and makes the point that while something may be possible it is not necessarily relevant. Since stromal environment plays an important role in tumor progression and no study has shown the role of cyclin D1 in the stroma, questions over the role of cyclin D1 in prostate cancer progression has driven our attention to study the consequences of cyclin D1 over expression in both epithelial and stromal tissues.

Prostate cancer research has been hindered by the lack of well established, characterized, immortalized benign prostatic epithelial cells lines and human models. In this project, we have used a few benign prostatic epithelial cell lines in an effort to build new *in vivo* models of human prostate cancer progression. We have already successfully built a new model of human prostate cancer progression by overexpression cMyc oncogene. The aim of this project to build less aggressive models that represent distinct grades of disease by manipulating different genes. Taken together, important oncogenes (such as cyclin D1) and tumor suppressor genes (such as PTEN) are expected to be the essential players in the stromal-epithelial interaction in prostate cancer progression. A detail understanding of the mechanism of this interaction by modifying either the epithelial or the stromal compartments will elucidate new therapeutic targets. The central hypothesis of this proposal is that stromal-epithelial interactions play a crucial role in prostate cancer progression and are a potential therapeutic target.

CHAPTER II

TISSUE-SPECIFIC CONSUQUENCES OF CYCLIN D1 OVEREXPRESSION IN PROSTATE CANCER PROGRESSION

Introduction

Prostate development is controlled by steroid hormones that induce and maintain a complex cross talk between the stromal and epithelial cells (Cunha and Young, 1992). The result of this intercellular communication depends upon the context and differentiation status of the cell type being stimulated (Hayward and Cunha, 2000; Hayward et al., 1998). The process of prostatic carcinogenesis includes aberrations in the interactions of the prostatic epithelium and its local microenvironment resulting in reciprocal de-differentiation of both the emerging carcinoma cells and the prostatic smooth muscle.

The vast majority of human prostatic cancers arise as adenocarcinomas which, by definition, are derived from the epithelial cells that form the glands and ducts of the prostate. As the carcinoma evolves, phenotypic changes and alterations in gene expression also occur in the adjacent stroma. These “changes” may enhance the invasive potential of the epithelial tumor (Grossfeld et al., 1998; Joesting et al., 2005). Chung and co-workers reported that co-inoculation of tumorigenic Nbf-1 fibroblasts with human PC-3 cells accelerated tumor growth (Chung, 1991; Chung, 1995; Chung et al., 1991). More recently it was shown that human CAFs were capable of stimulating carcinogenesis and inducing the progression of an initiated epithelium (the SV-40 immortalized BPH-1

cell line), while normal prostatic fibroblasts were incapable of stimulating such progression (Olumi et al., 1999). The mechanistic basis by which stromal-epithelial interactions enhance the process of carcinogenesis is still poorly understood.

The cells in the tumor microenvironment supporting and nurturing the developing tumor include stromal fibroblasts, infiltrating immune cells, blood and lymphatic vascular networks (Mueller and Fusenig, 2004; Tuxhorn et al., 2001). A detailed understanding of the changes occurring within tumor stroma and to the signaling mechanisms acting between stroma and epithelium will allow for the rational design of therapies aimed at inhibiting prostate tumor growth.

Cyclin D1 encodes the regulatory subunit of a holoenzyme that phosphorylates and inactivates the retinoblastoma protein and promotes progression through G1 to S phase of the cell cycle (Fu et al., 2004; Petty et al., 2003). Overexpression of cyclin D1 plays important roles in the development of human cancers including breast, colon and melanoma (Bartkova et al., 1995; Hunter and Pines, 1994; Polsky and Cordon-Cardo, 2003; Roy and Thompson, 2006; Sherr et al., 1992). Increased cyclin D1 expression occurs relatively early during tumorigenesis, however, its role in prostate cancer is not well understood. Studies have shown that mouse prostatic normal and Rb-/- epithelial cells have elevated cyclin D1 expression as they enter the cell cycle (Day et al., 2002). Human prostate carcinoma cell lines frequently express elevated levels of cyclin D1 protein, although the gene is not amplified in these cells (Day et al., 2002). This situation

is analogous to that seen in a subset of human breast cancer cell lines and tumors (Arnold and Papanikolaou, 2005; Caldon et al., 2006). Overexpression of cyclin D1 can increase tumorigenicity of LNCaP cell lines. Additionally, androgen ablation has a smaller inhibitory effect on tumors formed by cyclin D1 overexpressing LNCaP cells compared with tumors formed by parental LNCaP cells, which regress after castration. This phenomenon suggests that cyclin D1 overexpression might be related to the evolution of androgen-independent prostate cancer (Chen et al., 1998). Immunostaining studies indicated that primary prostate carcinoma samples displayed moderate or strong expression of cyclin D1 protein in the epithelial compartment compared to normal epithelium. Little is known about the role of cyclin D1 in the stromal compartment of tumors, especially in adenocarcinomas. One study of cyclin D1 expression in esophageal carcinomas indicated that cyclin D1 is strongly expressed in stromal fibroblasts (Pera et al., 2001).

In this chapter we examined the consequences of targeted regulation of cyclin D1 expression in epithelial or stromal cells in order to investigate the effects of cyclin D1 in prostate cancer progression.

Materials and Methods

Cells

BPH-1 (a non-tumorigenic prostate epithelial cell), and its tumorigenic derivatives BPH^{CAFTD1} and BPH^{CAFTD2} were from our own stocks. DU145, LNCaP and PC3 cells were obtained from ATCC (Rockville, MD, USA). NPFs, BPH fibroblasts and CAFs were isolated and bioassayed as previously described (Olumi et al., 1999). Prostatic Epithelial cell (PrE)1 cells were isolated from human benign prostate tissue. 957E/hTERT cells were generously supplied by Dr. John Issacs (Johns Hopkins). PrE3 cells were kindly provided by Dr. Dean Tang (M. D. Anderson). BPH-$1^{C7\text{-}cyclin\ D1}$, BPH-$1^{C7\text{-}\Delta}$, BPH-1^{NPF}, $NPF^{cyclin\ D1}$ and BPH-$1^{NPF\text{-}cyclin\ D1}$ cells were generated as described below. All of the epithelial cells were maintained in RPMI 1640 (Gibco, Carlsbad, CA) with 1% antibiotic/antimycotic (Life Technologies, Grand Island, NY) and 5% Cosmic Calf Serum (CCS) (HyClone, Logan, Utah). All of the stromal cells were maintained in the same condition except 5% Fetal Bovine Serum (FBS) (Atlanta Biologicals, Atlanta, GA) was used.

Construction of cyclin D1 expression vector

The plasmid C7-cyclin D1 was constructed using the LZRS-EGFP backbone (Nolan Laboratory, Stanford University, CA). The CMV promoter was cut from pIRES-EGFP (Clontech, Palo Alto, CA) as a BglII/BamHI fragment. The fragment was then ligated into the BamHI site of the LZRS-EGFP backbone to produce C7-Δ. The human cyclin D1 cDNA clone was obtained from ATCC (Rockville, MD) and amplified by PCR using a 5'

primer specific to translational start site and a 3' primer containing an XhoI restriction site and the consensus sequence for the translational stop site. After PCR amplification, the product was gel purified, and cloned into pGem T-Easy (Promega, Madison, WI). Following DNA sequence verification, the cyclin D1 coding region was cut using EcoRI/XhoI and sub-cloned into the EcoRI/XhoI sites of pLZRS-EGFP to obtain C7-cyclin D1 construct.

Generation of a stable cyclin D1 overexpressing BPH-1 cell line

Viral particles were prepared as previously described and used to infect BPH-1 cells (Williams et al., 2005). Fresh virus was placed onto target cells every 24 hours until green fluorescent protein expression was observed. Cell sorting was performed to select the GFP-expressing BPH-1 cells. Two stable cell lines were generated: C7-cyclin D1 overexpressing BPH-1 cell line and C7-Δ control BPH-1 cell line which were designated as BPH-1$^{\text{C7-cyclin D1}}$ and BPH-1$^{\text{C7-}\Delta}$ respectively.

Generation of NPF$^{\text{cyclin D1}}$ cells

Human prostatic cells were prepared as described previously (Williams et al., 2005). Cyclin D1 virus was generated using phoenix A cells, and the prostatic cells were infected as described (Williams et al., 2005). After 1 week of successive rounds of infection, some cells expressed EGFP when monitored by fluorescence microscopy. Differential trypsinization was used to separate fibroblasts from the epithelial cells. The resulting colonies were characterized by phenotype and their nature confirmed using

immunocytochemical staining against keratin and vimentin. After 12 passages, EGFP-expressing cells self sorted as all unstained cells became senescent and died.

Western blotting analysis

Cell lysates were prepared and western blotting was performed as previously described (Williams et al., 2005). Membranes were incubated with mouse monoclonal antibody to cyclin D1 (BD Biosciences Pharmingen, San Jose, CA, 1:1,000 dilution) or α-tubulin (Santa Cruz Biotechnology, Santa Cruz, CA, 1:1,000 dilution) overnight, washed with PBS-Tween 20 for 1 hour, and incubated with horseradish-Peroxidase linked anti-mouse or anti-rabbit secondary antibody (Amersham Biosciences, Piscataway, NJ, 1:1,000 dilution) for 1 hour. Bound antibodies were visualized using enhanced chemiluminescence western blotting detection reagents (Amersham Bioscences). Cyclin D1 expression levels were normalized to β-actin and quantitated using Image J software from the NIH (http://rsb.info.nil.gov/ij/).

Growth curves

BPH-1$^{C7\text{-}\Delta}$ and BPH-1$^{C7\text{cyclin D1}}$ cells were plated in a 24-well plate (1000 cells/well) in RPMI 1640 medium supplemented with 5% CCS. After the cells had attached overnight, 300 µl of Cell Titer 96 Aqueous One Solution (Promega, Madison, WI) was added at indicated times (1, 2, 3, 4, and 5 days) to each well and the absorbance was measured at 490 nm after 3 hours of incubation at 37^{o}C. Experiments were performed in triplicate.

Wound healing assays

Confluent monolayers of BPH-1$^{C7-\Delta}$ and BPH-1$^{C7\text{-cyclin D1}}$ cells were grown in 6 well plates. An even line of cells was displaced by scratching through the layer using a pipet tip. Specific points on the wounds were identified and marked. These open areas were then inspected microscopically over time as the cells move in and fill the damaged area. Wounds were imaged at 0, 3, 6, and 8 hours post wounding and the cell migration rate into the wound was calculated. Experiments were performed in triplicate.

Transwell migration assay

One hundred thousand BPH-1$^{C7-\Delta}$ or BPH-1$^{C7\text{-cyclin D1}}$ cells were plated on top of the 8µm pore polycarbonate culture inserts (Becton Dickinson labware, Franklin Lakes, NJ), which were situated in wells of a 24-well culture plate and immersed in RPMI 1640 medium supplemented with 5% CCS. The cells were incubated at 37ºC for 12 hours. The cells on the upper surface of the inserts were removed using cotton swabs and those which had migrated to the bottom side, were fixed with 11% glutaraldehyde (Sigma, St. Louis, MO) for 20 minutes, stained with 0.1% crystal violet (Sigma) for 20 minutes. Inserts were then washed with water 3 times. The number of cells that had migrated was counted using a microscope. The filters were viewed under bright-field optics to count stained cells in eight fields (with a 20X objective) for the two types of cells. The mean number of cells per field was determined, and results from at least three experiments were expressed as the mean relative cell migration ± Standard Deviation (SD), with that of BPH-1$^{C7-\Delta}$ cells set at 1.

Boyden chamber assay

Polycarbonate culture inserts with 8 μm-pores were coated with 20 μl 2.5 mg/ml matrigel (BD Biosciences, Bedford, MA). After the gel solidified, the chambers were equilibrated with RPMI 1640 with 5% CCS for 2 hours in a humidified tissue culture incubator at 37°C with 5% CO_2 atmosphere. More media were then added to the lower compartment, and 100k BPH-$1^{C7\text{-}\Delta}$ and BPH-$1^{C7\text{-}cyclinD1}$ cells were seeded in the upper compartment of the chamber. Each cell group was plated in 3 duplicate wells. After 12 hours incubation, the matrigel was removed using a cotton swab. The number of cells that had migrated to the lower sides of the membrane was then determined as described for the transwell migration assay.

Tissue recombination and xenografting

One hundred thousand epithelial cells and 300k stromal cells were recombined to make the BPH-$1^{C7\text{-}\Delta}$ + rUGM, BPH-$1^{C7\text{-}cyclinD1}$ + rUGM, BPH-1 + NPF and BPH-1 + $NPF^{cyclin\ D1}$ tissue recombinants as previously described (Hayward et al., 1999). After incubating overnight at 37^{o}C, the tissue recombinants were grafted under the kidney capsule of adult male SCID mice (Harlan, Indianapolis, IN). All the experiments were repeated 6 times. Mice were sacrificed after four weeks and grafts were harvested, fixed and imbedded.

Immunohistochemical staining

Immunohistochemical staining was performed following a protocol that was described previously (Williams et al., 2005). Tissue slides were incubated with the primary

antibody against SV40 (Santa Cruz Biotechnology, Santa Cruz, CA, 1:1000 dilution) overnight. The polyclonal rabbit immunoglobulins/biotinylated anti-mouse secondary antibody (DAKO, Carpentiria, CA) was incubated for 60 minutes after the slides were washed with PBS buffer for 1 hour. After washing the slides in PBS extensively, slides were incubated in ABC-HRP complex (Vector Laboratories) for 30 minutes. Bound antibodies were then visualized by incubation with 3,3' diaminobenzidine tetrahydrochloride (liquid DAB, DAKO). Slides were then rinsed extensively in tap water, counterstained with hematoxylin, and mounted.

Isolation of cell strains and regrafting

BPH-1^{NPF} and BPH-1$^{NPF\text{-}cyclin\ D1}$ cells were isolated and selected with 50µg/ml G418 (Clontech, Palo Alto, CA) from BPH-1 + NPF and BPH-1 + NPF$^{cyclin\ D1}$ grafts, and regrafted without stromal cells to SCID mice as previously described (Hayward et al., 1999). Four to fourteen weeks after grafting, the hosts were sacrificed. The harvested grafts were removed from the kidney and formalin-fixed for immunohistochemical analysis.

Cell Cycle Analysis

BPH-1^{NPF} cells and BPH-1$^{NPF\text{-}cyclin\ D1}$ cells were harvested from monolayer culture. The cell pellets were washed and resuspended in PBS and fixed with 80% ETOH with vortexing. Cells were then pelleted and resuspended with PBS containing 1% CCS for cell counting after storing at -20^{0}C for 4 hours. 100,000 cells were resuspended in

Propidium Iodide (PI) / RNase / 1% CCS / PBS. PI was used to stain double-stranded nucleic acids stoichiometrically. Cells were treated with RNase A in order to stain only the DNA. Cell cycle distribution was analyzed on the flow cytometer after at least 30 minutes.

Microarray analysis

We collaborated with Dr. Peter Nelson in Fred Hutchinson Research institute to perform the microarray analysis. Cells were made in our laboratory and the analysis was done in Dr. Peter Nelson's laboratory. $NPF^{cyclin\ D1}$ cells were generated from NPFs, which were isolated from two different patient samples; CAFs were isolated from two different patient samples as well. RNA was isolated from NPFs, CAFs, and $NPF^{cyclin\ D1}$ cells using total RNA isolation kit (Qiagen). Custom spotted cDNA microarrays were constructed as previously described (True et al., 2006) using a non-redundant set of 6,700 prostate-derived cDNA clones identified from the Prostate Expression Data Base (PEDB), a public sequence repository of expressed sequence tag data derived from human prostate cDNA libraries. Total RNA was amplified through one round of linear amplification using the MessageAmp aRNA kit (Ambion, Austin, TX). Sample quality and quantification was assessed by agarose gel electrophoresis and absorbance at A260. Cy3 and Cy5 labeled cDNA probes were made from 4 µg of amplified RNA. Two $NPF^{cyclin\ D1}$ and two CAF samples (labeled with Cy3) were hybridized head-to-head with an NPF control sample labeled with Cy5. Probes were hybridized competitively to microarrays under a coverslip for 16 h at 63°C. Fluorescent array images were collected

for both Cy3 and Cy5 by using a GenePix 4000B fluorescent scanner, and image intensity data were gridded and extracted using GenePix Pro 4.1 software. Differences in gene expression between $NPF^{cyclin\ D1}$/NPF and CAF/NPF groups were determined using a two-sample t-test with Significance Analysis of Microarrays (SAM) software (http://www-stat.stanford.edu/_tibs/SAM/) with a False Discovery Rate (FDR) of $\leq$ 10% considered significant. Similarities in gene expression between NPF $^{cyclin\ D1}$/NPF and CAF/NPF groups were determined using a one-sample t-test in SAM with an FDR of $\leq$ 0.1% considered significant. These results were reduced to unique genes by eliminating all but the highest scoring clones for each gene. A Pearson correlation coefficient was calculated in Excel to assess the strength of the linear relationship between $NPF^{cyclin\ D1}$/NPF and CAF/NPF average $\log_2$ ratios.

Results

Cyclin D1 expression levels are elevated in malignant human prostatic epithelial cell lines

Cyclin D1 expression was examined by Western blotting in the prostate cancer cell lines, DU145, LNCaP, BPH^{CAFTD1} and BPH^{CAFTD2} and in a subset of non-tumorigenic prostatic cells, PrE1, 957E/hTERT (Dalrymple et al., 2005; Yasunaga et al., 2001), PrE3 and BPH-1 cell line. Cyclin D1 expression was found to be higher in all of the cancer cells as compared to the non-tumorigenic prostatic cells. A representative Western Blot is shown in Figure 2-1.Primary epithelial cells had the lowest cyclin D1 expression. The SV40 T-antigen immortalized BPH-1 cells had higher cyclin D1 expression compared with PrE, 957/hTERT and PrE, but lower expression level than that in malignant cell lines. These data crudely correlate cyclin D1 with tumorigenicity but, as with similar correlations seen in patient samples, do not address whether cyclin D1 overexpression is a cause or an effect of malignant change. In order to address this question we tested the consequences of overexpressing cyclin D1 in non-tumorigenic prostatic epithelial cells.

Cyclin D1 overexpression in BPH-1 cells can increase cell proliferation rate, migration and invasive ability *in vitro*

Western blotting showed that the BPH-$1^{cyclin\ D1}$ cells have a 34 fold elevation in cyclin D1 expression compared with control BPH-$1^{C7\text{-}\Delta}$ cells (Figure 2-2, A). BPH-$1^{C7\text{-cyclin D1}}$ cells showed enhanced motile ability in wound healing, transwell migration and Boyden chamber assays. Wound healing assays showed that BPH-$1^{C7\text{-cyclin D1}}$ cells were

significantly more motile than BPH-1$^{C7-\Delta}$ cells. This difference was clear after 3 hours and was very marked after 8 hours (Student's t-test, P<0.001) (Figure 2-2, B). In a transwell migration study, the BPH-1$^{C7\text{-cyclin D1}}$ cells migrated through the uncoated Boyden chambers to the underside of the insert in greater numbers in a 12 hour response to conditional medium containing 1% CCS in the lower chamber than BPH-1$^{C7-\Delta}$ cells (Student's t-test, P<0.05) (Figure 2-2, C). These data confirmed the elevated motility of BPH-1$^{C7\text{-cycin D1}}$ cells, as seen in the wound healing assay. An invasion assay, in which the inside chamber was coated with matrigel to mimic the *in vivo* extracellular matrix, demonstrated that BPH-1$^{C7\text{-cyclin D1}}$ cells had significantly increased invasive activity *in vitro* (Student's t-test, P<0.01) (Figure 2-2, D). We used an MTT assay to assess the effect of cyclin D1 overexpression on the growth rate of BPH-1 cells. Our results showed that the cyclin D1 overexpressing cells proliferated faster than control cells. The difference was observed even after 24 hours incubation (Figure 2-2, E). Collectively the assays showed that when cyclin D1 is forcibly overexpressed, BPH-1 cells acquired an enhanced proliferation rate, motility and invasive ability *in vitro*.

Cyclin D1 overexpressing BPH-1 cells are not tumorigenic in tissue recombinants with rUGM

To determine whether cyclin D1 could exert a tumorigenic effect on prostate cells *in vivo,* 100k BPH-1$^{C7\text{-cyclin D1}}$ cells or control cells were recombined with 300k rUGM and grafted under the kidney capsule of SCID mice. The grafts were harvested after 4, 8, 12 and 16 weeks. The results showed that BPH-1$^{C7\text{-cyclin D1}}$ cells formed significantly larger and

more vascularized grafts under the induction of rUGM, compared with BPH-1$^{C7-\Delta}$ cells. An example of the gross morphology of grafts at 8 weeks is shown in Figure 2-3, A. These results are consistent with our *in vitro* experiments, which showed that BPH-1$^{C7\text{-}cyclinD1}$ cells proliferate faster than controls. Histologically, both experimental and control grafts exhibited the formation of solid epithelial cords surrounded by a muscular stroma. SV-40 T-antigen staining confirmed the origin of BPH-1 cells in both control and cyclin D1 overexpressing groups and showed that there were sharp delineations from the host kidney (denoted as k in the figure) with no sign of invasion (Figure 2-3 B and C). It was noteworthy that a clear layer of stromal cells was always seen between the graft and host kidney under both control and test conditions. In the control grafts few epithelial cells were phospho histone H_3 positive (indicating low proliferation rates). However, there were significantly more histone H_3 positive cells in BPH-1$^{cyclin\ D1}$ cords (Student's t-test, $P<0.01$, data not shown). These data indicated that BPH-1$^{cyclin\ D1}$ cells proliferated much faster than control cells (Figure 2-3, B and C). To assess whether cyclin D1 can transform BPH-1 cells in a longer period of time *in vivo*, we sacrificed mice every month for up to 4 months. The histological appearance of the grafts at 4 months was similar to the earlier grafts with solid cord structures and no invasion of the kidney (date not shown). Therefore, while cyclin D1 can increase BPH-1 cell motility and promote cell proliferation *in vitro*, overexpression of the gene did not induce BPH-1 cells to undergo malignant transformation with associated invasion.

NPF$^{cyclin\ D1}$ cells have increased life span compared with NPFs and CAF cells have upregulated cyclin D1 expression

Since the stroma is viewed as an important active contributor to tumor growth, and in order to understand whether cyclin D1 performs different functions in stromal and epithelial tissues, we generated NPF$^{cyclin\ D1}$ cells by overexpressing cyclin D1 in primary cultures of normal prostate stromal cells. To investigate whether the cyclin D1 overexpressing fibroblasts have an increased life span compared to control or non-infected cells, we passaged the cell mixtures 12 times. The uninfected cells underwent spontaneous senescence and died within 12 passages. The EGFP-expressing cells still looked healthy and grew well after 11 more passages (total 23 passages-Figure 2-3, A). Western blot analysis demonstrated that EGFP positive cells also overexpressed cyclin D1 (Figure 2-4, B). This result indicated that NPFs acquired a prolonged life span as a consequence of upregulated cyclin D1.

It has previously been shown that CAF cells can induce BPH-1 cells to undergo malignant transformation while normal prostatic fibroblasts cannot (Olumi et al., 1999). Cyclin D1 has been shown to be strongly expressed in stromal fibroblasts in carcinoma and adenocarcinoma (Pera et al., 2001). We were interested to determine whether human prostatic CAFs have elevated cyclin D1 expression and if so whether CAFs and NPF$^{cyclin\ D1}$ cells share common functional sequelae. Therefore, we examined the expression level of cyclin D1 in NPFs, BPH fibroblasts and CAF cells. These experiments showed that CAFs

expressed a much higher level of cyclin D1 protein than either NPFs or fibroblasts isolated from BPH patients (Figure 3B).

NPF$^{\text{cyclin D1}}$ cells elicit CAF-like effects promoting tumorigenesis

To investigate the *in vivo* consequences of overexpression of cyclin D1 in NPFs, 100k BPH-1 cells were recombined either with 300k NPF$^{\text{cyclin D1}}$ or NPF cells. Grafts were harvested after one month. Tissue recombinants composed of BPH-1 + NPF$^{\text{cyclin D1}}$ exhibited moderate growth, in contrast, consistent with previously published data, control recombinants composed of BPH-1 + NPFs demonstrated minimal growth. Control grafts of NPF and NPF$^{\text{cyclin D1}}$were likewise small and flattened (Figure 2-5, A a and b). Comparison between the volume of the control and test recombinants showed that the test samples were significantly larger (Student's t-test, $P<0.01$). The histological appearance of the BPH-1 + NPF$^{\text{C7-cyclin D1}}$ grafts, as assessed by H & E staining, resembled a poorly differentiated carcinoma with areas of squamous differentiation (Figure 2-5 B,a and b). Instead of forming solid cord structures, some epithelium fused to form large nests with keratinization and a broad pushing margin against the host kidney (Figure 2-5, B a and b). Tumors also contained irregular epithelial cords intermingled within a fibrous stroma (Figure 2-5, B e and f-right arrow). In other areas, single epithelial cells were intermixed with fibrous stroma (Figure 2-5, B c-arrow and f-left arrow). SV-40 T antigen staining confirmed the origin of the epithelial component of the tumors as being from the BPH-1 cells (Figure 2-5, B c and f). E-cadherin expression was patchy, with positive expression in cell-cell junctions in some areas, but weak or absent in many areas (Figure 2-5, B d). The histology of

recombinants of BPH-1 + NPF$^{cyclin\ D1}$ was similar to that previously described for BPH-1 + CAFs recombinants (Dalrymple et al., 2005; Olumi et al., 1999), although the overall tumor size was smaller. After 5 months of incubation in the kidney capsule, BPH-1 cells formed larger tumors with clear kidney invasion (Figure 2-5, B g and i). Small kidney tubes intermingled with tumor cells (Figure 2-5, B g-arrow and h-arrows) and there were no clear margins between the kidney and grafts.

In contrast to the malignant histological appearance of the BPH-1 + NPF$^{cyclin\ D1}$ recombinants, the BPH-1 + NPF recombinants appeared benign and, as previously described, the bulk of the grafts were composed of stromal cells. Occasional small epithelial cords are found (Figure 2-5, B k and l). This confirmed previous observations that stromal cells from normal peripheral zone recombined with BPH-1 cells produced benign or no visible grafts (Barclay et al., 2005; Olumi et al., 1999). To examine if NPF $^{cyclin\ D1}$ cells are tumorigenic, we grafted either NPF or NPF $^{cyclin\ D1}$ cells alone to SCID mice. Both control groups formed flattened grafts (Figure 2-5, A c and d). H & E staining showed that both grafts were present as a thin layer of fibrous tissue (data not shown).

Epithelial cells isolated from BPH-1 + NPF$^{cyclin\ D1}$ grafts (BPH-1$^{NPF\text{-}cyclin\ D1}$) are tumorigenic

After cell culture and G418 selection, two cells strains were derived from BPH-1 + NPF and BPH-1 + NPF$^{cyclin\ D1}$ grafts, designated BPH-1^{NPF} and BPH-1$^{NPF\text{-}cyclin\ D1}$. The two strains were grafted in collagen gels beneath the renal capsule of male SCID mice.

Grossly, after 3 months, the BPH-1$^{NPF\text{-}cyclin\ D1}$ cells formed significantly larger grafts than the control group (Figure 2-6, A-right). The control group formed small flattened grafts (Figure 2-6, A-left). Histologically, the BPH-1^{NPF} cells grew to form occasional small cords, which were SV-40 positive, similar to the grafts previously reported for BPH1 cells grafted alone (Figure 2-6, B). The BPH-1$^{NPF\text{-}cyclin\ D1}$ cells, in contrast, formed large fused nests generally with a broad pushing margin to the host kidney (Figure 5C,a-arrow). Many smaller nests with irregular shapes were scattered throughout the tumor and intermingled with stroma (Figure 2-6, C, d and e). Some infiltrative areas recapitulated prostatic carcinoma (Figure 2-6, C b-arrow). Cells contained a foamy cytoplasm and their borders were indistinct (Figure 2-6, C c-arrow) . Minimally invasive growth was found in some areas (Figure 2-6, C f). Tumors continued to express SV-40T-antigen confirming the BPH-1 origin of the malignant epithelium.

DNA flow cytometry analysis demonstrated that stromal cyclin D1 caused a shift of the cell cycle distribution of BPH-1 $^{NPF\text{-}cyclin\ D1}$ cells. An abnormal wider peak which contains 55% of the cell population is located close to where the G2/M peak (which has twice the normal copies of DNA) is supposed to be, but its position is below the G2/M peak position. It was reported that a wide peak may represent two populations of cells with different quantities of DNA (Seidman et al., 1992). Given that the original BPH-1 population has previously been described to have an abnormal chromosomal make up and further that this can be altered by exposure to cancer stroma it is possible that BPH-1$^{NPF\text{-}cyclin\ D1}$ cells become hyperdiploid or nearly tetraploid, and the hyperdiploid cell

population mixed with the tetraploid G2/M population to produce this abnormal peak. A large proportion (23.1%) of BPH-1$^{NPF\text{-}cyclin\ D1}$ cells also appear to be polyploid with varying but high DNA content. In marked contrast, only 0.9% of BPH-1^{NPF} cells were found to be polyploid and BPH-1^{NPF} cells showed a normal distribution of cell populations with 64% cells in the G1 phase of cell cycle (Figure 2-6, D).

Gene expression profiles were highly concordant between CAFs and NPF$^{cyclin\ D1}$ cells

This data were received from Dr. Peter Nelson lab. The gene expression patterns of NPFs, CAFs and NPF$^{cyclin\ D1}$ cells were compared by cDNA microarray analysis (GEO submission (GSE6936) [NCBI tracking system #15248638]. NPF$^{cyclin\ D1}$ cells and CAFs showed a high level of gene expression correlations when compared to NPFs (Pearson r = 0.65 across all 5652 clones returning data in all 4 samples.) A one-sample t-test in SAM identified 118 unique genes up-regulated and 51 unique genes down-regulated (q-value $\leq$ 0.1%) commonly expressed between NPF$^{cyclin\ D1}$ cells and CAFs when compared with NPFs. (Figure 2-7 A and B). Relatively few significant differences in transcript abundance measurements between NPF$^{cyclin\ D1}$ cells and CAFs were identified: a two-sample t-test in SAM identified 6 unique genes up-regulated and 20 unique genes down-regulated (q-value $\leq$ 10%) in CAFs when compared with cyclin D1 overexpressing fibroblasts (Figure 2-7 C).

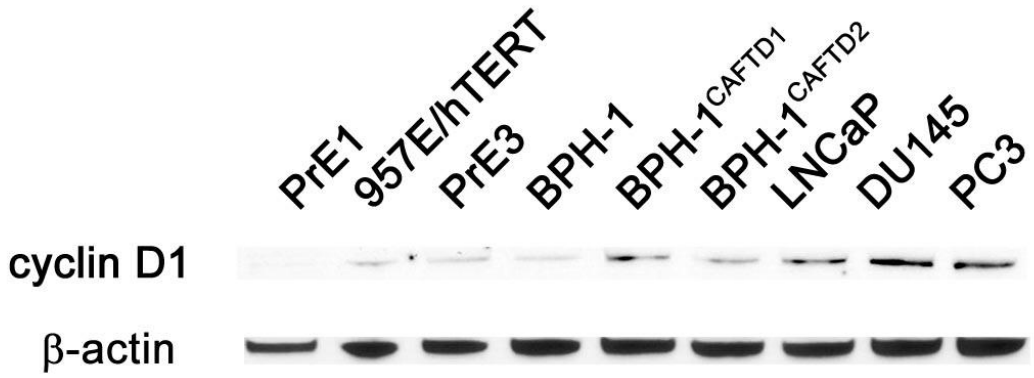

Figure 2-1. Cyclin D1 protein expression in a panel of human prostatic epithelial cells. Western blotting was performed to examine cyclin D1 protein expression levels in malignant (BPH-1^{CAFTD1}, BPH-1^{CAFTD2}, DU145, LNCaP and PC3) and non-tumorigenic (PrE1, 957E/hTERT, PrE3 and BPH-1) prostatic epithelial cell lines. The PrE1, 957/hTERT, PrE3 cells had the lowest cyclin D1 expression compared with other transformed prostate cell lines. BPH-1 cells had moderate level of cyclin D1 expression.

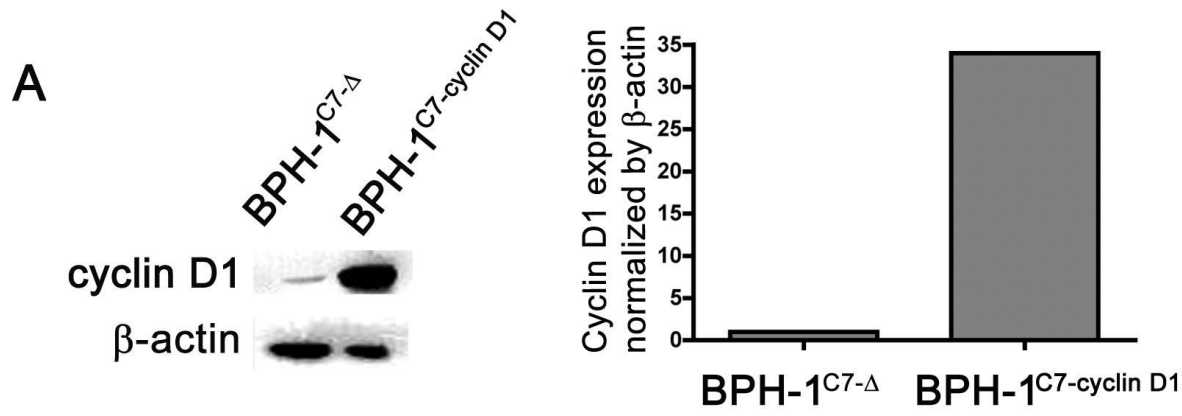

Figure 2-2. *In vitro* comparison of BPH-1$^{C7-\Delta}$ and BPH-1$^{C7\text{-cyclin D1}}$ cells.
(A) In order to examine the role of cyclin D1 in prostate cancer progression, C7-Δ (control - BPH-1$^{C7-\Delta}$) and cyclin D1 overexpressing (BPH-1$^{C7\text{-cyclin D1}}$) BPH-1 cell lines were generated by stable retroviral infection. Cyclin D1 overexpression in BPH-1$^{C7\text{-cyclin D1}}$ was confirmed by western blotting and band intensity quantitated.

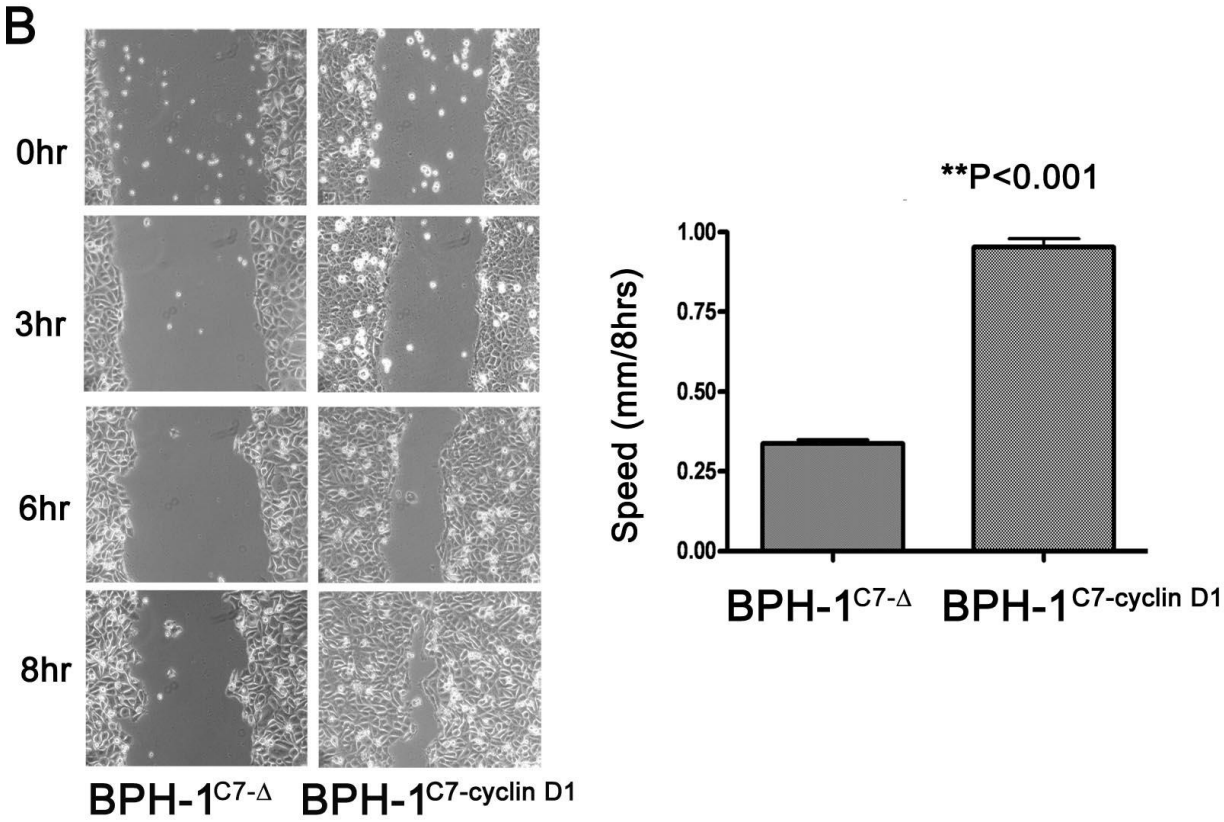

Figure 2-2 (B). Wound healing assay. BPH-1$^{C7\text{-}cyclin\ D1}$ closed wounds in the confluent monolayer significantly faster than BPH-1$^{C7\text{-}\Delta}$ cells. Images (left) and quantitation (right) shown. Student's t-test, P<0.001.

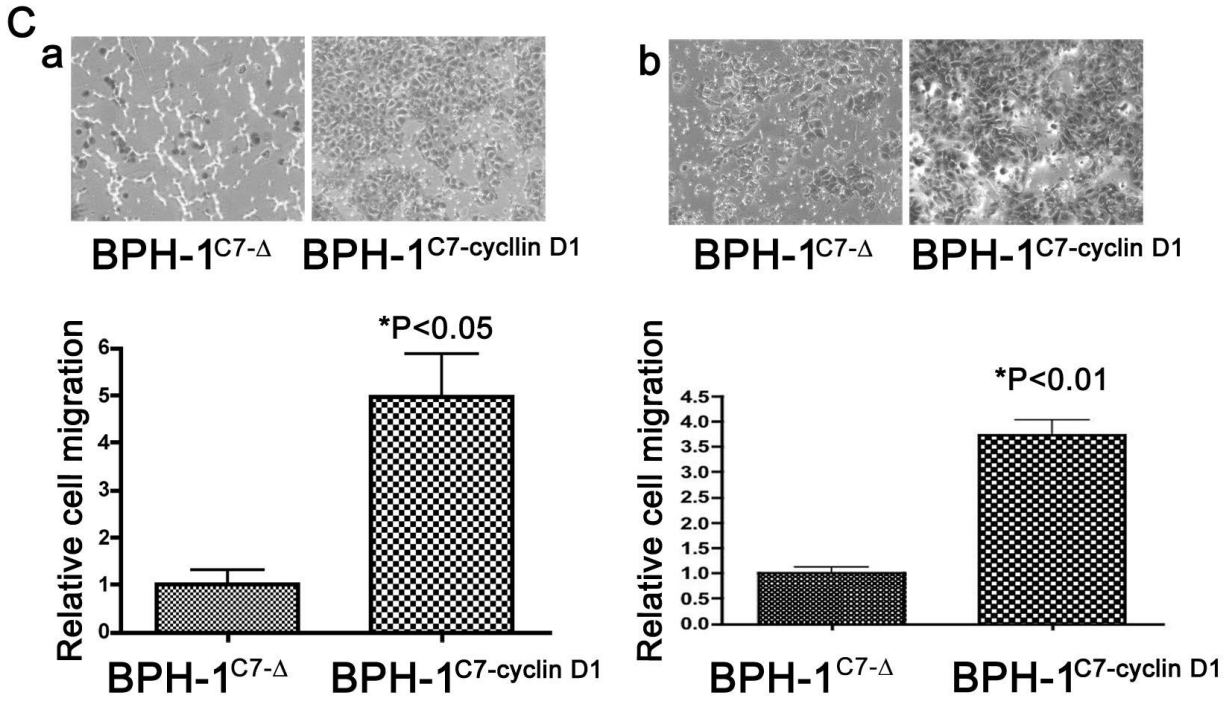

Figure 2-2 (C). Transwell migration study and invasion assay. BPH-1$^{C7\text{-}cyclin\ D1}$ migrated through the uncoated Boyden chamber significantly faster than BPH-1$^{C7\text{-}\Delta}$ Representative phase-contrast optical photomicrographs after overnight culture shown (a, above) and quantitated (a, bottom). Student's t-test, P<0.05. BPH-1$^{C7\text{-}cyclin\ D1}$ cells had increased invasive ability in a Matrigel coated Boyden chamber invasion assay compared to BPH-1$^{C7\text{-}\Delta}$□ □ Representative phasecontrast optical photomicrographs after overnight culture shown (b, above) and quantitated (b, bottom). Student's t-test, P<0.01.

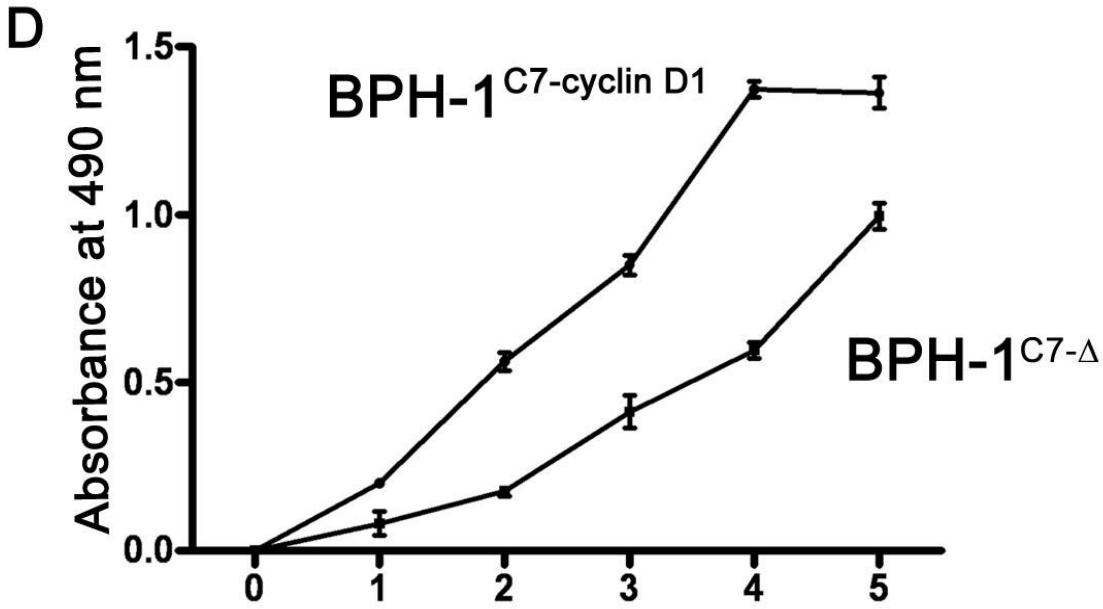

Figure 2-2 (D). Proliferation assay. Cyclin D1 overexpression promoted BPH-1 cell proliferation significantly over control growth rate. (Student's t-test, $P<0.001$).

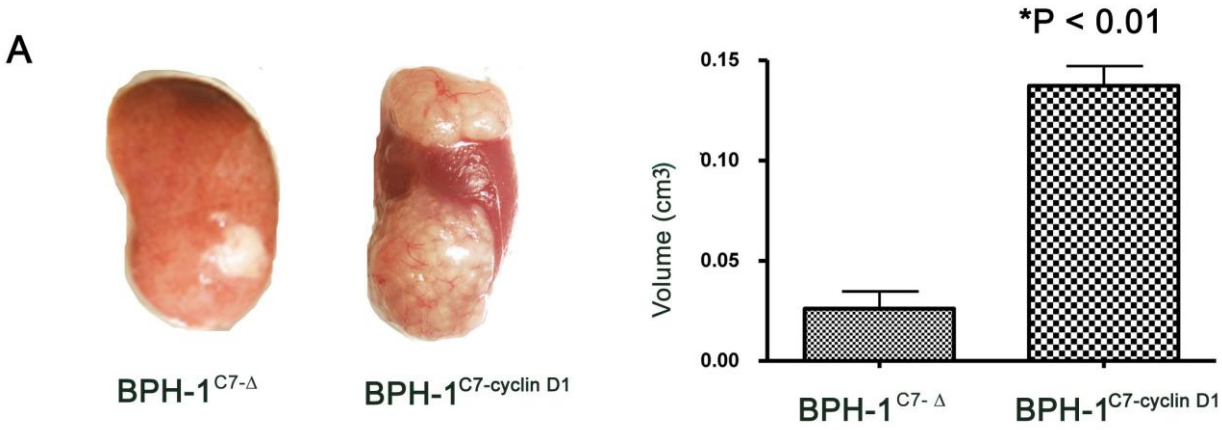

Figure 2-3. Overexpression of cyclin D1 in epithelium was insufficient to induce malignant transformation in BPH-1 cells as determined by *in vivo* assays.
(A) BPH-1$^{C7\text{-}cyclin\ D1}$ cells were not tumorigenic under the influence of the inductive rat UGM in the tissue recombination model. Gross morphology of 2 months grafts of BPH-1$^{C7\text{-}\Delta}$ + UGM (left) and BPH-1$^{C7\text{-}cyclin\ D1}$ + UGM (right). The volume of grafts containing BPH-1$^{C7\text{-}cyclin\ D1}$ was significantly larger than controls. Student's t-test, $P < 0.01$.

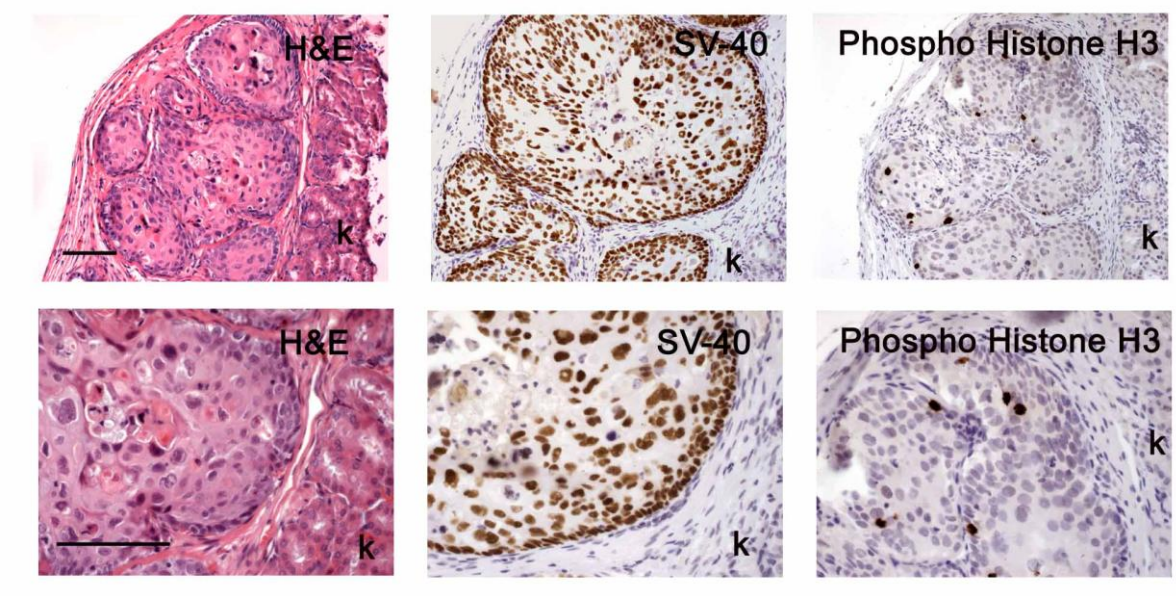

Figure 2-3 (B). H & E staining of BPH-$1^{C7-\Delta}$ + UGM grafts showed that the recombinants formed solid cord structures with no sign of invasion to the host kidney. SV40 T-antigen staining confirmed the cell origin of the epithelium. Phospho histone H_3 staining identified few positive cells in the solid cords. Higher magnification pictures were shown in bottom. Scale bar equals 50 µm.

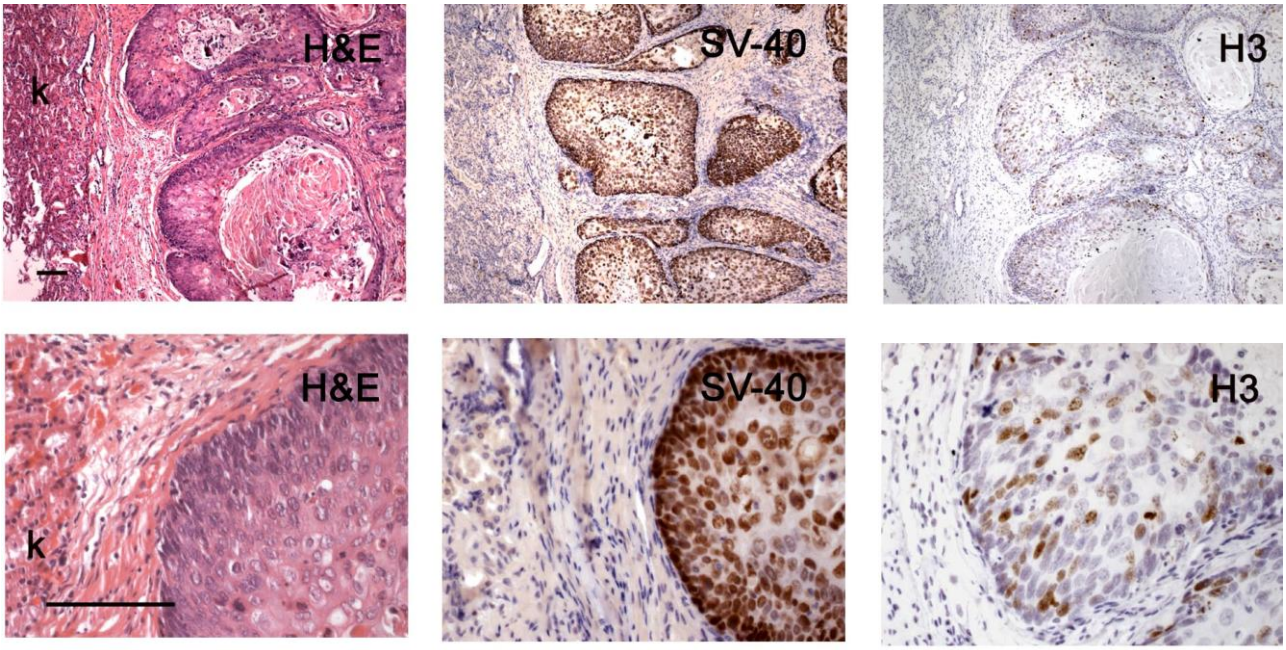

Figure 2-3(C). H & E and SV-40 T antigen staining of BPH-1$^{C7\text{-}cyclin\ D1}$ + UGM grafts. Histology is similar to that seen in the control groups. The basement membrane between kidney and graft was intact and there was no sign of invasion into the host kidney was seen. Phospho histone H_3 staining identified significantly more positive cells in the solid cords compared in B. Higher magnification pictures were shown in bottom. Scale bar equals 50 µm.

A

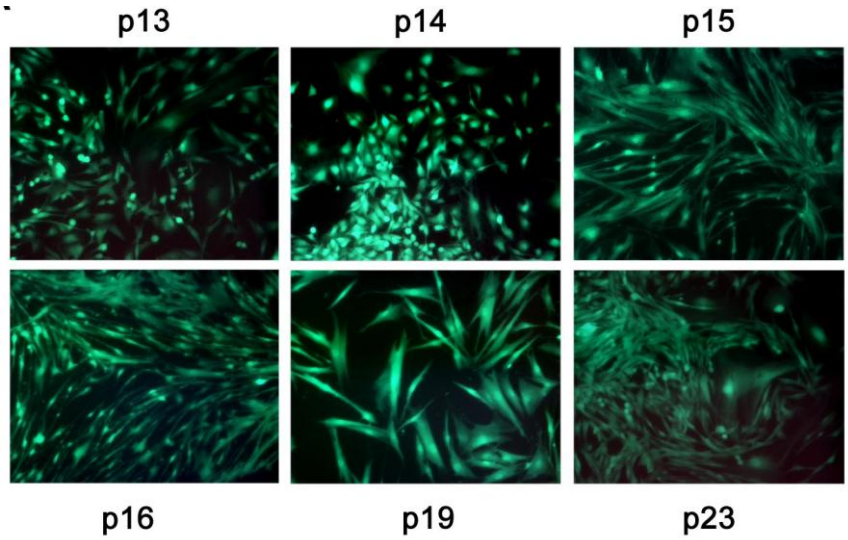

B

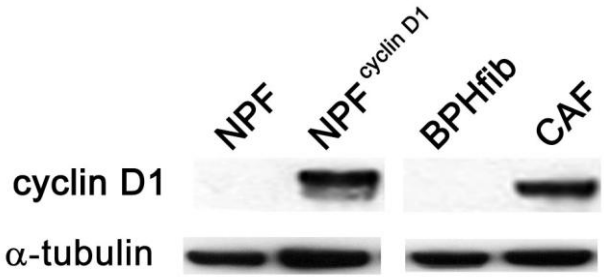

Figure 2-4. Expression of cyclin D1 in human prostatic fibroblasts. (A) $NPF^{cyclin\ D1}$ cells have increased life span compared with NPF cells. Control cells were all dead within 12 passages. The $NPF^{cyclin\ D1}$ cells appeared healthy after 23 passages (passage number shown adjacent to illustration) post-infection by C7-cyclin D1 overexpressing retroviral vector (total 23 passages). (B) Western blotting results confirmed cyclin D1 was overexpressed in $NPF^{cyclin\ D1}$ cells. Human prostatic carcinoma-associated fibroblasts (CAF) cells also expressed elevated levels of cyclin D1 protein as compared to NPF or to BPH-derived fibroblasts.

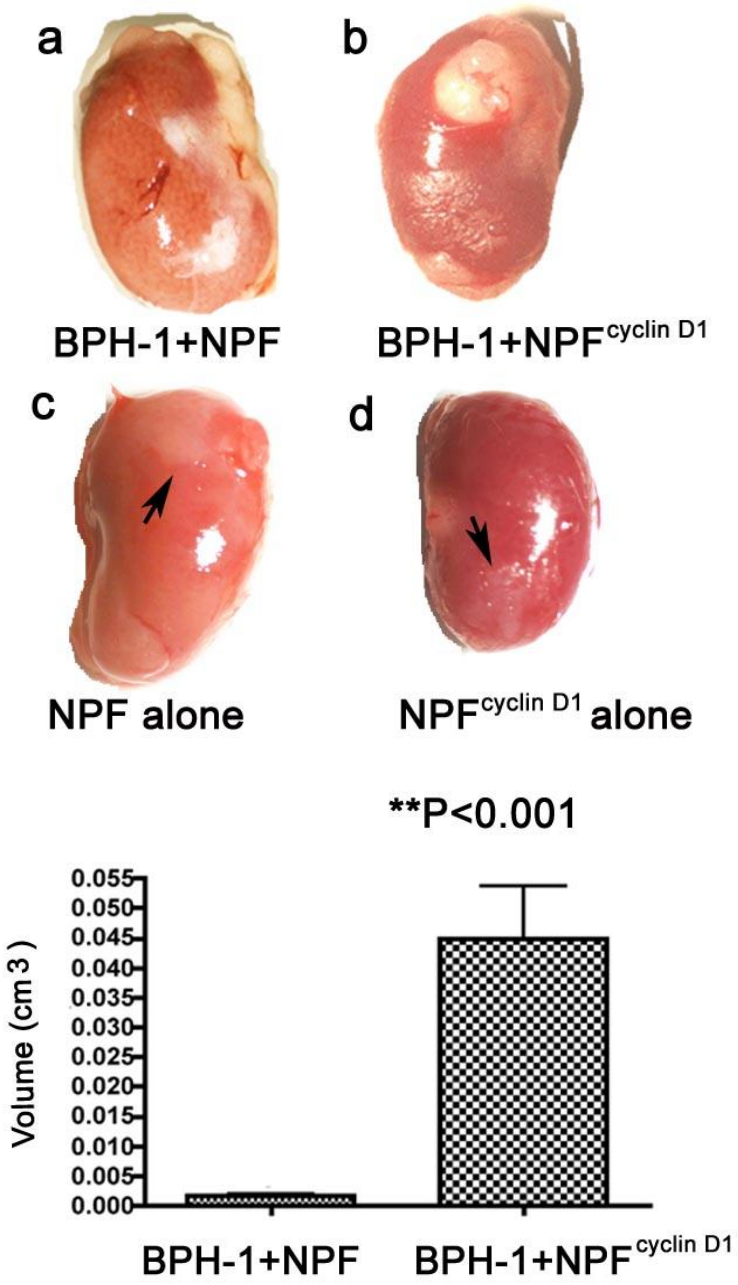

Figure 2-5. Effects of NPF$^{\text{cyclin D1}}$ cells on BPH-1 epithelium *in vivo*.(A) Gross morphology of one month grafts of tissue recombinants composed of BPH-1 + NPF(a), BPH-1 + NPF$^{\text{cyclin D1}}$ cells (b), NPF alone (c) and NPF$^{\text{cyclin D1}}$ alone (d). The graft volume of BPH-1 + NPF$^{\text{cyclin D1}}$ was significantly larger than that of BPH-1 + NPF. Student's t-test, P<0.001 (right).

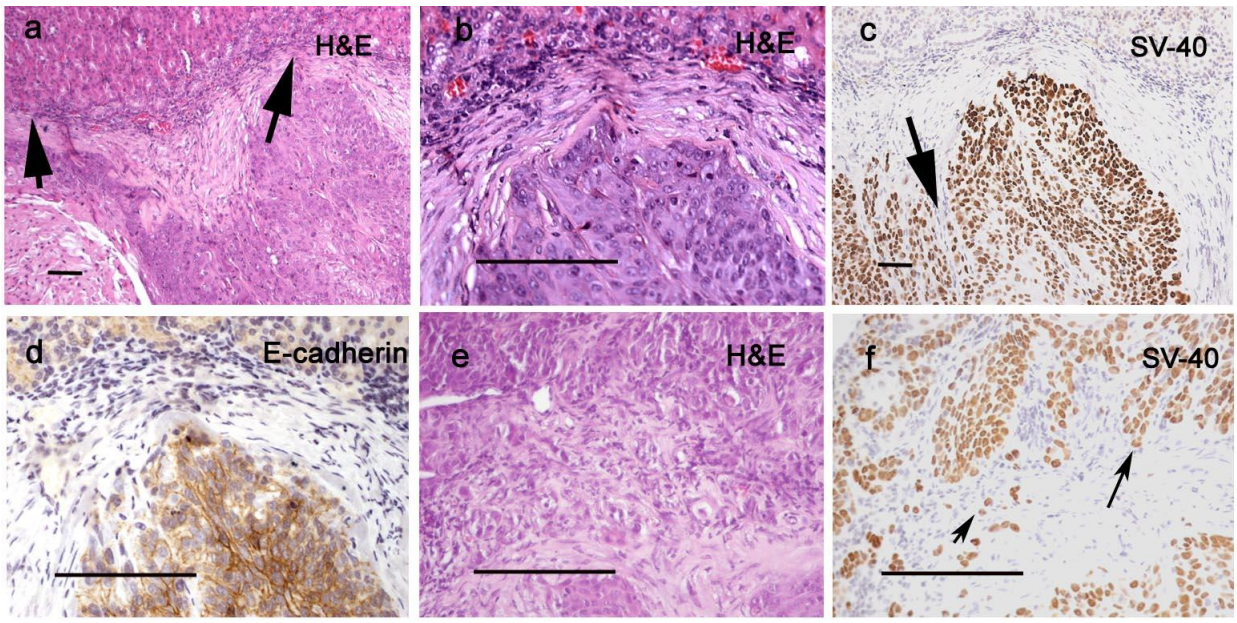

Figure 2-5 (B). Staining of BPH-1 + NPF$^{cyclin\ D1}$ recombinants revealed organization resembling a poorly differentiated carcinoma. Some epithelium fused to form large nests (a, b) with keratinization and a broad pushing margin to kidney (a, arrow). Tumors contained irregular epithelial cords and epithelial cells intermingled within a fibrous stroma (c, e and f-right arrow). Single epithelial cells were intermixed with fibrous stroma in other areas (c-arrow and f-left arrow). Immunohistochemical localization of SV-40 T antigen confirmed the origin of the tumors (c and f). E-cadherin staining was patchy (d).

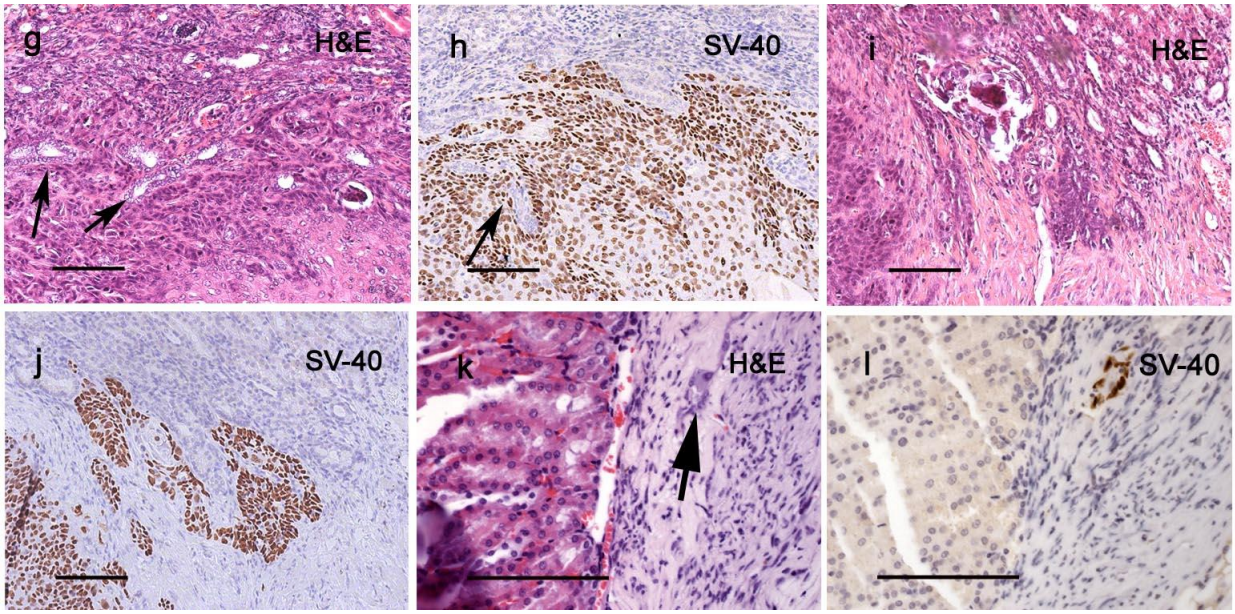

Figure 2-5 (C). After 5 months incubation in kidney capsule, BPH-1 cells formed larger tumors and invaded the host kidney (g, h, i, j). Tumor cells surrounded and intermingled with kidney tubes (Figure 4B, g and h-arrows). There were no clear margins between kidney and grafts. H & E staining of BPH-1 + NPF grafts revealed small grafts with minimal epithelial growth consistent with previous observations (k, arrow and l). Scale bar equals 50 µm.

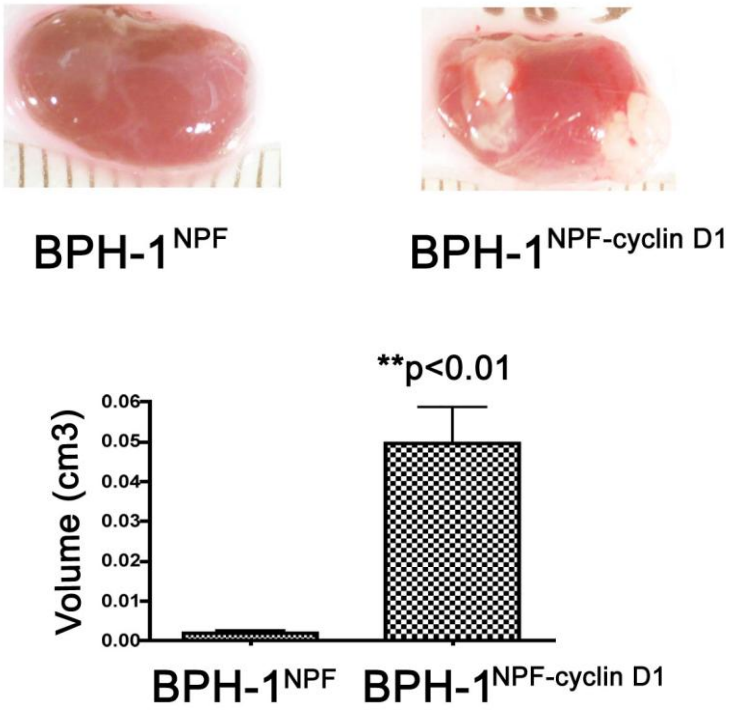

Figure 2-6. The BPH-1$^{NPF\text{-}cyclinD1}$ cells which were isolated from BPH-1 + NPF$^{cyclin\ D1}$ grafts exhibited a transformed phenotype. (A) Gross morphology of 3 months grafts of BPH-1^{NPF} (left) and BPH-1$^{NPF\text{-}cyclinD1}$ (right). The volume of the BPH-1$^{NPF\text{-}cyclinD1}$ grafts was significantly larger than the control grafts (Student's t-test, $P<0.01$).

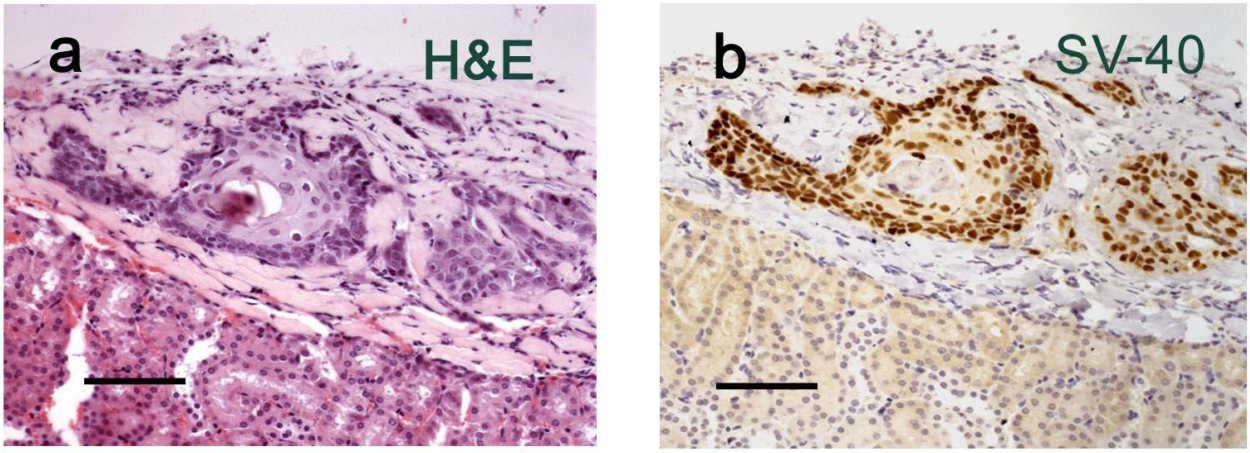

Figure 2-6 (B). In grafts of BPH-1^{NPF} cells, occasionally, epithelial cords were seen. (a) and their origin confirmed by SV-40 staining (b). No evidence of malignant growth or invasion was seen in these grafts. Scale bar equals 50 µm.

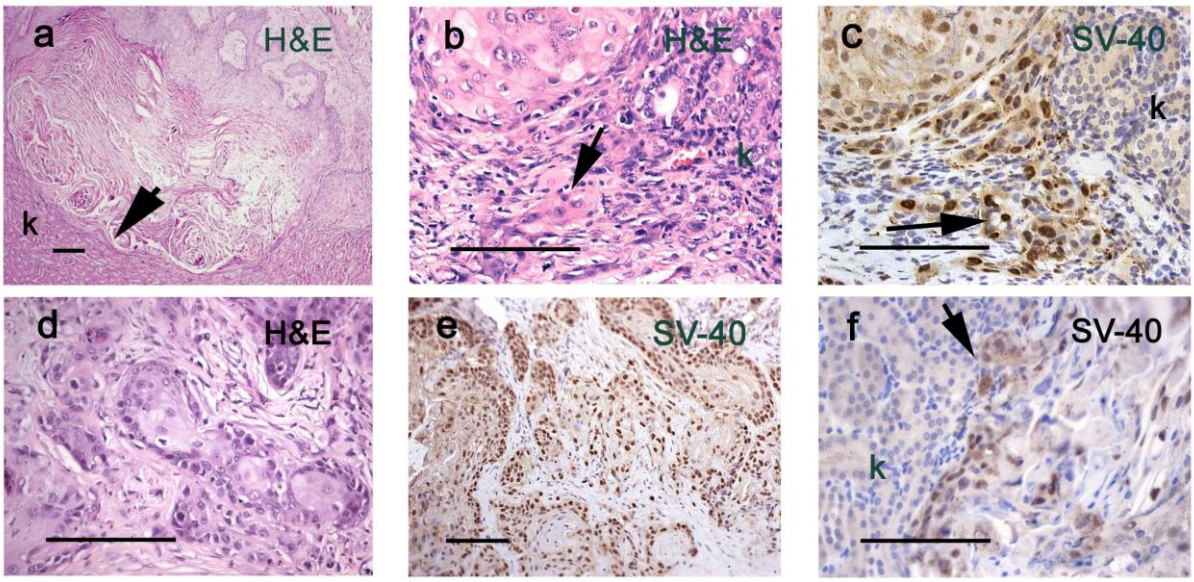

Figure 2-6 (C). BPH-1$^{\text{NPF-cyclin D1}}$ tumors were larger than controls with areas of keratinization. (a). The grafts formed a pushing margin directly touching the host kidney (a, arrow). Small nests of epithelial cells with irregular shapes intermingled with stroma (d and e). Some infiltrative areas (b-arrow) were found to be composed of bubbly cytoplasm and indistinct cells borders (c-arrow). Minimally invasive growth into the kidney was seen in a few areas. The invading cells expressed SV-40T antigen (f, arrow). Scale bar equals 50 µm. k = host kidney.

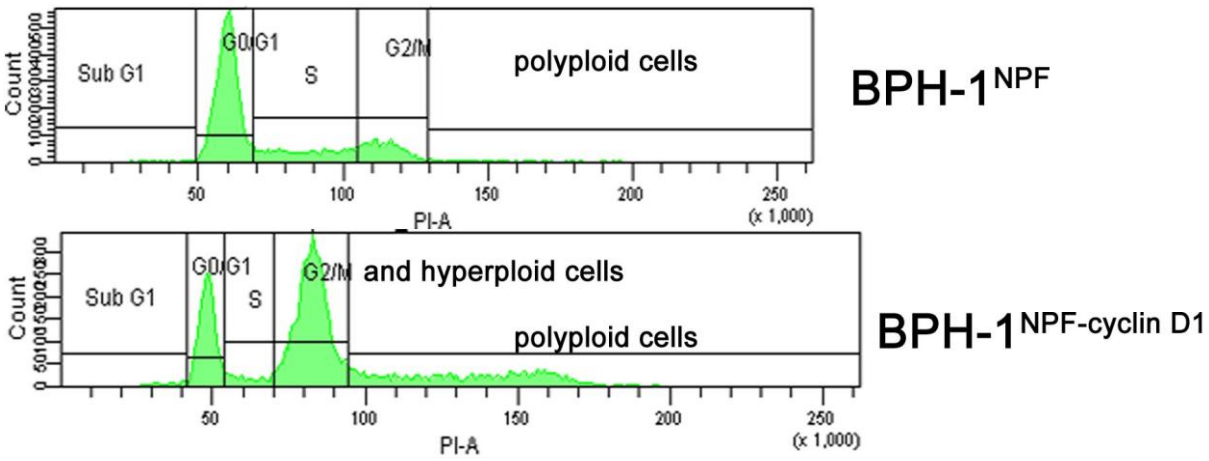

Figure 2-6 (D). FACS analysis demonstrated striking differences in cell population distribution between BPH-1^{NPF} and BPH-1$^{NPF\text{-}cyclin\ D1}$ cells. The majority (64%) of the BPH-1^{NPF} cells were in the G1/G0 phase of cell cycle. In contrast, in BPH-1$^{NPF\text{-}cyclin\ D1}$ cells an abnormal peak which contains 55% of the total cell population is located close to but somewhat below where the G2/M peak would be expected. Additionally, polyploid cells composed of 23.1% of the total population in the BPH-1$^{NPF\text{-}cyclin\ D1}$ cells.

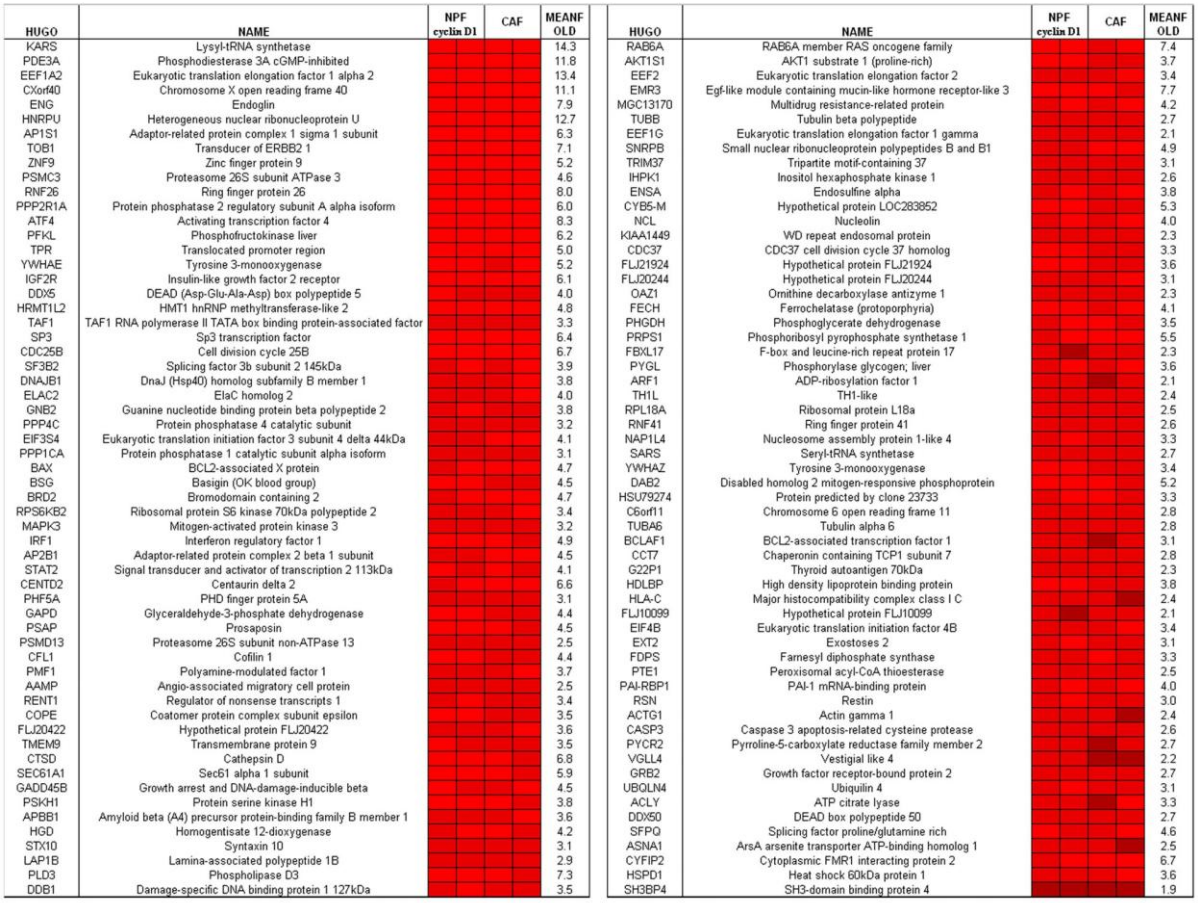

HUGO	NAME	NPF cyclin D1	CAF	MEANFOLD
KARS	Lysyl-tRNA synthetase			14.3
PDE3A	Phosphodiesterase 3A cGMP-inhibited			11.8
EEF1A2	Eukaryotic translation elongation factor 1 alpha 2			13.4
CXorf40	Chromosome X open reading frame 40			11.1
ENG	Endoglin			7.9
HNRPU	Heterogeneous nuclear ribonucleoprotein U			12.7
AP1S1	Adaptor-related protein complex 1 sigma 1 subunit			6.3
TOB1	Transducer of ERBB2 1			7.1
ZNF9	Zinc finger protein 9			5.2
PSMC3	Proteasome 26S subunit ATPase 3			4.6
RNF26	Ring finger protein 26			8.0
PPP2R1A	Protein phosphatase 2 regulatory subunit A alpha isoform			6.0
ATF4	Activating transcription factor 4			8.3
PFKL	Phosphofructokinase liver			6.2
TPR	Translocated promoter region			5.0
YWHAE	Tyrosine 3-monooxygenase			5.2
IGF2R	Insulin-like growth factor 2 receptor			6.1
DDX5	DEAD (Asp-Glu-Ala-Asp) box polypeptide 5			4.0
HRMT1L2	HMT1 hnRNP methyltransferase-like 2			4.8
TAF1	TAF1 RNA polymerase II TATA box binding protein-associated factor			3.3
SP3	Sp3 transcription factor			6.4
CDC25B	Cell division cycle 25B			6.7
SF3B2	Splicing factor 3b subunit 2 145kDa			3.9
DNAJB1	DnaJ (Hsp40) homolog subfamily B member 1			3.8
ELAC2	ElaC homolog 2			4.0
GNB2	Guanine nucleotide binding protein beta polypeptide 2			3.8
PPP4C	Protein phosphatase 4 catalytic subunit			3.2
EIF3S4	Eukaryotic translation initiation factor 3 subunit 4 delta 44kDa			4.1
PPP1CA	Protein phosphatase 1 catalytic subunit alpha isoform			3.1
BAX	BCL2-associated X protein			4.7
BSG	Basigin (OK blood group)			4.5
BRD2	Bromodomain containing 2			4.7
RPS6KB2	Ribosomal protein S6 kinase 70kDa polypeptide 2			3.4
MAPK3	Mitogen-activated protein kinase 3			3.2
IRF1	Interferon regulatory factor 1			4.9
AP2B1	Adaptor-related protein complex 2 beta 1 subunit			4.5
STAT2	Signal transducer and activator of transcription 2 113kDa			4.1
CENTD2	Centaurin delta 2			6.6
PHF5A	PHD finger protein 5A			3.1
GAPD	Glyceraldehyde-3-phosphate dehydrogenase			4.4
PSAP	Prosaposin			4.5
PSMD13	Proteasome 26S subunit non-ATPase 13			2.5
CFL1	Cofilin 1			4.4
PMF1	Polyamine-modulated factor 1			3.7
AAMP	Angio-associated migratory cell protein			2.5
RENT1	Regulator of nonsense transcripts 1			3.4
COPE	Coatomer protein complex subunit epsilon			3.5
FLJ20422	Hypothetical protein FLJ20422			3.6
TMEM9	Transmembrane protein 9			3.5
CTSD	Cathepsin D			6.8
SEC61A1	Sec61 alpha 1 subunit			5.9
GADD45B	Growth arrest and DNA-damage-inducible beta			4.5
PSKH1	Protein serine kinase H1			3.8
APBB1	Amyloid beta (A4) precursor protein-binding family B member 1			3.6
HGD	Homogentisate 12-dioxygenase			4.2
STX10	Syntaxin 10			3.1
LAP1B	Lamina-associated polypeptide 1B			2.9
PLD3	Phospholipase D3			7.3
DDB1	Damage-specific DNA binding protein 1 127kDa			3.5

HUGO	NAME	NPF cyclin D1	CAF	MEANFOLD
RAB6A	RAB6A member RAS oncogene family			7.4
AKT1S1	AKT1 substrate 1 (proline-rich)			3.7
EEF2	Eukaryotic translation elongation factor 2			3.4
EMR3	Egf-like module containing mucin-like hormone receptor-like 3			7.7
MGC13170	Multidrug resistance-related protein			4.2
TUBB	Tubulin beta polypeptide			2.7
EEF1G	Eukaryotic translation elongation factor 1 gamma			2.1
SNRPB	Small nuclear ribonucleoprotein polypeptides B and B1			4.9
TRIM37	Tripartite motif-containing 37			3.1
IHPK1	Inositol hexaphosphate kinase 1			2.6
ENSA	Endosulfine alpha			3.8
CYB5-M	Hypothetical protein LOC283852			5.3
NCL	Nucleolin			4.0
KIAA1449	WD repeat endosomal protein			2.3
CDC37	CDC37 cell division cycle 37 homolog			3.3
FLJ21924	Hypothetical protein FLJ21924			3.6
FLJ20244	Hypothetical protein FLJ20244			3.1
OAZ1	Ornithine decarboxylase antizyme 1			2.3
FECH	Ferrochelatase (protoporphyria)			4.1
PHGDH	Phosphoglycerate dehydrogenase			3.5
PRPS1	Phosphoribosyl pyrophosphate synthetase 1			5.5
FBXL17	F-box and leucine-rich repeat protein 17			2.3
PYGL	Phosphorylase glycogen; liver			3.6
ARF1	ADP-ribosylation factor 1			2.1
TH1L	TH1-like			2.4
RPL18A	Ribosomal protein L18a			2.5
RNF41	Ring finger protein 41			2.6
NAP1L4	Nucleosome assembly protein 1-like 4			3.3
SARS	Seryl-tRNA synthetase			2.7
YWHAZ	Tyrosine 3-monooxygenase			3.4
DAB2	Disabled homolog 2 mitogen-responsive phosphoprotein			5.2
HSU79274	Protein predicted by clone 23733			3.3
C6orf11	Chromosome 6 open reading frame 11			2.8
TUBA6	Tubulin alpha 6			2.8
BCLAF1	BCL2-associated transcription factor 1			3.1
CCT7	Chaperonin containing TCP1 subunit 7			2.8
G22P1	Thyroid autoantigen 70kDa			2.3
HDLBP	High density lipoprotein binding protein			3.8
HLA-C	Major histocompatibility complex class I C			2.4
FLJ10099	Hypothetical protein FLJ10099			2.1
EIF4B	Eukaryotic translation initiation factor 4B			3.4
EXT2	Exostoses 2			3.1
FDPS	Farnesyl diphosphate synthase			3.3
PTE1	Peroxisomal acyl-CoA thioesterase			2.5
PAI-RBP1	PAI-1 mRNA-binding protein			4.0
RSN	Restin			3.0
ACTG1	Actin gamma 1			2.4
CASP3	Caspase 3 apoptosis-related cysteine protease			2.6
PYCR2	Pyrroline-5-carboxylate reductase family member 2			2.7
VGLL4	Vestigial like 4			2.2
GRB2	Growth factor receptor-bound protein 2			2.7
UBQLN4	Ubiquilin 4			3.1
ACLY	ATP citrate lyase			3.3
DDX50	DEAD box polypeptide 50			2.7
SFPQ	Splicing factor proline/glutamine rich			4.6
ASNA1	ArsA arsenite transporter ATP-binding homolog 1			2.5
CYFIP2	Cytoplasmic FMR1 interacting protein 2			6.7
HSPD1	Heat shock 60kDa protein 1			3.6
SH3BP4	SH3-domain binding protein 4			1.9

Figure 2-7 (A). cDNA Microarray analysis identified similar gene expression profiles of the cyclin D1 overexpressing normal fibroblasts and CAFs compared with NPFs. Heat map colors reflect fold ratio values between each sample and NPF reference (see scale.) Results of a one-sample t-test comparing $NPF^{cyclin\ D1}$ cells and CAFs vs. normal fibroblasts. Shown are the 118 unique genes up-regulated in both $NPF^{cyclin\ D1}$ cells and CAFs compared to normal fibroblasts (q-value $\leq$ 0.1%.).

HUGO	NAME	NPF cyclin D1		CAF		MEANFOLD
KDR	Kinase insert domain receptor					-53.5
KRT7	Keratin 7					-15.8
BMP5	Bone morphogenetic protein 5					-4.5
PISD	Phosphatidylserine decarboxylase					-5.9
RHOB	Ras homolog gene family member B					-8.2
SLC27A2	Solute carrier family 27 member 2					-25.6
WISP2	WNT1 inducible signaling pathway protein 2					-7.6
BMP6	Bone morphogenetic protein 6					-10.2
CTGF	Connective tissue growth factor					-7.5
ADAMTS1	A disintegrin-like and metalloprotease with thrombospondin type 1 motif 1					-13.7
REL	V-rel reticuloendotheliosis viral oncogene homolog					-5.3
WFDC1	WAP four-disulfide core domain 1					-17.1
ITGAV	Integrin alpha V					-8.2
PPAP2A	Phosphatidic acid phosphatase type 2A					-8.6
ADAMTS8	A disintegrin-like and metalloprotease with thrombospondin type 1 motif 8					-7.2
MAOA	Monoamine oxidase A					-8.5
DKFZp762K222	Hypothetical protein DKFZp762K222					-5.8
AHCYL1	S-adenosylhomocysteine hydrolase-like 1					-3.0
TGFBR1	Transforming growth factor beta receptor I					-3.0
PRG1	Proteoglycan 1 secretory granule					-4.3
COL27A1	Collagen type XXVII alpha 1					-3.2
MCP	Membrane cofactor protein					-3.0
CMKOR1	Chemokine orphan receptor 1					-10.0
AK3	Adenylate kinase 3					-4.7
KIAA1272	KIAA1272 protein					-3.1
CRYAB	Crystallin alpha B					-11.6
C1GALT2	Core 1 UDP-galactose:N-acetylgalactosamine-alpha-R beta 13-galactosyltransferase 2					-5.4
ACTB	Actin beta					-2.9
ARHGEF5	Rho guanine nucleotide exchange factor 5					-5.2
PTGER2	Prostaglandin E receptor 2 53kDa					-3.0
CHSY1	Carbohydrate synthase 1					-3.9
WDFY1	WD repeat and FYVE domain containing 1					-2.9
IGFBP5	Insulin-like growth factor binding protein 5					-16.4
B4GALT4	UDP-Gal:betaGlcNAc beta 14- galactosyltransferase polypeptide 4					-6.5
PCSK1	Proprotein convertase subtilisin/kexin type 1					-4.8
MYLK	Myosin light polypeptide kinase					-7.1
GTF2IP1	General transcription factor II i pseudogene 1					-3.9
ARHGAP9	Rho GTPase activating protein 9					-2.1
ITGB1	Integrin beta 1					-2.1
FNDC3	Fibronectin type III domain containing 3					-3.0
CPNE3	Copine III					-2.0
CSNK1A1	Casein kinase 1 alpha 1					-3.8
DHRS9	Dehydrogenase/reductase member 9					-2.3
THBS4	Thrombospondin 4					-4.6
FLJ20160	FLJ20160 protein					-2.8
MKLN1	Muskelin 1 intracellular mediator containing kelch motifs					-2.0
PERP	PERP TP53 apoptosis effector					-3.3
MUC13	Mucin 13 epithelial transmembrane					-3.6
DMN	Desmuslin					-4.6
RBPMS	RNA binding protein with multiple splicing					-5.0
DUSP1	Dual specificity phosphatase 1					-3.3

Figure 2-7 (B). Shown are the 51 unique genes down-regulated in both NPF$^{\text{cyclin D1}}$ cells and CAFs compared to normal fibroblasts (q-value $\leq$ 0.1%.).

HUGO	NAME	NPF cyclin D1		CAF		MEANFOLD
SYNPO2	Synaptopodin 2					10.2
MAF	V-maf musculoaponeurotic fibrosarcoma oncogene homolog					23.0
PCSK7	Proprotein convertase subtilisin/kexin type 7					4.6
ACTA2	Actin alpha 2 smooth muscle aorta					6.4
TPD52	Tumor protein D52					12.9
RODH	3-hydroxysteroid epimerase					16.6
PTPN11	Protein tyrosine phosphatase non-receptor type 11					-2.6
PTGS2	Prostaglandin-endoperoxide synthase 2					-50.9
IL8	Interleukin 8					-171.4
EDG7	Endothelial differentiation lysophosphatidic acid G-protein-coupled receptor 7					-4.3
ACADVL	Acyl-Coenzyme A dehydrogenase very long chain					-3.4
IER3	Immediate early response 3					-8.6
IL1B	Interleukin 1 beta					-42.4
CDKN2B	Cyclin-dependent kinase inhibitor 2B					-4.2
VEGF	Vascular endothelial growth factor					-3.0
PLAUR	Plasminogen activator urokinase receptor					-6.1
ITGA2	Integrin alpha 2					-9.9
RAB27B	RAB27B member RAS oncogene family					-8.8
SLC26A6	Solute carrier family 26 member 6					-3.4
D2S448	Melanoma associated gene					-5.3
BDNF	Brain-derived neurotrophic factor					-5.9
C8orf1	Chromosome 8 open reading frame 1					-4.9
ABCC4	ATP-binding cassette sub-family C member 4					-4.3
NFKBIZ	Nuclear factor of kappa light polypeptide gene enhancer in B-cells inhibitor zeta					-4.7
AHR	Aryl hydrocarbon receptor					-6.9
SPON2	Spondin 2 extracellular matrix protein					-7.0

Figure 2-7 (C). Results of a two-sample t-test comparing $NPF^{cyclin\ D1}$ cells with CAFs. Shown are the six unique genes upregulated in CAFs and 20 unique genes down-regulated in CAFs compared to cyclin D1 overexpressing cells (q-value ≤ 10%.)

Discussion

The concept of stroma as a contributor to, and potentially as an initiator of, carcinogenesis have led to altered perceptions of the development and progression of epithelial malignancies. Histopathologic examination has shown clear differences in gene expression patterns between the reactive stroma of tumors and normal stroma, additionally these differences have clinical prognostic value (Ayala et al., 2003; Bosman et al., 1993; Tuxhorn et al., 2002). The importance of stromal-epithelial interactions in tumorigenesis has been demonstrated in many malignancies, including, carcinoma of the skin, colon, breast and prostate (De Cosse et al., 1973; Fukamachi et al., 1986; Singer et al., 1995; Wright et al., 1994). Stromal-epithelial interactions not only play an important role in normal development and adult growth quiescence of the prostate (Cunha et al., 2004) but changes in these interactions can promote a malignant progression of initiated epithelium and result in tumorigenesis (Grossfeld et al., 1998; Hayward et al., 1997; Mueller and Fusenig, 2004).

There are cases in which addition of a single dominant-acting oncogene is sufficient to transform a non-tumorigenic cell. For example, massive overexpression of c-myc converted normal prostatic epithelial cells to rapidly become an invasive prostate carcinoma cell (Williams et al., 2005), while lower levels of c-myc expression had similar but slower effects (Ellwood-Yen et al., 2003). Similarly loss of genes with tumor suppressor function can also contribute to malignancy (Wang et al., 2003). These observations emphasize the importance of genetic changes as key factors in malignancy.

Alterations in the microenvironment adjacent to the epithelial cells can drive non-tumorigenic cells to become malignant both *in vivo* and *in vitro* (Hayward et al., 2001; Maffini et al., 2004; Pierce, 1974). Stromal factors can also elicit reversion of a malignant teratocarcinoma to a benign phenotype despite of genetic changes within the epithelial cells (Hayashi and Cunha, 1991; Mintz, 1978). The growth and differentiation of epithelial cells from R3327 Dunning prostatic adenocarcinoma (DT) were modified when reassociated with normal stromal environment. The epithelial cells were induced to differentiate to tall columnar secretory epithelial cells and tumorigenesis was remarkably diminished (Hayashi and Cunha, 1991; Hayashi et al., 1990). Experiments in mice suggested that genetic inactivation of the stromal TGF-□ RII receptor resulted in the transformation of normal epithelial cells (Bhowmick et al., 2004b). Bissell's group demonstrated that by manipulating ECM proteins, human breast cancer cells reverted to normal functional cells in culture and tumorigenicity was reduced dramatically in mice (Weaver et al., 1997).

Cyclin D1 is an important oncogene in many human cancers, but its function in prostate cancer is not clear (Bubendorf et al., 1999; Gumbiner et al., 1999; Kallakury et al., 1997). We show here that cyclin D1 is upregulated in prostate cancer cell lines indicating that it might be associated with prostate tumorigenicity. Overexpression of cyclin D1 can increase tumorigenicity of LNCaP cell lines (Chen et al., 1998). We have observed that BPH-1 cells in which cyclin D1 was overexpressed did not become tumorigenic under the influence of inductive rUGM in the tissue recombination model when grafted to SCID

mice. However, the cyclin D1 overexpressing cells did have a higher proliferation rate *in vitro* and *in vivo* and motility *in vitro*. Such observations indicated that this single gene is not enough to transform BPH-1 cells even in the face of SV40 large T antigen, which is expressed in these cells. This underlines the important point that increased proliferation *per se* is insufficient for malignant transformation.

In marked contrast to the effects in epithelial cells, overexpression of cyclin D1 in primary cultures of benign human prostatic fibroblasts extended the lifespan and altered the behavior of the stromal cells, nonetheless falling short of directly inducing malignant transformation. Cyclin D1 induced these cells to behave in a manner similar to CAFs, imparting an ability to elicit malignant transformation in BPH-1 epithelial cells in a tissue recombination model. The cyclin D1 overexpressing fibroblasts have increased life span compared with NPFs. NPFs were all dead within 12 passages. However, the $NPF^{cyclin\ D1}$ cells appeared healthy after an additional 11 passages. NPFs overexpressing cyclin D1 may be selectively advantageous for the proliferation and survival characteristics often associated with oncogenesis compared with non-infected cells in the same mixture. However it should be noted that, as when expressed in epithelial cells, expression of cyclin D1 did not result in transformation of the stromal cell population. As a result of *in vitro* adaptation, cells may pick up generic alterations such as the mRNA changes we have seen in microarray data. However, $NPF^{cyclin\ D1}$ cells are not fully immortal and are not tumorigenic by themselves. This is consistent with observations that CAFs are also not immortal and not tumorigenic per se, but have the ability to transform adjacent BPH-1

cells.

By expressing cyclin D1 in stromal cells we demonstrated that benign stromal cell behavior can be modified to mimic that of cancer stromal cells. $NPF^{cyclin\ D1}$ cells have a potential to transform BPH-1 cells similar to that seen with CAFs although with a reduced intensity. Tissue architecture in recombinants showed irregular epithelial cords and epithelium infiltrating into the stroma. This observation indicated that the presence of altered stromal cells in proximity to an initiated epithelium has an important biological impact on prostatic carcinogenesis. Expression of this single oncogene in the stroma may mimic the effects of CAFs on epithelium by modifying the local microenvironment. Specifically altering the expression of growth factors and ECM proteinases results in expansion and malignant progression of the initiated epithelial cells.

BPH-1 cells form tumors after recombination with CAFs, and epithelial cells derived from these tumors ($BPH1^{CAFTD}$) are tumorigenic without the stimulation of stromal cells when re-grafted to mice (Hayward et al., 2001). The present study shows that the tumorigenic behavior of $BPH\text{-}1^{NPF\text{-}cyclin\ D1}$ cells (derived from recombination of BPH-1 + $NPF^{cyclin\ D1}$ cells) also resulted in a permanent malignant transformation of epithelial cells similar to that seen with CAF.

Cell cycle analyses of cells from malignant tissues have demonstrated the presence of aneuploid cells as well as normal diploid cells (Givan, 2001). In the present study, an

abnormal peak in cell cycle histogram of BPH-1$^{\text{NPF-cyclin D1}}$ likely represented hyperdiploid cells. Many of these cells had multiple nuclei. It has been shown that aneuploidy is the possible underlying mechanism and potential consequences in the pathogenesis of human lung cancer (Masuda and Takahashi, 2002). Clinical progression of prostate cancer is also associated with formation of DNA aneuploidy (Koivisto, 1997). These data suggested that BPH-1$^{\text{NPF-cyclin D1}}$ cells might be transformed through chromosomal changes (aneuploidy).

The histological appearance BPH-1$^{\text{NPF-cyclin D1}}$ tumors was consistent with poorly differentiated carcinoma. It is important to note that CAFs have elevated expression levels of cyclin D1 protein, and therefore many of their characteristics could be linked to the downstream consequences of this change. Microarray comparison of the NPF$^{\text{cyclin D1}}$ and CAFs vs. NPF showed highly concordant gene expression profiles. The same 118 unique genes were up-regulated and 51 unique genes were down-regulated in NPF$^{\text{cyclin D1}}$ cells and CAFs when compared with NPFs. Relatively few significant differences in transcript abundance measurements between NPF$^{\text{cyclin D1}}$ cells and CAFs were identified. These data indicate that cyclin D1 expression in stroma can critically affect paracrine interactions with adjacent epithelial cells in a manner resembling CAFs.

In summary, the present study in this chapter demonstrated for the first time the importance of cyclin D1 as a potential regulator of paracrine interactions in prostate cancer progression. The cyclin D1 overexpressing fibroblasts have an increased life span

and share many commonalities with CAFs making them a potentially useful research tool. Traditional therapy for all epithelial malignancies, including prostate cancer, has been targeted at the epithelial cells which progressively acquire genetic changes. The stroma may provide a more stable target at which to direct treatment, since the gene expression profile differs from that seen in normal tissues. We should also bear in mind that the tumor stromal compartment is heterogeneous and that CAFs are a mixed population of fibroblastic cells. Juxtacrine signaling between fibroblastic cells of different types may contribute to changes in overall paracrine signaling which boosts the growth of epithelial cells. Interactions with other stromal cell types including inflammatory cells or nerve cells also turn out to be of critical importance. A better understanding of these complex interactions within the stroma and between stroma and epithelium, and the manner in which these are influenced by gene expression in stromal cells will allow for the rational design of therapies aimed at inhibiting prostate tumor growth.

CHAPTER III

CATHEPSIN D ACTS AS AN ESSENTIAL MEDIATOR TO PROMOTE MALIGNANCY OF BENIGN PROSTATIC EPITHELIUM.

Introduction

Cathepsin D is a ubiquitous lysosomal aspartyl endoproteinase which is overexpressed and hypersecreted by human breast cancer cells (Rochefort, 1992). Overexpression of cathepsin D has been shown to increase the risk of breast cancer metastasis. (Ferrandina et al., 1997; Foekens et al., 1999; Rochefort, 1992). Cathepsin D was shown to stimulate cancer cell proliferation (Westley and May, 1999). Cathepsin D may be responsible for positive regulation of proliferation, motility, and/or invasion of cells by triggering activation of ras/MAPK/ERKs (Laurent-Matha et al., 2005). Immunohistochemical studies indicated that cathepsin D not only promoted cancer cell proliferation by an autocrine mechanism, but also tumor angiogenesis via a paracrine mechanism by staining with PCNA, whose expression is associated with proliferating cells in late G1 and S phase (Berchem et al., 2002). It is the first time that the potential paracrine action of cathepsin D was found in the context of a tumor.

Cathepsin D overexpression was shown to be important in epithelial growth, but also affects fibroblast behavior. Cathepsin D was required for fibroblast invasive growth using a three-dimensional (3D) coculture assay with breast cancer cells. Cathepsin D was found to be crucial for fibroblast invasive outgrowth and could act as a key paracrine communicator between breast cancer and stromal cells, independently of its catalytic

activity (Laurent-Matha et al., 2005). The mechanism of how cathepsin D involves in the paracrine signaling is still under investigation.

There are a few studies which examined the function of cathepsin D in prostate cancer progression. Some data demonstrated that a greater expression of mature cathepsin D with a higher catalytic activity in prostate cancer specimens is the most notable difference from normal specimens (Cherry et al., 1998). The normal glands were, in general, found to be negative for cathepsin D expression, but carcinoma samples have greater positive punctate lysosomal staining. Therefore, cathepsin D may prove to be a useful marker of prostate cancer progression (Makar et al., 1994). Endogenous cathepsin D can possibly modulate androgen receptor function in LNCaP cells and in prostate cancer specimens. Its activity appears to differ significantly between normal and malignant tissue. Cathepsin D may play a pivotal role as a growth modulator in androgen-dependent prostate cancer (Mordente et al., 1998). Some studies also indicated that cathepsin D, which is produced by reactive stromal cells but not the cancer cells, influence the prognosis of breast cancer (Tetu et al., 1999).

As the carcinoma evolves, phenotypic changes and alterations in gene expression in the adjacent stroma may enhance the invasive potential of the epithelial tumor (Cunha et al., 2002; Cunha et al., 2003). The microenvironment affects tumor formation, growth, invasiveness and metastasis. Stromal-epithelial interactions are mediated, in large part, by paracrine signaling between epithelial tumor cells and neighboring stromal fibroblasts (Ao

et al., 2007). In addition to receiving signals from epithelial cells, the stromal fibroblasts can also stimulate tumorigenesis by releasing factors which act on epithelial cells or exchange enzymes, growth factors and cytokines with epithelium to modify local extracellular matrix (ECM), stimulate migration and invasion, and promote proliferation and survival of tumor cells (Liotta and Kohn, 2001).

In tissue recombination model, it was shown that human prostatic CAFs are capable of stimulating carcinogenesis and inducing the progression of an initiated epithelium (BPH-1 cell line), while normal prostatic fibroblasts were incapable of stimulating such tumorigenesis (Olumi et al., 1999). The mechanistic basis by which stromal-epithelial interactions enhance the process of prostatic carcinogenesis and tumor invasion is beginning to be dissected and studied. TGF-β pathway is a crucial component in this interaction (Ao et al., 2007; Ao et al., 2006). Cyclin D1 was also shown to be a mediator of carcinogenesis. Our previous study in chapter II demonstrated that cyclin D1 overexpressing prostate fibroblasts ($NPF^{cyclin\ D1}$) transformed BPH-1 cells and drove BPH-1 cells to be invasive in a similar manner to CAFs. Cathepsin D expression was increased 7 fold in $NPF^{cyclin\ D1}$ cells and also in CAFs, indicating a possible role of cathepsin D as a paracrine mediator of cancer progression.

In the chapter, we highlight the possibility that cathepsin D may participate in paracrine signaling interactions between epithelial cancer cells and $NPF^{cyclin\ D1}$ cells or CAF cells. The expression of cathepsin D was examined in clinical samples and tissue recombinants.

The function of cathepsin D in NPF$^{cyclin\ D1}$ cells was examined in a 3D coculture assay. We then went on to study the effects of knocking down cathepsin D in CAFs to investigate the importance of cathepsin D in this paracrine signaling interaction.

Methods

Cells

BPH-1 (a non-tumorigenic human prostatic epithelial cell), NPF and CAF cells were from our own stocks (Hayward et al., 2001). BPHfib and CAF cells were isolated from human prostate samples. $NPF^{cyclin\ D1}$ cells was generated as discribed in chapter II (He et al., 2007). Cells were maintained in RPMI 1640 (Gibco, Carlsbad, CA) with 1% antibiotic/antimycotic (Life Technologies, Grand Island, NY) and 5% Cosmic Calf Serum (CCS-HyClone, Logan, Utah).

Generating genetically modified cell lines

The pSuper.Retro-control (PSR- OligoEngine, Seattle, WA) and pSuper.Retro-cyclin D1 shRNA (PSR-cyclinD1sh-kindly provided by Dr. Rene Bernards and Dr. Daniel Peeper from the Netherlands Cancer Institute) were transduced into CAFs by retroviral infection as described previously (Williams et al., 2005). The successfully infected cells were selected using puromycin (5ug/ml) to generate two cell lines (CAF^{PSR} and $CAF^{PSR\text{-}cyclin\ D1sh}$). The pSilencer 2.1-cathepsin D1 shRNA vector was kindly provided by Dr. Daniel E. Johnson from the University of Pittsburgh Cancer Institute. We cut both pSilencer 2.1-cathepsin D1shRNA and pSuper.Retro plasmids with HindIII and BamH1, and inserted the cathepsin D shRNA sequence to pSuper.Retro vector to generate the retroviral cathepsin D knockdown vector which is designated as PSR-cathepsinDsh. The PSR and PSR-cathepsinDsh were transduced into CAFs by retroviral infection as described previously (Williams et al., 2005). The successfully infected cells were selected

using puromycin (5μg/ml) to generate two cell lines (CAF^{PSR} and $CAF^{PSR\text{-}cathepsinDsh}$). PSR and PSR-cathepsinDsh vector was retrovirally infected to $NPF^{cyclin\ D1}$ cells to generate $NPF^{cyclin\ D1\text{-}\ control}$ and $NPF^{cyclin\ D1\text{-}cathepsin\ Dsh}$ respectively.

Western blotting analysis

Cells were grown in T75 cell culture flasks at 37^{o}C until they were confluent. After washing with PBS three times, 300 μl cold lysis buffer (10 mM HEPES pH 7.9; 10mM KCl: 0.1mM EDTA; 0.1mM EGTA; 0.1mM DTT; 1 protease complete tablet (Roche, Indianapolis, IN)) were added to each flask. The cells were cooled on ice for 30 minutes with lysis buffer, and then were scraped from flasks. Cell lysates were sonicated 5 times (10 second/time) and centrifuged for 20 minutes at 4°C. Protein concentrations were measured for western blotting. Twenty μg protein was loaded and electrophoresed through 10% NuPAGE BisTris gel (Invitrogen, Carlsbad, CA) and electrophoretically transferred to nitrocellulose membranes. Membranes were blocked with PBS-Tween20 with 5% non fat milk and incubated with mouse primary antibody to PTEN (1:1000, Santa Cruz Biotechnology, Santa Cruz, CA), Cdk2 (1:1000, Santa Cruz), Cdk4 (1:1000, Santa Cruz), Cdk6 (1:1000, Santa Cruz), cyclin E (1:1000, Santa Cruz), cyclin D1 (1:1000, BD Biosciences Pharmingen, San Jose, CA) ,□β-actin (1:5000, Sigma) or cathepsin D (1:1000, Cell Signaling, Denvers, MA) overnight and washed with PBS-Tween 20 for 1 hour, and incubated with horseradish-Peroxidase linked anti-mouse secondary antibody (Amersham Biosciences, Piscataway, NJ, 1:1,000 dilution) for 1 hour. Bound antibodies

were visualized using enhanced chemiluminescence western blotting detection reagents (Amersham Bioscences).

Tissue recombination and xenografting

BPH + CAF^{PSR}, BPH-1+ $CAF^{PSR\text{-}cyclinD1sh}$, BPH-1 + $CAF^{PSR\text{-}cathepsin\ Dsh}$ tissue recombinants were made as described in chapter II (Williams et al., 2005). 100k epithelial cells and 600k stromal cells were recombined to make the resultant recombinants. All the experiments were repeated 6 times. Mice were sacrificed after 6 weeks and grafts were harvested, fixed, and paraffin embedded.

Wound healing assays

Confluent monolayers of NPF, $NPF^{cyclin\ D1}$, $NPF^{cyclin\ D1\text{-}cathepsinD\ control}$ and $NPF^{cathepsin\ Dsh}$ cells were grown in 6 well plates. Wound healing assays were performed as described in chapter II. Wounds were imaged at 0, 3, 6, and 8 hours post wounding and the cell migration rate into the wound was calculated. Experiments were performed in triplicate.

Outgrowth assay

100k NPF, $NPF^{cyclin\ D1}$, $NPF^{cyclin\ D1\text{-}cathepsinD\ control}$ or $NPF^{cyclin\ D1\text{-}cathepsin\ Dsh}$ were resuspended at 4°C in Matrigel (0.2 ml, 10 mg/ml; Becton and Dickinson), and quickly added to a preset layer of Matrigel in 24-well plates as described previously (Garcia et al., 1990). The top Matrigel layer was solidified at 37°C for 30 minutes and covered with

culture medium containing 10% FCS (0.5 ml). Cells outgrowth from the Matrigel was monitored under microscope after 14 days.

Conditioned Medium

NPF, $NPF^{cyclin\ D1}$, $NPF^{cyclin\ D1-\ control}$ or $NPF^{cyclin\ D1\text{-}cathepsin\ Dsh}$ cells were seeded with 5% FCS in RPMI 1640 at a density of 500k per 75-cm^2 flask, allowed to grow, and attached overnight. Confluent cultures of cells were rinsed twice in PBS and incubated for 3 days in RPMI + 0.5% FCS. The medium was collected, centrifuged, passed through a 0.45-μm filter (Millipore), and stored at –80°C for later use. Conditioned medium was thawed and diluted 1:1 with fresh DMEM + 0.5% FCS before use. BPH-1 cells were seeded at 20k per well in six-well plates in conditioned medium. The cultures were incubated for 3 days and the total number of BPH-1 cells was determined by direct counting in a hemacytometer.

Immunofluorescence staining

Cells were plated on glass (Superfrost) slides and allowed to attach and grow overnight. After fixation in methanol for 5 minutes at –20°C, samples were washed twice in PBS, blocked for 30 minutes with 5% goat serum (Vector Laboratories, Burlingame, CA), and incubated at room temperature for 1 hour with primary antibodies against α-actin (1:500, Sigma), γ-actin (1:500, Sigma), vimentin (1:100; Sigma,) and wide spectrum keratin (1:100; DAKO, Carpinteria, CA) followed by washing for 30 minutes in PBS. Staining was visualized using fluorescence-conjugated secondary anti-rabbit IgG (whole

molecule) TRITC Conjugate (Sigma) or anti-mouse IgG (whole molecule) FITC Conjugate (Sigma). Slides were visualized and imaged using a Zeiss upright microscope with an attached Axiocam camera and proprietary software.

Immunohistochemical staining

Immunohistochemical staining was performed as previously described in chapter II. Tissue slides were then incubated with the primary antibody against cathepsin D (1:1000, Cell Signaling), Vimentin (1:500, Sigma) overnight. The polyclonal rabbit or mouse immunoglobulins/biotinylated anti-mouse secondary antibody (DAKO, Carpentiria, CA) was incubated for 60 minutes after the slides were washed with PBS buffer for 1 hour. After washing the slides in PBS extensively, slides were incubated in ABC-HRP complex (Vector Laboratories) for 30 minutes. Bound antibodies were then visualized by incubation with 3,3' diaminobenzidine tetrahydrochloride (liquid DAB, DAKO). Slides were then rinsed extensively in tap water, counterstained with hematoxylin, and mounted.

Results

Characterization of cyclin D1 overexpressing fibroblast cells

Expression of epithelial and stromal markers was examined by immunofluorescence in cultured fibroblasts to monitor the phenotypic characteristics. Three markers of stromal differentiation (α-actin, γ-actin and vimentin) were examined in NPF, $NPF^{cyclinD1}$, BPHfib and CAF cells. Keratin staining (wide spectrum) was be used to confirm lack of epithelial contamination. It was found that all the cells maintain fibroblastic or myofibroblastic characteristics with high expression of vimentin, and moderate expression of α-actin and γ- actin (Figure 3-1). Keratin expression was negative in all four cell lines which indicated that they are all fibroblasts without epithelial cell contamination.

Cathepsin D increased the motile ability of $NPF^{cyclin\ D1}$cells

Chapter II showed that $NPF^{cyclin\ D1}$ cells can elicit permanent malignant transformation in initiated but non-tumorigenic BPH-1 cells, similar to the malignant changes which have been described in BPH-1 + CAF tissue recombinants. In order to investigate the underlying mechanism of this malignant transformation, we at first compared the effect of cyclin D1 overexpression on the migration of NPFs. It was shown that $NPF^{cyclin\ D1}$ cells were found to have enhanced motile ability in wound healing assay compared with control NPFs (Figure 3-2, A). This difference was clear after 3 hours and was very marked after 8 hours (Student's t-test, $P<0.01$). However, when cathepsin D was knocked down by retroviral infection in $NPF^{cyclin\ D1}$ cells, the motile ability was reduced in $NPF^{cyclin\ D1\text{-}cathepsin\ Dsh}$ cells.

The observation suggested that cathepsin D may be an essential mediator of NPF$^{cyclin\ D1}$ migration *in vitro*.

Cathepsin D is important for 3D outgrowth of NPF$^{cyclin\ D1}$ fibroblasts

We next studied if cathepsin D is important for NPF$^{cyclin\ D1}$ fibroblast outgrowth in 3D matrices. As shown in Figure 3B, overexpression of cyclin D1 promoted outgrowth of normal prostatic fibroblasts embedded into Matrigel. After 14 days of culture, NPF$^{cyclin\ D1}$ cells had adopted a stellate morphology of growing and invasive colonies with protrusions sprouting into the surrounding matrix (Figure 3-2, B). In contrast, normal prostatic fibroblasts presented a well-delineated spherical appearance of quiescent cells and grew poorly, neither invading nor forming protrusions to the surrounding matrix (Figure 3-2, B). We then went on to examine if cathepsin D is important for NPF$^{cyclin\ D1}$ outgrowth from matrigel. Cathepsin D was knocked down in NPF$^{cyclin\ D1}$ cells by retroviral infection. It was found that the invasive outgrowth of NPF$^{cyclin\ D1}$ was reversed by knocking down cathepsin D those cells (Figure 3-2, B). Neither invasion nor protrusion formation into the surrounding matrix was found in NPF$^{cyclin\ D1\text{-}cathepsin\ Dsh}$ cells. But the NPF$^{cyclin\ D1\text{-}control}$ cells maintained the invasive growth feature. These data indicated that cathepsin D is an essential factor of promoting NPF$^{cyclin\ D1}$ cells invasion *in vitro.* Inhibition of cathepsin D leads to a decreased in fibroblast invasive growth. These data indicated that cathepsin D might also be an potential paracrine factor in stromal-epithelial interaction *in vivo*.

Evaluation of cathepsin D as a paracrine mediator of neoplastic epithelial cell growth *in vitro*

The identification of cyclin D1 induced expression of transcripts encoding cathepsin D with the potential to influence epithelial proliferation *in vitro* prompted experiments designed to determine whether conditional medium from NPF$^{\text{cyclin D1}}$ fibroblasts could stimulate the growth of immortalized prostate epithelial cells (BPH-1). To determine whether the influence of NPF$^{\text{cyclin D1}}$ on epithelial growth resulted from secretary factors. We generated conditioned medium from NPF and NPF$^{\text{cyclin D1}}$ cells, and measured BPH-1 cell numbers after growth for 3 days in the different conditioned media. The proliferation of BPH-1 cells was stimulated 1.7-fold (P<0.01) with medium from NPF$^{\text{cyclin D1}}$, when compared with medium from with NPF (Figure 3-2, C). Cathepsin D expression in NPF$^{\text{cyclin D1}}$ conditional medium was also upregulated compared with NPF conditional medium (Figure 3-2, D). These results suggest that a significant component of NPF$^{\text{cyclin D1}}$ proliferative influence toward epithelium is mediated through secreted cathepsin D.

Evaluation of cathepsin D as a paracrine mediator of neoplastic epithelial cell growth in tissue recombinants *in vivo*

To examine whether CAF or NPF$^{\text{cyclin D1}}$ induces cathepsin D expression *in vivo* and also to examine if cathepsin D expression in tissue recombinants correlates what we have seen in clinical samples, we checked cathepsin D expression in BPH-1 + NPF, BPH-1 + NPF$^{\text{cyclin D1}}$, BPH-1 + rUGM and BPH-1+CAF tissue recombinants. Among these recombinants, CAF and NPF$^{\text{cyclin D1}}$ can drive non-tumorigenic BPH-1 cells to undergo malignant

transformation (Hayward et al., 2001; He et al., 2007). BPH-1 + NPF, and BPH-1 + UGM formed benign structures and none of the epithelial cells were transformed. Immunohistochemical staining revealed minimal expression of cathepsin D in BPH-1 + NPF and BPH-1 + UGM recombinants. In marked contrast, cathepsin D expression in was elevated in BPH-1 + $NPF^{cyclin\ D1}$ and BPH-1 + CAF recombinants (Figure 3-3, A). This observations are consistent with what we have seen in clinical samples. This result indicated that upregulation of cathepsin D might be involved in the interaction that between $NPF^{cyclin\ D1}$ or CAFs and non-tumorigenic BPH-1 cells. However, this correlation did not address the question whether the upregulation is an effect of tumorigenicity or is a required paracrine signaling event for epithelial transformation *in vivo*.

BPH-$1^{NPF\text{-}cyclin\ D1}$ cells had increased cathepsin D and CDK2, but not CDK4/6 expression

In order to understand the mechanism by which stromal cyclin D1 or CAFs affects the prostate cancer cellular processes through paracrine signaling, western blotting assays were performed on BPH-1^{NPF}, BPH-1^{CAFTD1} and BPH-$1^{NPF\text{-}cyclin\ D1}$ cells (the epithelial cells isolated from BPH-1 + $NPF^{cyclin\ D1}$ tumors) to examine expression levels of several genes which are involved in cell cycle regulation. Our results showed that overexpression of cyclin D1 in the stroma increased CDK2 and cyclin E protein expression in the adjacent epithelium (Figure 3-3, B). No change was seen in CDK4 and CDK6 protein levels. These data indicated that the tumorigenic response of BPH-1 to either CAFs or $NPF^{cyclin\ D1}$ cells resulted in an increased expression of cyclinE/cdk2, but not cyclin D1/cdk4/cdk6 in the

permanent transformed epithelium. These data were consistent with our previous finding that cyclin D1 upregulation in epithelium might not be essential for tumorigenicity (He et al., 2007). Cathepsin D protein expression level was upregulated in BPH-1^{CAFTD1} and BPH-1$^{NPF\text{-}cyclin\ D1}$ cells compared with control BPH-1^{NPF} cells. This observation suggested that NPF$^{cyclin\ D1}$ secreted cathepsin D which could affect adjacent BPH-1 cells. The stromal fibroblasts stimulated epithelial tumorigenesis by releasing cathepsin D which acts on epithelial cells to stimulate proliferation and invasion.

Cyclin D1 and cathepsin D are both required for CAF induced tumorigenicity *in vivo*

To examine the function of cyclin D1 and cathepsin D in CAF-induced tumorigenicity in BPH-1 transformation, we used retroviral transfection of shRNA vectors to knock down either cyclin D1 or cathepsin D expression in CAF cells. Western blotting indicated there were approximately 50% knockdown of cyclin D1 and 95% cathepsin D protein expression respectively (Figure 3-4, C). It was found that BPH-1 + CAF^{cyclinD1sh} and BPH-1 + CAF$^{cathepsin\ Dsh}$ recombinants formed significantly smaller grafts compared with BPH-1+ CAF grafts (Figure 3-4, A). Histologically, BPH-1 + CAF recombinants formed adenosquamous carcinoma as previously described. Knockdown of either cyclin D1 or cathepsin D recombinants formed small, benign cords with no tumorigenic response (Figure 3-4, B). Similarly, after cathepsin D is knocked down in NPF$^{cyclin\ D1}$ cells, their ability to transform BPH-1 cells was reduced (data not shown). Interestingly, cathepsin D expression in CAF^{cyclinD1sh} cells was downregulated and cyclin D1 expression in CAF$^{cathepsin\ D}$ cells was also downregulated suggesting some form of co-regulation of these

proteins (Figure 3-4, C).

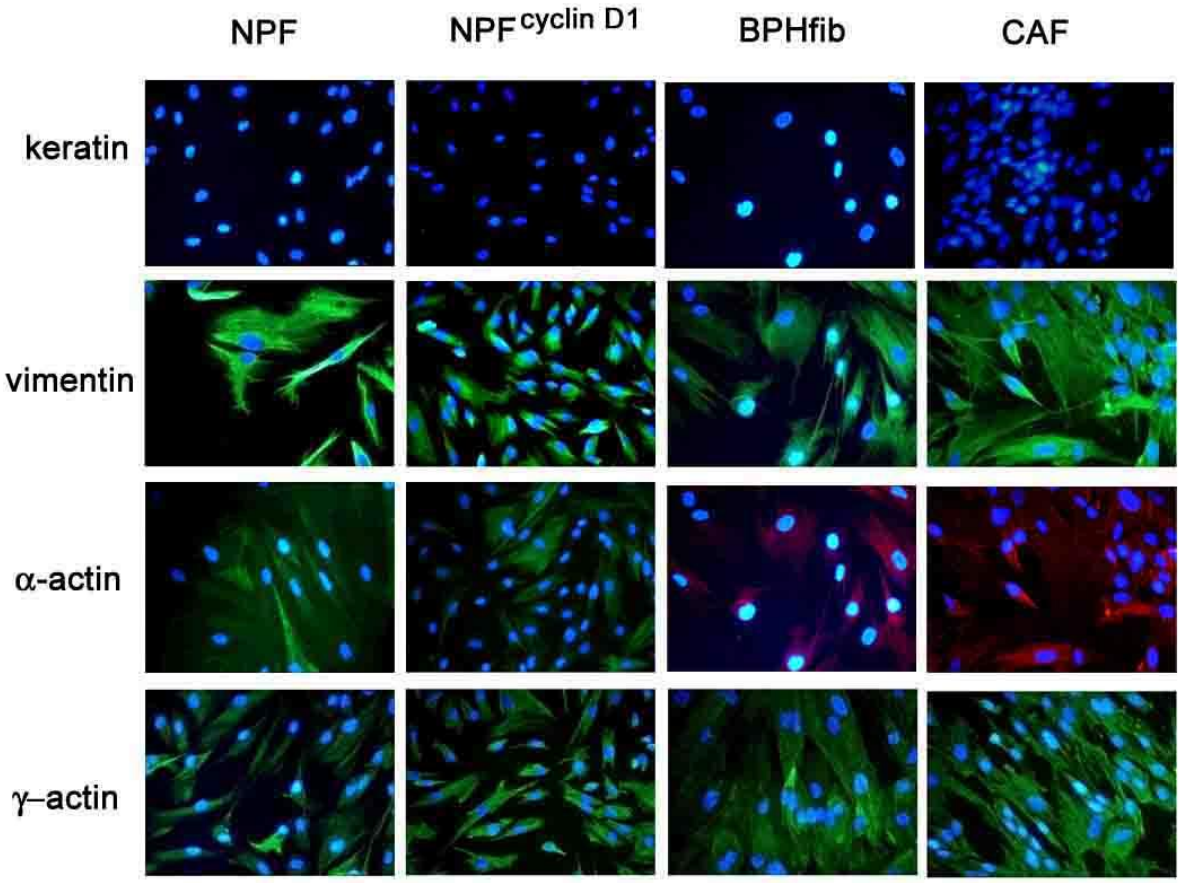

Figure 3-1. Characterization of cyclin D1 overexpressing fibroblasts. Three markers of stromal differentiation (α-actin, γ-actin and vimentin) were examined in NPF, $NPF^{cyclinD1}$, BPHfib and CAF cells. Keratin staining was be used to confirm lack of epithelial contamination. All the cells maintain fibroblastic characteristic with high expression of vimentin, and moderate expression of α-actin and γ-actin. Keratin expression was negative in all four cell lines.

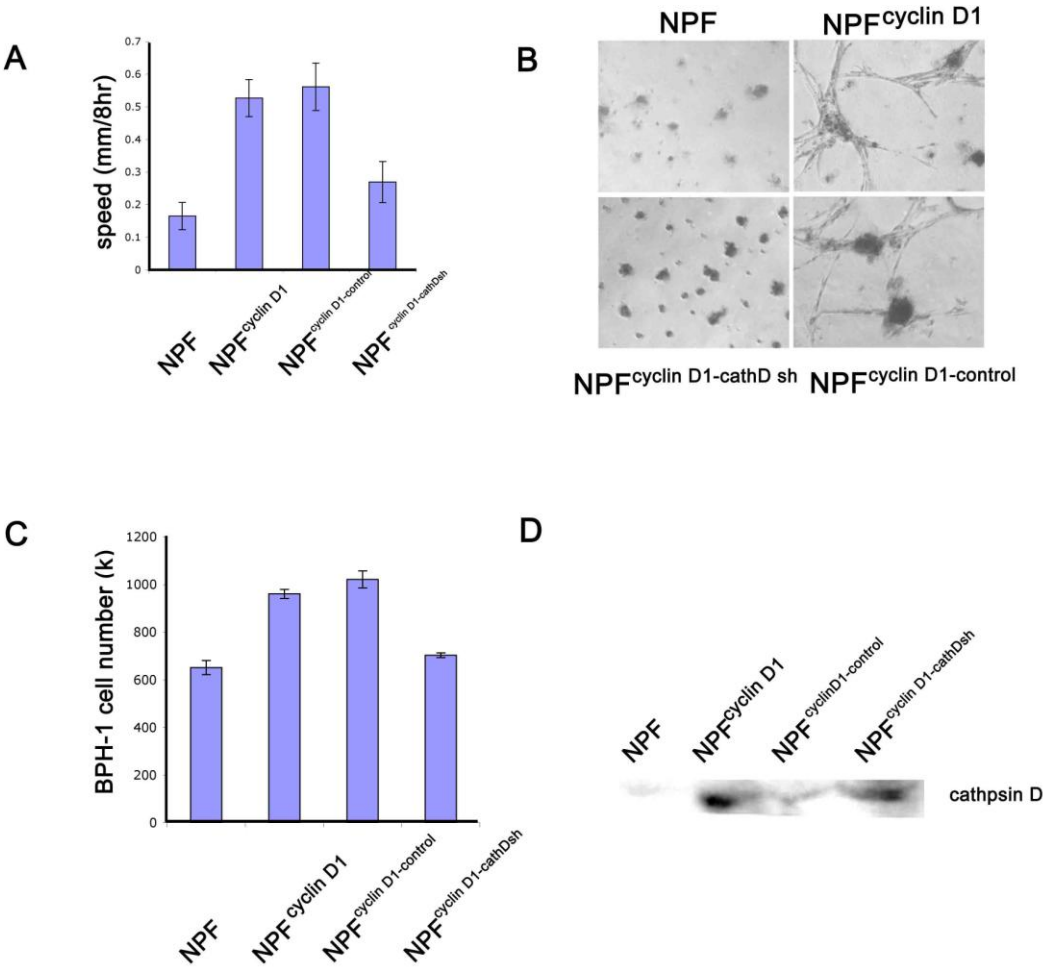

Figure 3-2. Cathepsin D is a critical mediator between BPH-1 cells and NPF$^{\text{cyclin D1}}$ *in vitro*. (A) NPF$^{\text{cyclin D1}}$ cells had enhanced motile ability in wound healing assay compared with control NPFs. The motile ability was reduced in NPF$^{\text{cyclin D1-cathepsin Dsh}}$ cells. (B) Cathepsin D is important on 3D outgrowth of NPF$^{\text{cyclin D1}}$ fibroblasts. Overexpression of cyclin D1 promoted outgrowth of normal prostatic fibroblasts embedded into Matrigel after 14 days of culture. The invasive outgrowth of NPF$^{\text{cyclin D1}}$ was reversed by knocking down cathepsin D those cells. (C) Evaluation of cathepsin D as a paracrine mediator of neoplastic epithelial cell growth *in vitro*. (D) Cathepsin D expression in NPF$^{\text{cyclin D1}}$ conditional medium was also upregulated compared with NPF conditional medium

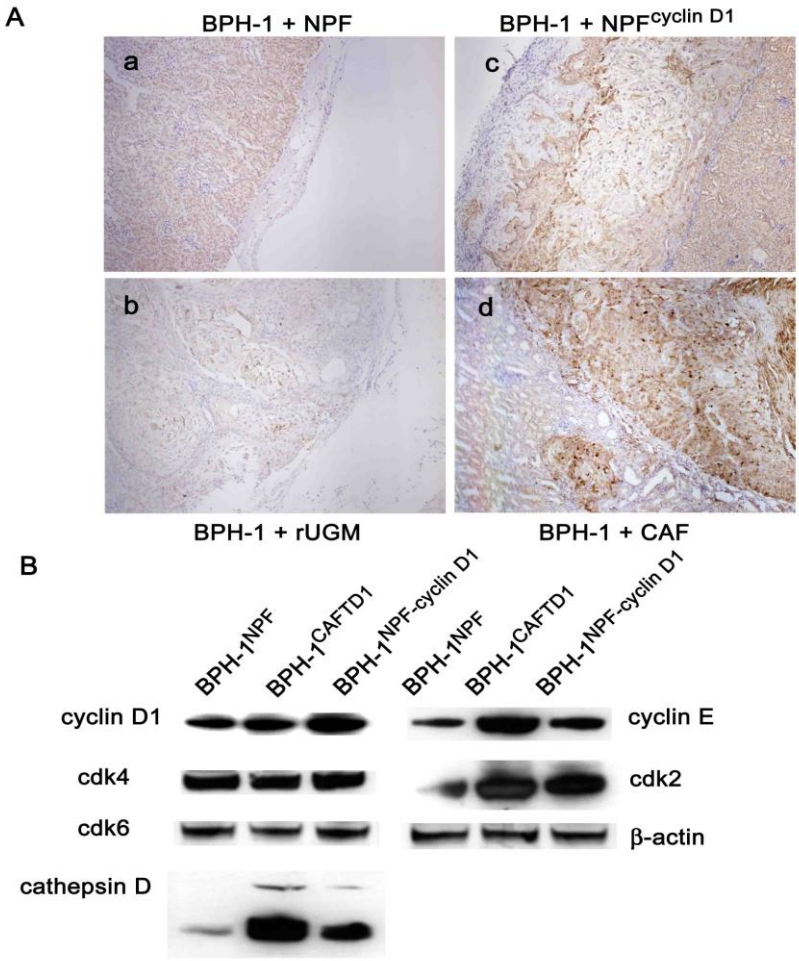

Figure 3-3. Evaluation of cathepsin D as a paracrine mediator of neoplastic epithelial cell growth in tissue recombinants *in vivo*. (A) Immunohistochemical staining revealed minimal expression of cathepsin D in BPH-1 + NPF and BPH-1 + UGM recombinants. In marked contrast, cathepsin D expression in BPH-1 + $NPF^{cyclin\ D1}$, BPH-1 + CAF were induced. (B) BPH-$1^{NPF\text{-}cyclin\ D1}$ cells had increased cathepsin D and CDK2/cyclin E, but not cyclin D1 expression. Overexpression of cyclin D1 in stromal environment could increase CDK2 and cyclin E protein expression in the adjacent epithelium. But there was no change in CDK4 and CDK6 protein levels. Cathepsin D protein expression level was upregulated in BPH-$1^{NPF\text{-}cyclin\ D1}$ and BPH-1^{CAFTD1} compared with control BPH-1^{NPF} cells.

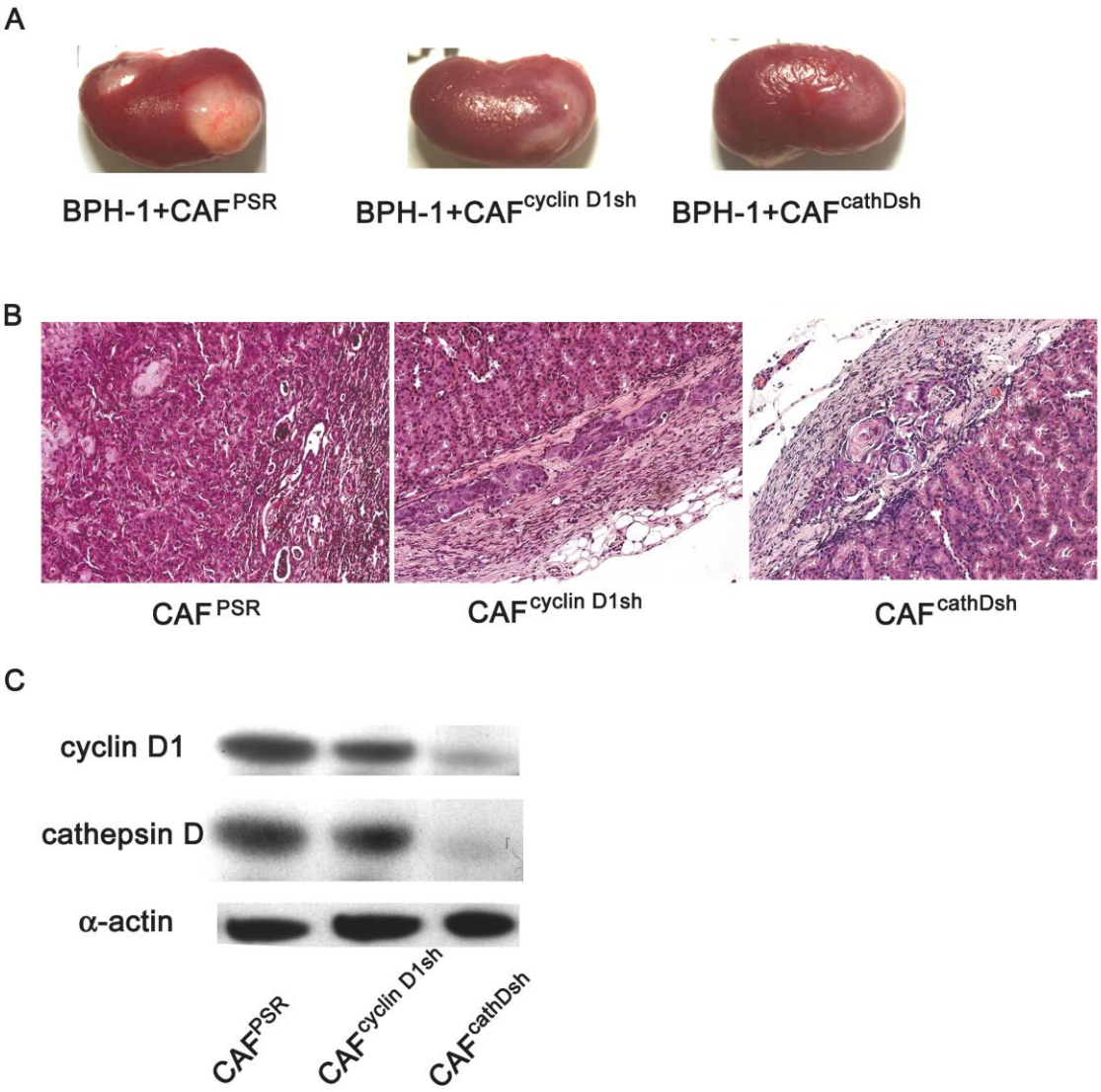

Figure 3-4. Cyclin D1 and cathepsin D are required for CAF induced tumorigenicity *in vivo*. (A) BPH-1 + $CAF^{cyclinD1sh}$ and BPH-1 + $CAF^{cathepsin\ Dsh}$ recombinants formed significantly smaller grafts compared with BPH-1+ CAF grafts. (B) Histologically, BPH-1 + CAF recombinants formed adenosquamous carcinoma. Knockdown recombinants formed benign, small cords structure with no tumorigenic response. (C) Western blotting indicated there were 50% knockdown of cyclin D1 and 95% cathepsin D protein expression $CAF^{cyclinD1sh}$ and $CAF^{cyclinD1sh}$ cells respectively. Cathepsin D expression in $CAF^{cyclinD1sh}$ cells was downregulated and cyclin D1 expression in $CAF^{cathepsin\ D}$ cells was downregulated as well.

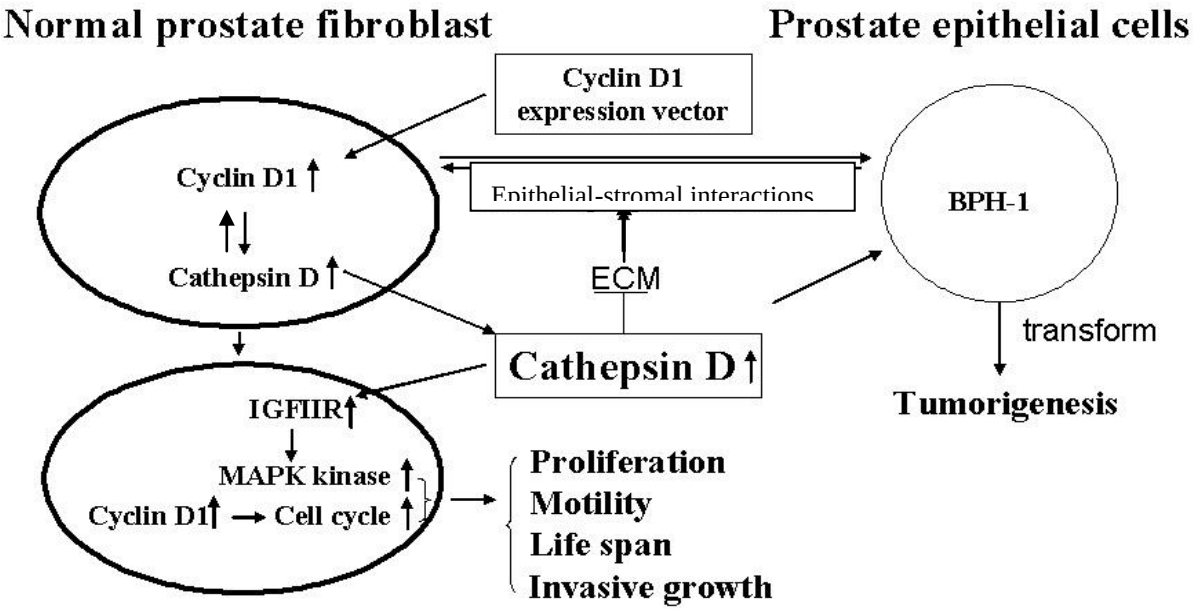

Figure 3-5. Cathepsin D plays a crucial role for prostatic fibroblast outgrowth and may favor prostate tumor progression via a paracrine loop.

Discussion

A number of chemokines and cytokines have been shown to involve in stromal-epithelial interaction in prostate cancer progression. Recent report suggested that cross talk between paracrine-acting cytokine and chemokine pathways promotes malignancy in benign human prostatic epithelium (Ao et al., 2007). The authors highlighted the links between TGF-β CXCR12/SDF-1 pathways and showed that these pathways are linked paracrine factors contributing to in CAF-driven tumorigenesis *in vivo*.

Tumor is a heterogenous disease, therefore many additional pathways are likely involved in stromal-epithelial interaction. Invasive prostate tumor stroma displayed induction of genes encoding ECM proteins and ECM degrading enzymes including members of the cathepsin family. Recent elegant study indicated that cathepsin D was robustly induced in stromal cells derived from prostate intraepithelial neoplasia (PIN) and invasive cancer in a multistage model of prostate carcinogenesis by cDNA microarray analysis of laser-microdissection (Bacac et al., 2006). The human ortholog of cathepsin D identified in the stromal reaction to tumor progression in this mouse model was observed to be expressed in several human cancers, including prostate cancer. Cathepsins have been suggested to participate in the progression of a variety of human cancers (Gocheva et al., 2006; Joyce et al., 2004; Joyce and Hanahan, 2004; Nomura and Katunuma, 2005). Cathepsins have recently been shown to be upregulated in pancreatic tumor model and contribute to invasive tumor growth (Gocheva et al., 2006). Cathepsin D is overexpressed and hypersecreted by epithelial breast cancer cells and stimulates their proliferation (Laurent-Matha et al., 2005). Clinical studies indicated that cathepsin D overexpression is

associated with increased risk of breast cancer metastasis and patient survival rate (Foekens et al., 1999; Maurizi et al., 1996). Cathepsin D is also crucial for fibroblast invasive outgrowth and acts as a paracrine communicator between the epithelial and stromal tissues. Cathepsin D was proposed to be mitogenic and to assist cancer cells in digesting ECM during tumor invasion (Laurent-Matha et al., 2005).

Our previous data have shown that overexpression of cyclin D1 in primary cultures of benign human prostatic fibroblasts extended the lifespan, altered the behavior of the stromal cells and induced malignant transformation of adjacent epithelium *in vivo* (chapter II) (He et al., 2007). Cyclin D1 induced these cells to behave in a manner similar to CAFs, towards the non-tumorigenic BPH-1 cells in a tissue recombination model. Stromal reactions to tumor growth are accepted to support tumor progression by providing growth factors, cytokines or chemokines that promote tumor cell survival, proliferation and migration (Ao et al., 2007; Olumi et al., 1999). The data presented here provide important messages by which paracrine signaling can promote tumorigenesis between tumor stroma and epithelium.

In this chapter, we proposed that cathepsin D is a crucial mediator between BPH-1 and either $NPF^{cyclin\ D1}$ or CAFs. Cathepsin D is upregulated in both $NPF^{cyclin\ D1}$ cells and CAFs as determined by microarray and western blot analysis (He et al., 2007). $NPF^{cyclin\ D1}$ cells have increased motile ability compared with control NPFs in a wound healing assay. By knocking down cathepsin D in $NPF^{cyclin\ D1}$ cells, their motile ability was decreased. Also,

the invasive growth of NPF$^{cyclin\ D1}$ cells was inhibited by knocking down cathepsin D in those cells. The stellate morphology of growing and invasive colonies with protrusions sprouting into the surrounding matrix of NPF$^{cyclin\ D1}$ cells disappeared after cathepsin D expression was decreased. The cell went back to a quiescent growth status as seen in NPFs.

Since cathepsin D is a secreted factor, we showed here that NPF$^{cyclin\ D1}$ conditioned medium promoted the growth of BPH-1 cells. In order to determine that cathepsin D is the mediator of this growth promotion, we used the conditioned medium from the cathepsin D knock down NPF$^{cyclin\ D1}$ cells to culture BPH-1 cells. It was found the growth promotion to BPH-1 cells was partially inhibited. Therefore, cathepsin D is necessary for NPF$^{cyclin\ D1}$ cells to promote the epithelium growth *in vitro*.

In a tissue recombination model, cyclin D1 and cathepsin D upregulation in NPF$^{cyclin\ D1}$ fibroblasts or CAFs favors BPH-1 growth *in vivo* by secreting and exchanging this protease to help BPH-1 cells digest ECM and invade to host kidney. As tumorigenesis progresses, the tumor cells express elevated cathepsin D. We showed that during malignant transformation, the isolated BPH-1$^{NPF\text{-}cyclin\ D1}$ cells from BPH-1 + NPF$^{cyclin\ D1}$ tumors continued to express upregulated cathepsin D. The data might suggest that the BPH-1$^{NPF\text{-}cyclin\ D1}$ cells were tumorigenic alone when grafted to kidney capsule of SCID mice as a result of upregulated cathepsin D.

Our previous data showed that NPF$^{cyclin\ D1}$ cells and CAFs elicited permanent malignant transformation of BPH-1 cells (Hayward et al., 2001; He et al., 2007). Both cyclin D1 and cathepsin D were shown to be upregulated in NPF$^{cyclin\ D1}$ cells and CAFs. When cyclin D1 or cathepsin D expression was knocked down in CAFs by retroviral transduction, CAFs had much reduced activity to transform BPH-1 cells. In the CAF$^{cyclin\ D1sh}$ cells, cathepsin D was also downregulated. This confirmed our hypothesis that cathepsin D is an important mediator between BPH-1 and CAFs. Interestingly, in the CAF$^{cathepsin\ Dsh}$ cells, cyclin D1 is also downregulated. This phenomenon makes sense because cyclin D1 is an cell cycle mediator, CAF$^{cathepsin\ Dsh}$ cells had lost their ability to transform BPH-1 resulting in reduced proliferation and growth. The reduced proliferation and growth reciprocally promoted cells to secrete less cathepsin D. This loop effect between cyclin D1 and cathepsin D disfavored the interactions between stroma and epithelium. Similarly, when cathepsin D was knocked down in NPF$^{cyclin\ D1}$ cells, these cells also had reduced ability to transform BPH-1 cells. These data indicated cathepsin D is not only in important mediator of stroma-epithelial cross talk *in vitro*, but also an essential component to favor this interaction *in vivo*.

Our study demonstrated that cathepsin D plays a crucial role in prostatic fibroblast outgrowth and may favor prostate tumor progression acting via a paracrine loop. Under these circumstances, cathepsin D is overexpressed and secreted by fibroblasts, and is captured *in vivo* by epithelial cells. The resultant cathepsin D overexpression in tumor epithelium promotes proliferation and stimulates motility and invasion of epithelium and

consequently enhance tumor-host homeostasis (Figure 3-6). The identification of factors such as cathepsin D that participate in the tumor-stroma communication might be crucial for the development of new stromal therapy of prostate cancer based on the fact that stroma might be a more stable target compared with the moving epithelium.

CHAPTER IV

FUNCTION OF PTEN IN NEW HUMAN IN VIVO MODELS REPRESENTING DISTINCT GRADES OF PROSTATE CANCER

Introduction

PTEN is one of the most frequently inactivated tumor suppressor genes in human tumors including prostate cancer. In humans, PTEN undergoes loss of heterozygosity (LOH) at relatively advanced stages in many cancers (Di Cristofano et al., 1998; Fujiwara et al., 2000; Garcia et al., 1999). The PTEN gene encodes a dual specificity phosphatase that regulates signal transduction pathways. PTEN mainly functions as a lipid phosphatase and targets phosphatidylinositol 3,4,5-trisphosphate (PIP-3) (Maehama and Dixon, 1998). By dephosphorylating PIP-3, PTEN can downregulate the Akt/PKB signaling pathway thus promoting cell survival and inhibiting apoptosis. PTEN can also antagonize the activity of PIP-3 affecting the G1 cell cycle transition (Wymann and Pirola, 1998).

PTEN is located at 10q23, a commonly deleted region in prostate cancer (DeMarzo et al., 2003; Visakorpi, 1999; Visakorpi, 2003). The biological importance of PTEN is evident from the early embryonic lethality of homozygous mutants. PTEN heterozygous mice develop cancers or dysplasias of multiple tissues including prostate (Di Cristofano et al., 2001; Di Cristofano et al., 1998; Suzuki et al., 1998). Loss of function of Nkx3.1 and PTEN cooperate in transgenic mouse models of prostate cancer progression (Abate-Shen et al., 2003). Since heterozygous and homozygous deletion of PTEN in animal models can result in prostate cancer, we were interested in identifying if and how PTEN suppression could play a role in initiation and progression of models of human prostate cancer and investigating responses to stromal environment.

Genetic insults to prostatic epithelium have been postulated to alter paracrine signaling to the prostatic smooth muscle (Hayward et al., 1997). Phenotypic changes consistent with this concept have been reported in stromal cells associated with human prostate tumors (Tuxhorn et al., 2002). Such changes have been demonstrated to be prognostic indicators of disease progression (Ayala et al., 2003). Presently, the profile of genetic changes in epithelium which results in a loss of normal stromal differentiation is not clearly understood. Stromal-epithelial interactions play a key role in the development and adult maintenance the prostate (Cunha and Young, 1992). Previous studies have shown that the inductive mesenchymal cells of normal prostate can suppress the growth of well differentiated prostate tumor cells (Hayashi et al., 1990). These results suggest that not all genetic lesions are sufficient to elicit significant alterations in the stromal-epithelial signaling axis with the additional possibility that fully differentiated prostate smooth muscle acts to restrain prostate tumor growth perhaps until a threshold of genetic damage has occurred. Such a mechanism suggests that stroma normally acts to suppress tumorigenesis and may explain the high incidence of small slow growing or latent prostate tumors which are found at autopsy in men who die from causes unconnected to prostate cancer (Franks, 1954b; Franks, 1976). In such a scenario these foci will not progress to an invasive phenotype until they accumulate a profile of genetic changes allowing them to escape the growth control exerted by the normal adjacent stroma. After the threshold is reached, the stromal microenvironment is altered in comparison to normal stroma and exhibits features of stroma involved in wound repair. The reactive stroma includes elevated numbers of myofibroblasts and fibroblasts with induced vimentin expression (Tuxhorn et al., 2002).

In this chapter, we examined the hypothesis that the ability of human prostatic epithelial cells to induce and maintain smooth muscle differentiation in adjacent stroma is negatively related to the level of genetic damage sustained by those epithelial cells. Suppression of PTEN was examined to determine the effects of stromal cells on the ability to transform epithelial cells and to affect differentiation of the local microenvironment.

Methods

Cells

BPH-1 (a non-tumorigenic human prostatic epithelial cell), and its tumorigenic derivatives BPH^{CAFTD1} and BPH^{CAFTD2}, PrE (prostatic epithelial cells)1 and PrE3 were from our own stocks (Hayward et al., 1995; Hayward et al., 2001). PrE cells were isolated from human benign prostate tissue and spontaneouly immortalized.PC3, DU145 and LNCaP were obtained from ATCC (Rockville, MD, USA). BPH-1^{PSR} (pSuper.Retro empty vector infected BPH-1 cells), BPH-1^{PTENsh} (pSuper.Retro PTEN shRNA vector infected BPH-1 cells), $PrE1^{PSR}$ (pSuper.Retro empty vector infected PrE1 cells), $PrE1^{PTENsh,}$ (pSuper.Retro PTEN shRNA infected PrE1 cells), $PrE3^{PSR}$ (pSuper.Retro empty vector infected PrE3 cells) $PrE3^{PTENsh}$ (pSuper.Retro PTEN shRNA vector infected PrE2 infected cells), $PrE3^{pLNCX\text{-}control}$ (pLNCX control vector infected PrE3 cells), $PrE3^{pLNCX\text{-}PTENsh}$ (pLNCX PTEN shRNA vector infected PrE3 cells) and $PrE3^{pLNCX\text{-}myrAKT}$ (pLNCX myristolated-Akt vector infected PrE3) cells were generated as described below. 957E/hTERT cells were generously supplied by Dr. John Issacs (Johns Hopkins). Cells were maintained in RPMI 1640 (Gibco, Carlsbad, CA) with 1% antibiotic/antimycotic (Life Technologies, Grand Island, NY) and 5% Cosmic Calf Serum (CCS-HyClone, Logan, Utah).

Generating genetically modified cell lines

pSuper.Retro vector (OligoEngine, Seattle, WA) was used as a backbone to clone a PTEN short hairpin RNA (shRNA) sequence. A 19 nucleotide PTEN target sequence (5'AGATGAGAGACGGCGGCGG3') corresponding to nucleotides 206-224 of PTEN mRNA was selected for constructing PTEN shRNA vector (Ning, 2004 #8479). pSuper.Retro empty and pSuper.Retro-PTENsh constructs were transduced to targeted

BPH-1 and PrE3 cells using retroviral infection as described in chapter II. Successfully infected cells were selected by 5μg/ml puromycin (Sigma) for 3 days. pLNCX control and pLNCX myr-Akt vectors were kindly provided by Dr. Hideyuki Miyauchi at Chuba University in Japan. PrE3 cells were gifts from Dr. Dean Tang at MD Anderson Cancer Center. PrE3$^{pLNCX\ control}$ and PrE3$^{pLNCX\text{-}myr\text{-}Akt}$ cells were generated by retroviral infection as described in chapter II and selected by 400μg/ml G418 for a week.

Western blotting analysis

Western blotting analysis was performed as previously described in chapter II. Membranes were incubated with mouse monoclonal antibody to PTEN (Santa Cruz Biotechnology, Santa Cruz, CA, 1:1,000 dilution), rabbit polyclonal phospho-Akt (Ser 473) (1:1000, Cell Signaling, Denvers, MA) and β-actin (1:5000, Sigma) overnight and washed with PBS-Tween 20 for 1 hour, and incubated with horseradish-Peroxidase linked anti-mouse secondary antibody (Amersham Biosciences, Piscataway, NJ, 1:1,000 dilution) for 1 hour. Bound antibodies were visualized using enhanced chemiluminescence western blotting detection reagents (Amersham Bioscences). PTEN expression levels were normalized to β-actin and quantitated using NIH Image J software (http://rsb.info.nih.gov/ij/).

Growth curves

BPH-1^{PSR} and BPH-1^{PTENsh} cells were plated in a 24-well plate (1000 cells/well) in RPMI 1640 medium supplemented with 5% CCS. After the cells had attached overnight, 300 μl Cell Titer 96 Aqueous One Solution (Promega, Madison, WI) was added at indicated times (1, 2, 3, 4, and 5 days) to each well and the absorbance was measured at 490 nm after 3 hours incubation. Experiments were performed in triplicate.

Wound healing assays

Confluent monolayers of BPH-1^{PSR} and BPH-1^{PTENsh} cells were grown in 6 well plates. Wounds were imaged at 0, 3, 6, and 9 hours post wounding and the cell migration rate into the wound was calculated. Experiments were performed in triplicate.

Transwell migration assay

Detail method was described in chapter II. Results from at least three experiments were expressed as the mean relative cell migration ± SD, with that of BPH-1^{PSR} cells set at 1.

Boyden chamber assay

Detail method was described in chapter II.

Tissue recombination and xenografting

BPH-1^{PSR} + rUGM, BPH-1^{PTENsh} + rUGM, PrE3$^{pLNCX\text{-}control}$ + rUGM and PrE3$^{pLNCX\text{-}myrAkt}$ + rUGM tissue recombinants were made as previously described in chapter II (Hayward et al., 1999). 100k BPH-1^{PSR} or BPH-1^{PTENsh}, 600k PrE3 $^{pLNCX\text{-}control}$ or PrE3$^{pLNCX\text{-}myrAk}$ were recombined with 300k rUGM cells. All the experiments were repeated 6 times. Mice with BPH-1 grafts were sacrificed after 2 months and mice with PrE grafts were sacrificed after 6 months and grafts were harvested, fixed, and paraffin embedded.

Immunohistochemical and Immunofluorescence staining

Immunohistochemical and immunofluorescence methods have been described previously in chapter II (Ao et al., 2006; Williams et al., 2005). Briefly, primary antibodies against α-actin (1:1000, Sigma), γ-actin (1:1000, Sigma), vimentin (1:1000, sigma), AR (1:1000, Santa Cruz

Biotechnology,), E-cadherin (1:1000, BD Biosciences PharMingen, San Diego, CA), anti-phospho histone H_3 (1:200, Upstate, Lake Placid, NY), CK14 (1:100, gift from E. B. Lane, University of Dundee), and Rabbit polyclonal to Ku 70 (1:500, Abcam, Inc., Cambrige, MA) were incubated with tissue sections at $4^{\circ}C$ overnight. Polyclonal rabbit immunoglobulins/biotinylated anti-mouse or mouse immunoglobulins/biotinylated anti-rabbit secondary antibody (DAKO, Carpinteria, CA) were incubated for 60 minutes the next day after the slides were washed with PBS buffer for 1 hour for immunohistochemical staining of α-actin, γ-actin, vimentin, AR, E-cadherin and anti-phospho histone H_3. The secondary anti-rabbit IgG (whole molecule) TRITC Conjugate (Sigma) or anti-mouse IgG (whole molecule) FITC Conjugate (Sigma) was used for immunofluorescence staining of Ku 70, CK14 or vimentin for immunofluorescence.

Cell Cycle Analysis

Cell cycle analysis of BPH-1^{PSR} cells and BPH-1^{PTENsh} cells was performed using the method described in chapter II.

Results

PTEN expression is downregulated in prostate cancer cell lines

PTEN expression was examined by Western blotting in the prostate cancer cell lines, PC3, DU145, LNCaP, BPH^{CAFTD1} and BPH^{CAFTD2} and in a subset of non-tumorigenic PrE1, 957E/hTERT, PrE3 and BPH-1 prostatic cells. PTEN expression was found to be lower in all of the cancer cells as compared to the non-tumorigenic prostatic cells (Figure 4-1, A). Non-tumorigenc epithelial cells had the highest PTEN expression, but malignant cell lines have a lower PTEN expression level. These data crudely correlate PTEN expression with tumorigenicity.

Internal mutation and deletion of PTEN is detected in BPH^{CAFTD} cell lines but not in PH-1 cells

To better understand the genomic instability of the BPH-1 derived human prostate cancer cell lines (BPH^{CAFTD1} and BPH^{CAFTD2}), leading to decrease of PTEN expression, we designed primers to amplify the PTEN genomic DNA sequence by RT-PCR. The PCR products were cloned into T-easy and sequenced to examine differences between cell lines. Sequence analysis indicated that the entire coding sequence was intact in the parental BPH-1 cells. In contrast, the BPH^{CAFTD} cell lines, contained point mutations, insertions and deletions in the five prime untranslated region(5'UTR) of mRNA (messenger RNA) . As shown in Figure 4-1, B, two obvious insertions (9 bp and 15 bp) and one deletion (28 bp) were found in BPH^{CAFTD1} cells in the 5'UTR. Since no deletions, insertions, or mutations were found in the coding sequence of BPH^{CAFTD} cell lines, the downregulation of PTEN in

these cells may be due to problems related to transcription initiation, incorrect translation start site, or mRNA instability. These data are consistent with findings that clinical tumors frequently have acquired mutations in noncoding regions of PTEN (Liaw et al., 1997; Liu et al., 1997). Our data correlate loss of PTEN with tumorigenicity but, like similar correlations seen in patient samples, do not address whether this correlation is a cause or an effect of malignant change. In order to address this question, we tested the consequences of knocking down PTEN in non-tumorigenic prostatic epithelial cells.

Suppression of PTEN in BPH-1 cells can increase cell migration, and invasion *in vitro*

Western blotting showed that BPH-1^{PTENsh} cells have a 0.55 fold decrease in PTEN expression compared with control BPH-1^{PSR} cells after normalization to β-actin expression (Figure 4-2, A). Phospho-Akt expression was elevated in the PTEN knockdown cells (2.2 fold), confirming functional changes predicted by this manipulation. BPH-1^{PTENsh} cells showed enhanced mobility in wound healing, transwell migration, and Boyden chamber assays. Wound healing assays showed that BPH-1^{PTENsh} cells were significantly more motile than control BPH-1^{PSR} cells. This difference was clear after 6 hours (Student's t-test, $P<0.01$) (Figure 4-2, B). In a transwell migration study, more BPH-1^{PTENsh} cells migrated through the uncoated Boyden chambers to the underside of the insert in a 12 hour response to conditional medium containing 1% CCS than BPH-1^{PSR} cells (Student's t-test, $P<0.01$) (Figure 4-2, C). These data confirmed the elevated motility of BPH-1^{PTENsh} cells. An invasion assay, in which the inside chamber was coated with matrigel to mimic the *in vivo* extracellular matrix, demonstrated that BPH-1^{PTENsh} cells had

significantly increased invasive activity *in vitro* (Student's t-test, P=0.01) (Figure 4-2, D). Collectively these assays showed that when PTEN expression is suppressed, BPH-1 cells acquired an enhanced motility and invasive ability *in vitro*.

BPH-1^{PTENsh} cells were deficient in cell cycle control and had a higher proliferation rate compared with control cells

Previous reports demonstrated that PTEN induced cell cycle arrest by decreasing the number of cells in S phase, which is indicative of S-phase entry inhibition (Paramio et al., 1999). Consistent with this, we saw that BPH-1 cells with PTEN knocked down had an increased fraction of cells in the S and G2/M phases of the cell cycle (Figure 4-2, E b and c). Cell cycle analysis was also consistent with proliferation where we observed that PTEN knock down cells proliferated faster than control cells (Figure 4-2, E a).

Partial loss of PTEN expression drove BPH-1 cells to grow as an invasive tumor To determine whether PTEN loss could exert a tumorigenic effect on prostate cells *in vivo*, 100k BPH-1^{PTENsh} or control epithelial cells were recombined with 300k rUGM cells and grafted under the kidney capsule of SCID mice. The grafts were harvested after 4 weeks. The results showed that recombinants contains BPH-1^{PTENsh} cells were significantly larger grafts than BPH-1^{PSR} containing recombinants (Figure 4-3, A, P<0.01). These results were consistent with our *in vitro* observations. Grossly, control grafts formed white solid cores. Histologically, they exhibited the formation of solid epithelial cords surrounded by a muscular stroma, as previously described (Cunha et al., 2002). There were sharp

delineations between the grafts and the host kidney with no sign of invasion (Figure 4-3, B a and b). In clear contrast, based on gross observation the grafts using PTEN knockdown epithelium contained areas where blood vessels were formed and areas composed of either cysts or necrotic tissue. The histological appearance of the BPH-1^{PTENsh} + rUGM grafts, as assessed by H & E staining and SV-40 T-antigen staining, resembled a poorly differentiated carcinoma phenotype (Figure 4-3, B e and f). There was heterogeneity in the resultant tumors in that some cases grew as noninvasive proliferative lesions on the surface of the host kidney, some contained individual cells with large nuclei and dense cytoplasm scattered with stroma, while others formed invasive lesions that engulfed and destroyed kidney tissue (Figure 4-3, B e and f). Irregular areas of necrotic tissue also extended throughout the grafts with positive SV-40 T antigen staining which confirmed the BPH-1 cell origin of the tumor epithelium (Figure 4-3, B f and inset). Invasion and infiltration into the kidney were observed. Previous unpublished data showed that LNCaP + rUGM grafts contained much less stroma compared with BPH-1 + rUGM grafts, indicating a rapid tumor growth. The same observation was also seen in recombinants of c-myc overexpressing epithelial cells with rUGM (Williams et al., 2005). The present chapter also showed that no fibromuscular stroma was observed in the invading area. Tumor cells invaded the kidney and engulfed nephrons after 1 month of growth. In contrast, control grafts did not invade the kidney and graft epithelium was separated from kidney by a stromal layer. Well defined epithelial cell junctions demonstrated by E-cadherin staining were noted (Figure 4-3, B c). In the PTEN knockdown cells, E-cadherin expression was almost absent, consistent with the malignant

phenotype (Figure 4-3, B g). BPH-1^{PTENsh} cells have significantly elevated phosphorylated histone H3 (pHisH3) cells throughout the grafts compared with control grafts (Figure 3 B, d and h, 0.7/100μm^2 positive cells in BPH-1^{PSR} grafts, 4.33/100μm^2 positive cells in BPH-1^{PTENsh} grafts, $P<0.001$). These data show that a moderate suppression (55%) PTEN in BPH-1 cells not only significantly increased motility and promoted cell proliferation, and invasion *in vitro*, but also was sufficient to induce malignant transformation and invasion *in vivo*.

Suppression of PTEN in BPH-1 cells caused a loss of stromal differentiation

Immunohistochemical analysis was used to assess the effect of epithelial cells on adjacent stroma. The three markers used, vimentin, smooth muscle α-actin, smooth muscle γ-actin, representing respectively, a fibroblastic marker, an early marker of smooth muscle differentiation, and a late marker of smooth muscle differentiation. The stromal cells in BPH-1^{PSR} + rUGM tissue recombinants had abundant α-actin and γ-actin expression, but almost no vimentin expression (Figure 4-3, C a, b and c), which indicated a well differentiated stroma surrounding the epithelium. In stromal cells of BPH-1^{PTENsh} + rUGM tissue recombinants, there was suppression of α-actin expression, moderate γ-actin expression(Figure 4-3C, d) and induction of vimentin expression (Figure 4-3, C f, arrow and I), indicating poorly differentiated stroma correlating with a cancer phenotype.

Activation of Akt signaling pathway elicited an atypical hyperplasia phenotype

To determine whether constitutive activation of Akt could exert a tumorigenic effect on prostate cells *in vivo*, 100k BPH-1^{Akt} cells (generated as described as previously- ((Ao et al., 2006)) or BPH-1 cells were recombined with 300k rUGM and grafted under the kidney capsule of SCID mice. The grafts were harvested after 4 weeks. The BPH-1^{Akt} cells formed larger grafts under the induction of rUGM, compared with BPH-1 groups (data not shown). Histologically, both control grafts and Akt overexpressing grafts had sharp delineations from the host kidney with no sign of invasion (Figure 4-4, A a and e). However, the BPH-1^{Akt} cells formed small solid cord structures and many cells had enlarged and elongated nuclei, which indicated an atypical hyperplasia phenotype (Figure 4-4, A e). Both BPH-1 and BPH-1^{Akt} cells continued to express SV-40 T antigen (Figure 4-4, A b and f). Control grafts had well defined cell junctions demonstrated by E-cadherin staining (Figure 4-4, A c). E-cadherin expression was almost absent in the BPH-1^{Akt} cells consistent with a malignant phenotype (Figure 4-4, A g). BPH-1^{Akt} cells have significantly increased number of pHisH3 positive cells throughout the grafts compared with control grafts (Figure 4-4, A d and h, 0.3/100μm^2 positive cells in BPH-1grafts, 2.33/100μm^2 positive cells in BPH-1^{Akt} grafts, $P<0.01$). These data showed activation of Akt in BPH-1 cells could also promote cell proliferation, and induce transformation *in vivo*.

Activation of Akt in BPH-1 cells caused a loss of stromal differentiation

The stromal cells in BPH-1 + rUGM tissue recombinants had a well differentiated stroma with abundant α-actin and γ-actin expression, but very low vimentin expression (Figure

4-4, B a, b and c). In stromal cells of BPH-1^{Akt} + rUGM tissue recombinants, there was suppression of α-actin expression, moderate expression of γ-actin (Figure 4-4, B d) and induction of vimentin expression (Figure 4-4, B f, arrow and I), consistent with a poorly differentiated stroma.

The effect of PTEN knock down is consistent by using a new human prostatic epithelial cells line

In order to assess whether the results obtained in BPH-1 cells were consistent we repeated the experiments using a new human prostatic epithelial cell line PrE3, which has been immortalized by retrovirally introduced SV-40 T antigen by retroviral infection. These cells give rise to a normal-appearing glandular structures when recombined with rUGM (Figure 4-5, A a) In order to test the consequences of suppression of PTEN in these cells, PTEN knocked down and control constructs were retrovirally infected to PrE3 cells. The knocked down cells were then grafted under the renal capsule of SCID mice after recombined with rUGM. After 5 months of growth under the kidney capsule of SCID mice, $PrE3^{PSR}$ + rUGM tissue recombinants formed glandular structures, Ku 70 immunofluorescence staining and SV-40 T antigen staining (data not shown) were positive in the nuclei of the epithelial cells, indicating that the glands were formed from the grafted human cells. (Figure 4-5, A b). In contrast, in + rUGM tissue recombinants the epithelial cells formed large solid cords with enlarged nuclei (Figure 4-5, A f). Multilayered cells forming nests recapitulated a PIN structure. Since the parental PrE3 cells formed normal glandular structure, knocking down only one tumor suppressor even

in the face of SV-40 may not be enough for these cells to undergo malignant change. PrE3^{PTENsh} cells continued to express Ku 70 (Figure 4-5 A, g) and SV-40 T antigen (data not shown). Consistent with the consequences of suppression of PTEN in BPH-1 cells, recombinants of PrE^{PTENsh} + rUGM showed expression of vimentin in adjacent stroma (Figure 4-5A, j). The stromal cells in PrE3^{PSR} + rUGM and PrE3^{PTENsh} + rUGM grafts expressed α-actin and γ–actin (Figure 4-5, A c, d, h and i). Epithelial cells in both control and knock down recombinants continuously expressed AR (Figure 4-5, B a and e). E-cadherin staining was positive at the cell-cell junctions of control recombinants (Figure 4-5, B b), however, in the PTEN knockdown recombinants, staining was patchy and, in many places, undetectable (Figure 4-5, B f). PrE3^{PTENsh} cells proliferated much faster *in vivo* than control PrE3^{PSR} cells, demonstrated by significantly increased pHisH3 positive cells (Figure 4-5, A d and h, 0.3/100μm^2 positive cells in PrE3 grafts, 3/100μm^2 positive cells in PrE3^{PTENsh} grafts, $P<0.01$). pHisH3 positive cells could only occasionally be found in control grafts (Figure 4-5, B c and g). CK 14 expression was absent in PrE^{PTENsh} cells, indicating that as PIN lesions progressed, basal cells were lost. In contrast, normal glands were CK14 positive in the basal layer (Figure 4-5, B d and h).

Constitutive expression of myrislated Akt in PrE3 cells caused a high-grade cribriform PIN phenotype

In order to confirm the consequences of PTEN suppression in prostate cancer progression, we retrovirally overexpressed Akt in PrE3 cells. After 5 months of growth under the kidney capsule of SCID mice PrE3$^{pLNCX\text{-}control}$ + rUGM tissue recombinants

formed benign appearing glandular structures (Figure 4-6, A a), with Ku 70-positive nuclei. PrE3$^{myr\text{-}Akt}$+ rUGM tissue recombinants fused into large ducts lined with epithelial cells with a cribriform high grade PIN-like structure (Figure 4-6, A f). Cells in these structures continued to express Ku 70 (Figure 4-6, A g). There were multiple epithelial layers in the cords and cells have enlarged nuclei consistent with a PIN phenotype. PrE3$^{myr\text{-}Akt}$ cells had induced vimentin expression in stroma (Figure 4-6, A g and j). α-actin and γ-actin expression did not change much in the rUGM compared with control recombinants. Both control and knock down recombinants expressed AR (Figure 4-6, B a and e). E-cadherin expression was detected in cell-cell junctions of control recombinants (Figure 4-6, B b), however, the PrE3$^{myr\text{-}Akt}$ cells had decreased E-cadherin staining (Figure 4-6, B f). PrE3$^{myr\text{-}Akt}$ cells proliferated significantly faster *in vivo* than control PrE3$^{pLNCX\text{-}control}$ cells as demonstrated by increased pHisH3 staining (0.3/100μm^2 positive cells in PrE3$^{pLNCX\text{-}control}$ grafts, 1.7/100μm^2 positive cells in PrE3$^{myr\text{-}Akt}$ grafts, $P<0.01$). (Figure 4-6, B c and g). Control glands retained CK14 expression in the basal layer. However, lack of CK 14 expression in structures generated by PrE3$^{myr\text{-}Akt}$ cells indicated that basal cells were lost. (Figure 4-6, B d and h).

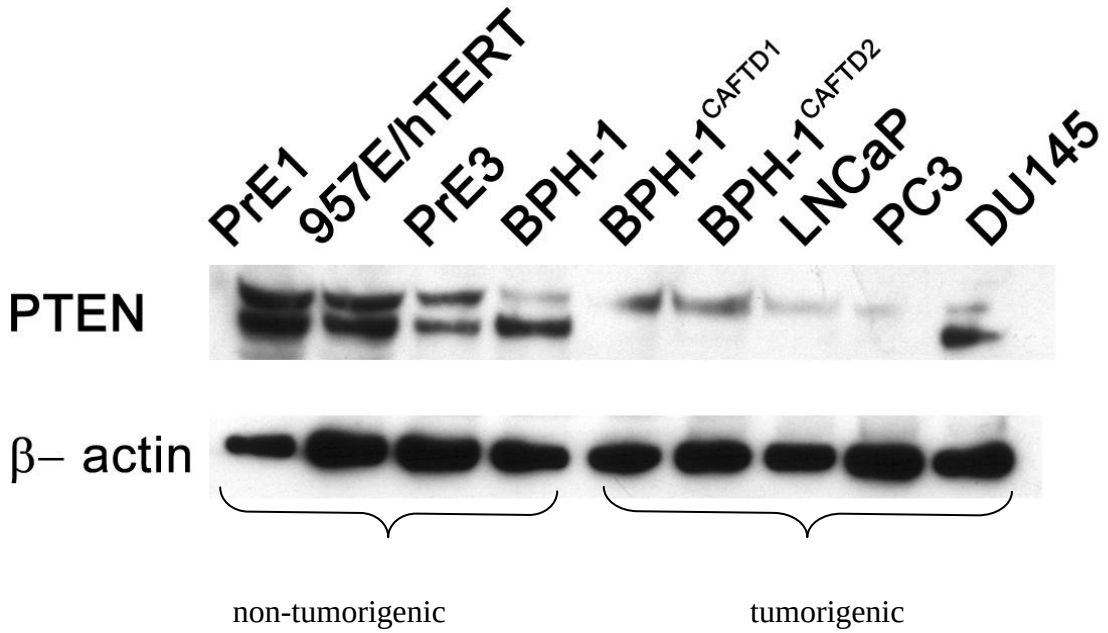

Figure 4-1. PTEN protein expression in a panel of human prostatic epithelial cells and internal mutation or deletion of PTEN in BPH^{CAFTD} cell lines. (A) Western blotting was performed to examine PTEN protein expression levels in malignant (BPH-1^{CAFTD1}, BPH-1^{CAFTD2}, DU145, LNCaP and PC3) and non-tumorigenic (PrE1, 957E/hTERT, PrE3 and BPH-1) prostatic epithelial cell lines. The PrE1, 957/hTERT, PrE3 cells had the highest PTEN expression compared with other transformed prostate cell lines. BPH-1 cells had a moderate level of PTEN expression. These two bands might correspond to two isoforms of the PTEN protein

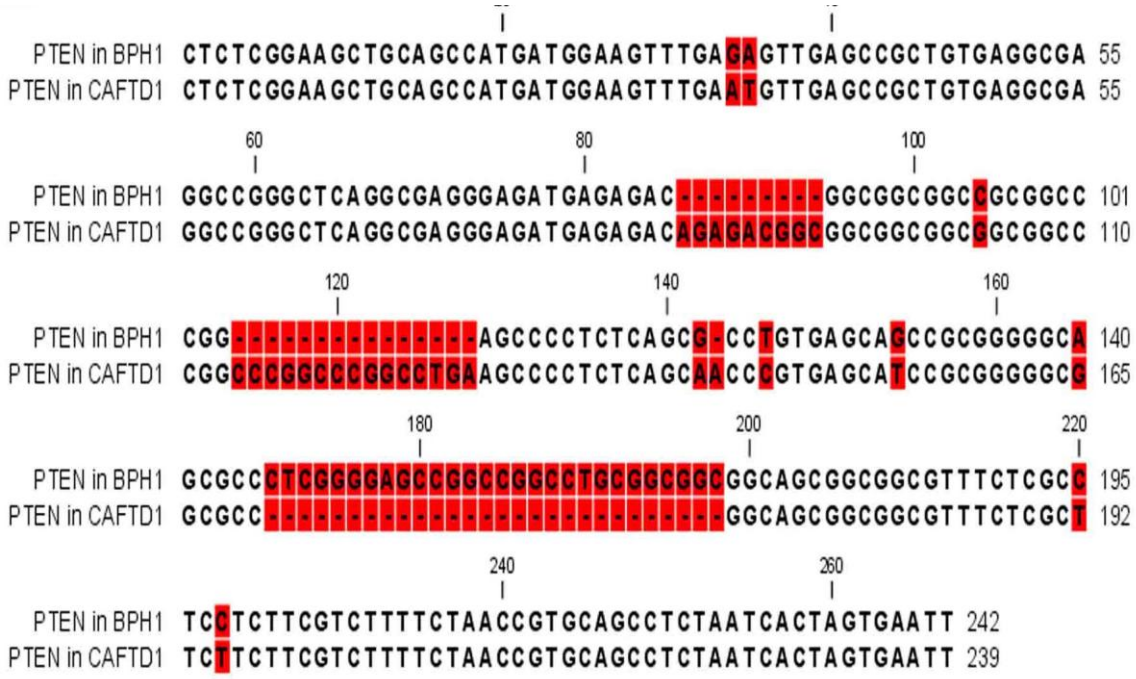

Figure 4-1 (B) Two obvious insertions (9 bp and 15 bp) and one deletion (28 bp), all highlighted, were found in BPH^{CAFTD1} cells in the 5'UTR region of the mRNA.

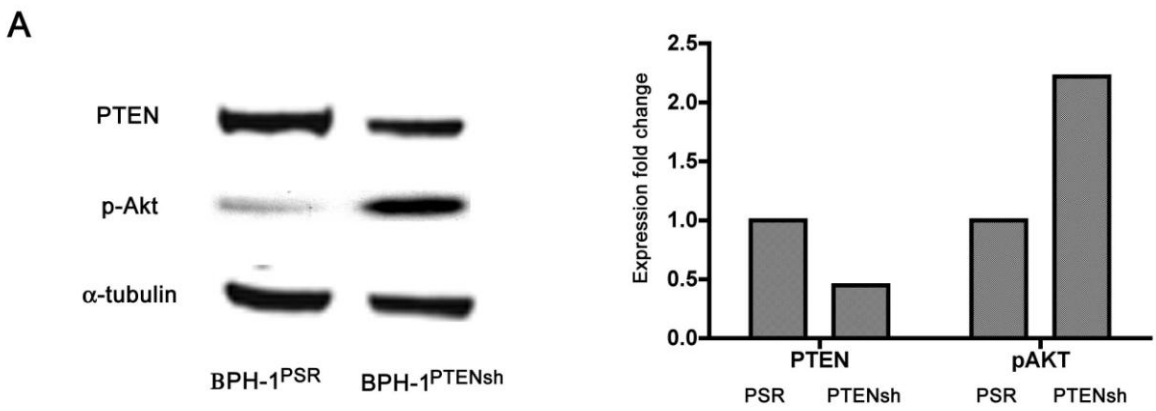

Figure 4-2. *In vitro* assays for BPH-1^{PSR} and BPH-1^{PTENsh} cells. (A) In order to examine the role of PTEN in prostate cancer progression, PSR (control - BPH-1^{PSR}) and PTEN knock down (BPH-1^{PTENsh}) BPH-1 cell lines were generated by stable retroviral infection. PTEN downregulation in BPH-1^{PTENsh} was confirmed by western blotting and band intensity quantitated. There was 55% PTEN protein downregulation and 2.2 fold pAKT upregulation in BPH-1^{PTENsh} cells.

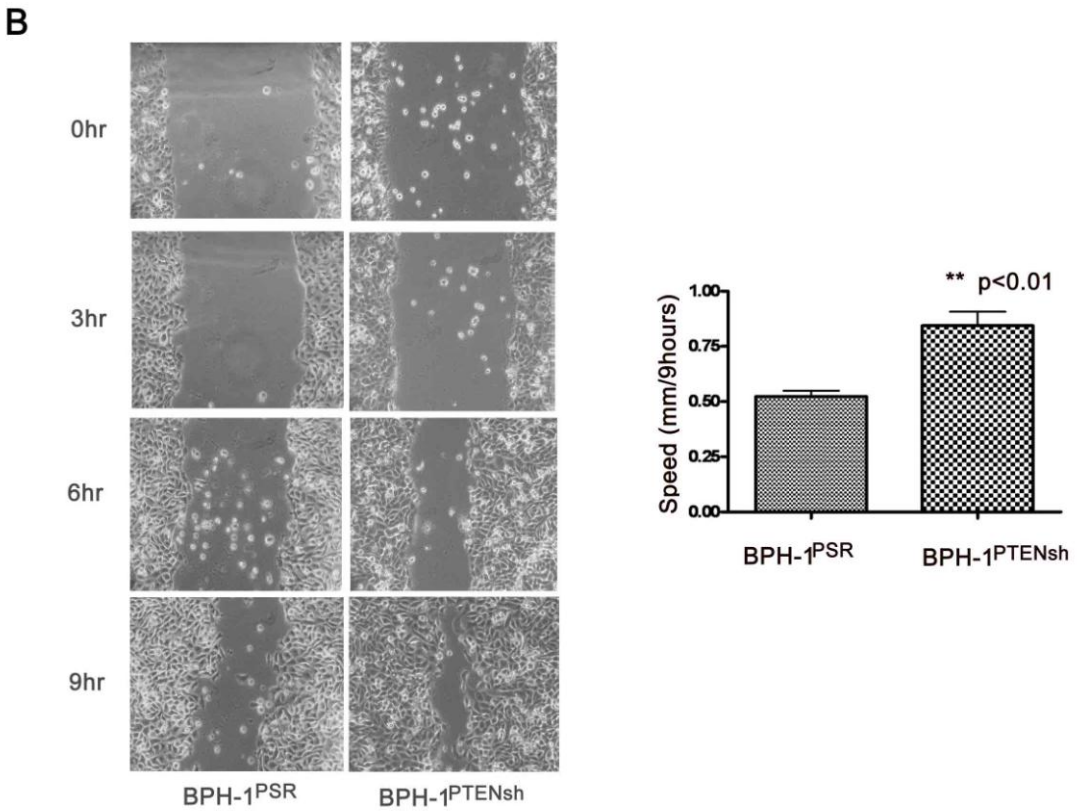

Figure 4-2 (B). Wound healing assay. BPH-1^{PTENsh} closed wounds in the confluent monolayer significantly faster than BPH-1^{PSR} cells. Images (left) and quantitation (right) shown. Student's t-test, P<0.001.

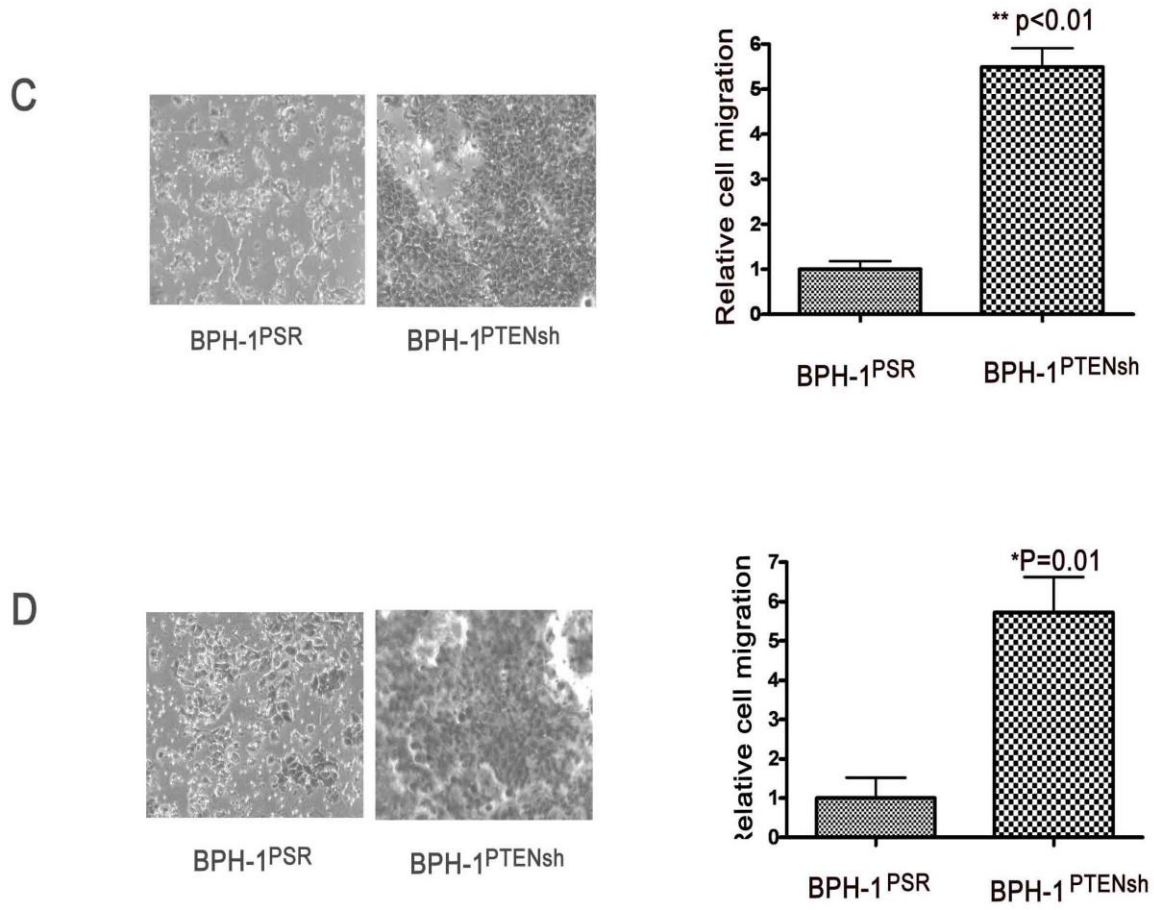

Figure 4-2 (C). Transwell migration study. BPH-1^{PTENsh} migrated through the uncoated Boyden chamber significantly faster than BPH-1^{PSR} Representative phase-contrast optical photomicrographs after overnight culture shown (a, left) and quantitated (a, right). Student's t-test, P<0.01. (D) Invasion assay. BPH-1^{PTENsh} cells had increased invasive ability in a Matrigel coated Boyden chamber invasion assay compared to BPH-1^{PSR}. Representative phase-contrast optical photomicrographs after overnight culture shown (left) and quantitated (right). Student's t-test, P=0.01.

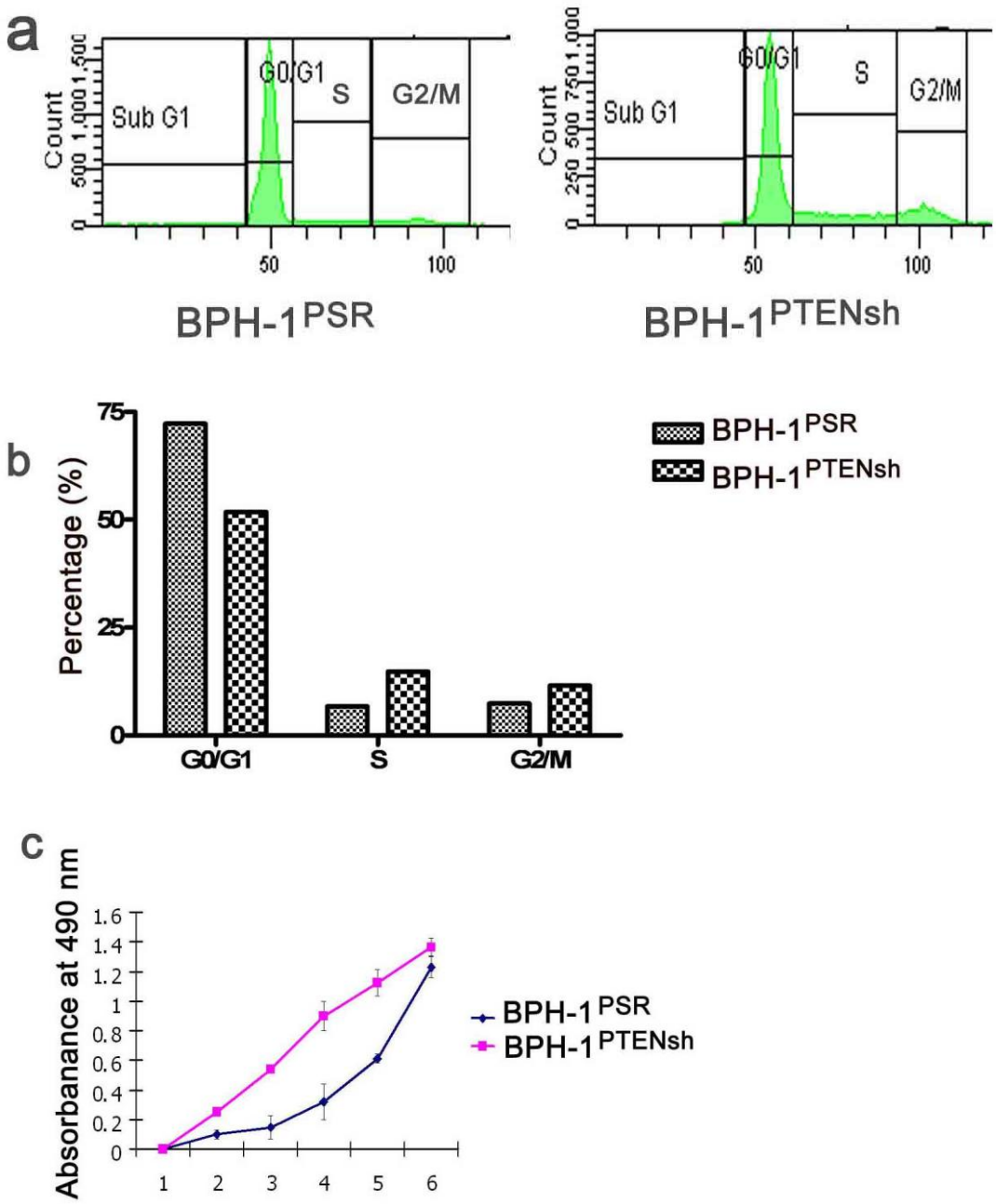

Figure 4-2 (E). Cell cycle analysis and proliferation assay. BPH-1 cells with PTEN knockdown had an increased fraction of cells in the S and G2/M phases of the cell cycle (a and b). PTEN knockdown promoted BPH-1 cell proliferation significantly over control growth rate. (Student's t-test, $P<0.001$) (c).

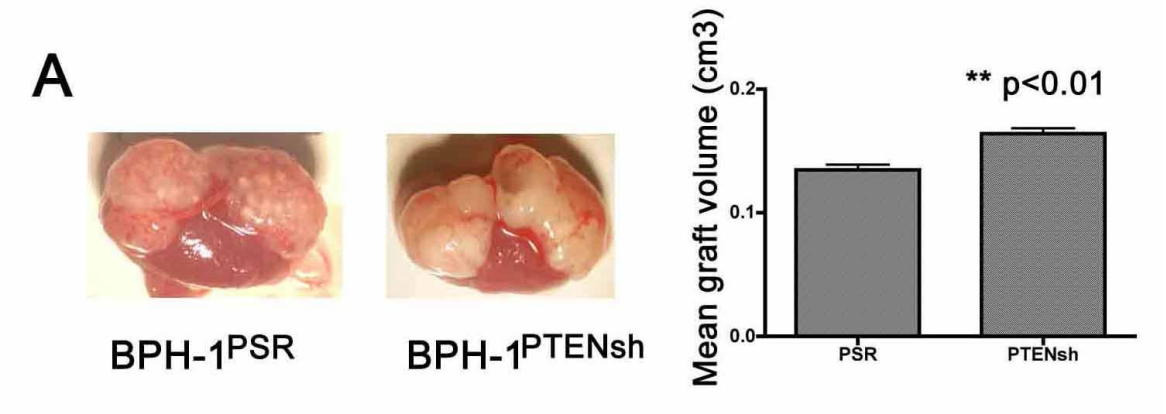

Figure 4-3. *In vivo* comparisons of BPH-1^{PSR} and BPH-1^{PTENsh} cells. (A). BPH-1 ^{PTENsh} cells (right) formed significantly larger grafts than control (left) after 3 months of growth under the kidney capsule of SCID mice (P<0.01).

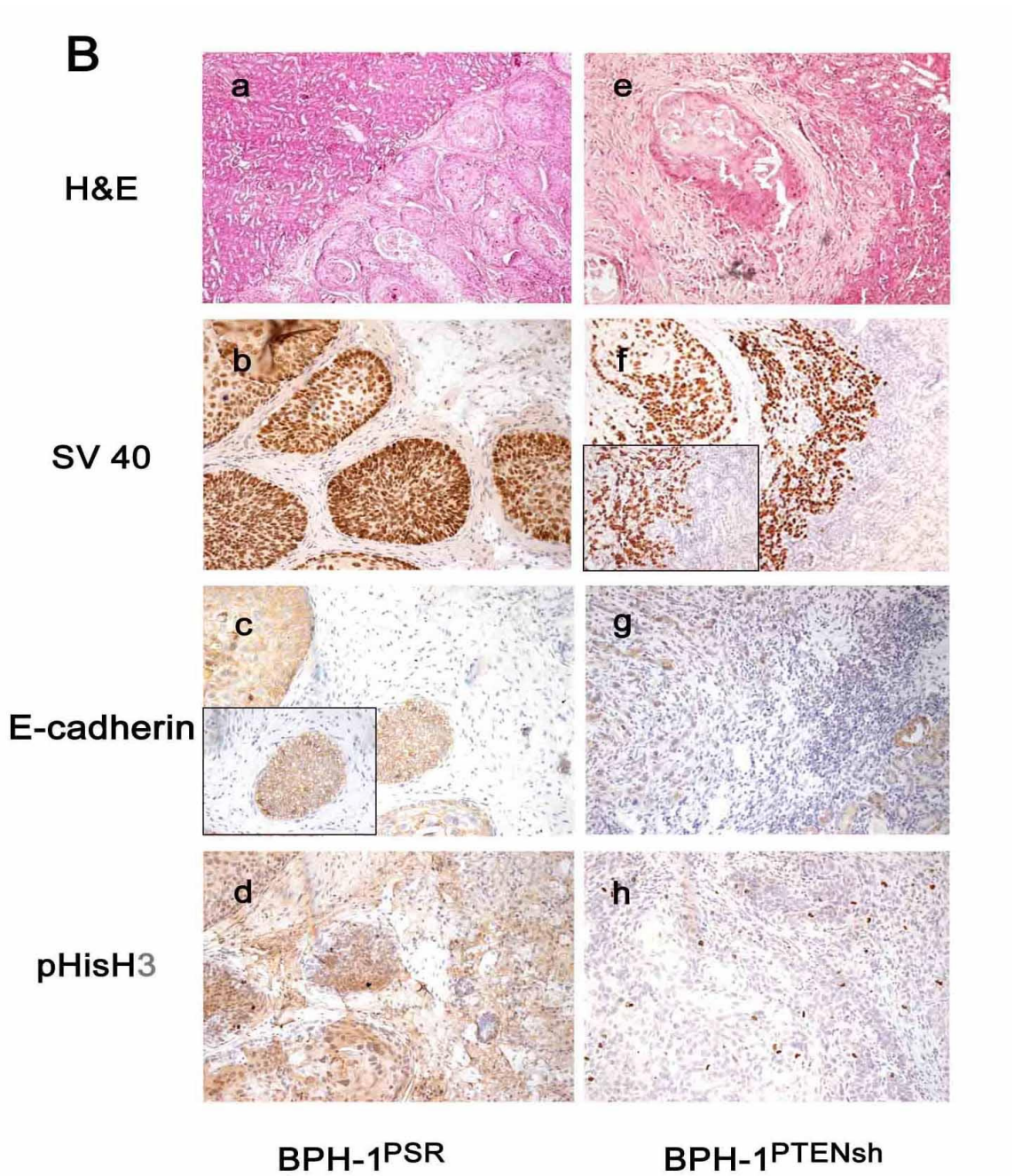

Figure 4-3 (B) (a). H & E staining and SV-40 T-antigen staining demonstrated that BPH-1^{PTENsh} cells invaded to kidney (e, f and inset). E-cadherin was clear in cell-cell junctions of control grafts (c), however, E-cadherin expression was low in the PTEN knock down cells (g). BPH-1^{PTENsh} cells had increased pHisH3 positive cells (h) indicating increased proliferation compared with control.

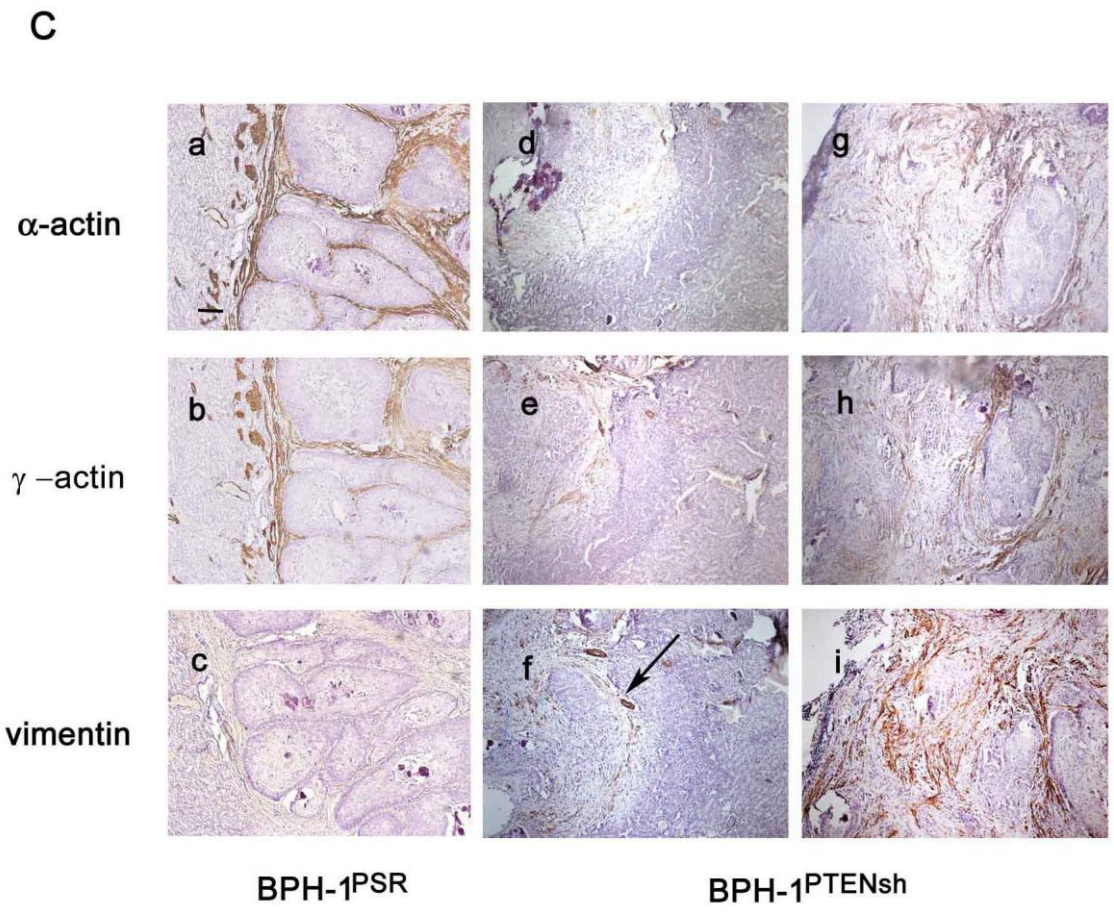

Figure 4-3 (C). Suppression of PTEN in BPH-1 cells caused a loss of stromal differentiation. BPH-1^{PSR} + rUGM tissue recombinants had abundant α-actin and γ-actin expression, but almost no vimentin expression (a, b and c) In BPH-1^{PTENsh} + rUGM tissue recombinants, there was suppression of α-actin expression (d and g), no significant change of γ- actin expression (e and h) and induction of vimentin expression (f and i)

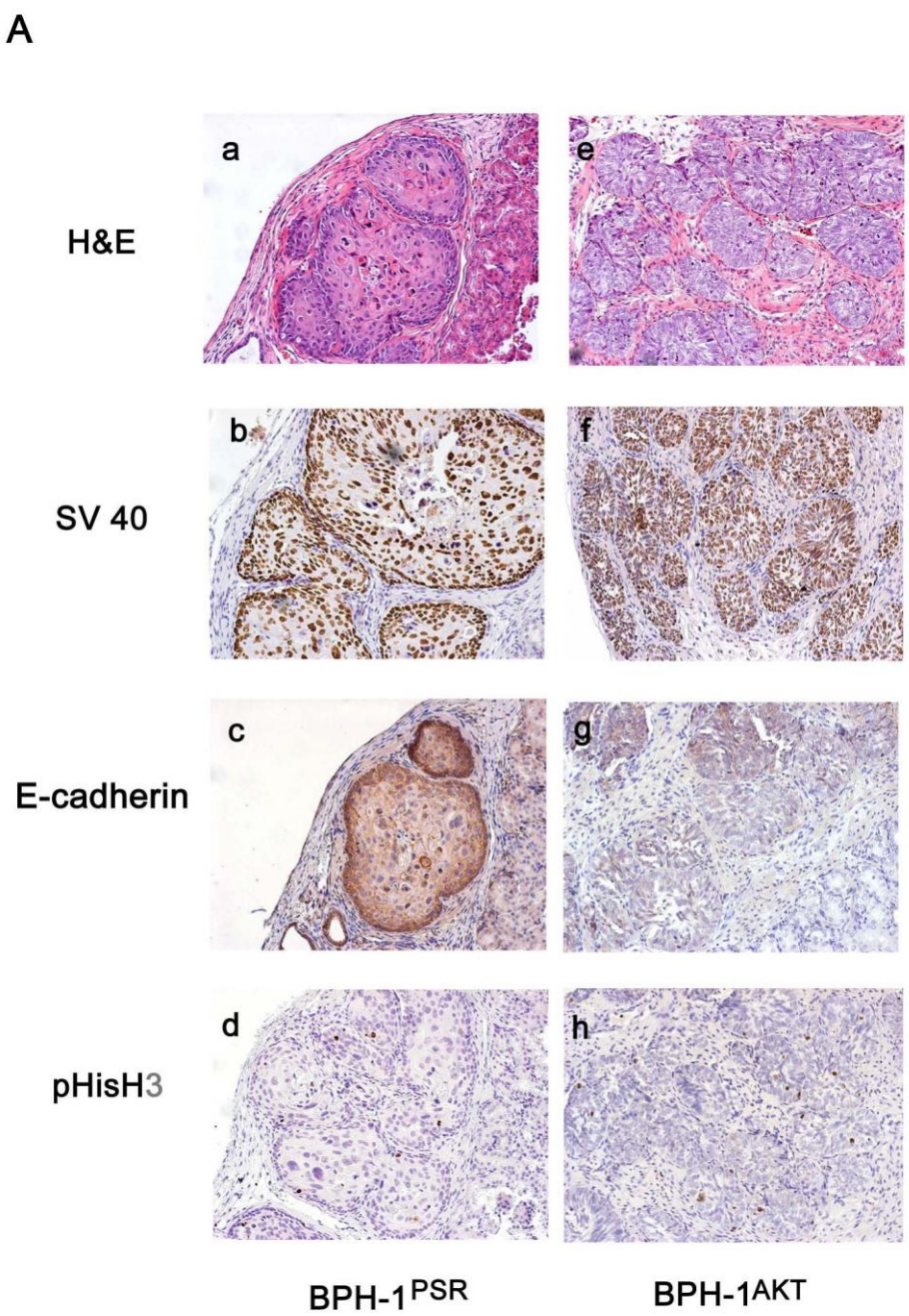

Figure 4-4. Activation of Akt signaling pathway elicited a atypical hyperplasia phenotype**.** (A) Both control grafts and Akt overexpressing grafts had no sign of invasion (a and e). BPH-1^{Akt} cells formed smaller solid cord structures and many cells had enlarged and elongated nuclei within the cords which indicated a atypical hyperplasia phenotype (e). Both BPH-1 and BPH-1^{Akt} cells continued to express SV-40 T antigen (b and f). Control grafts had clear cell junctions demonstrated by E-cadherin staining (c). E-cadherin expression was almost absent in the BPH-1^{Akt} cells (g). BPH-1^{Akt} cells have significantly increased number of pHisH3 positive cells throughout the grafts.

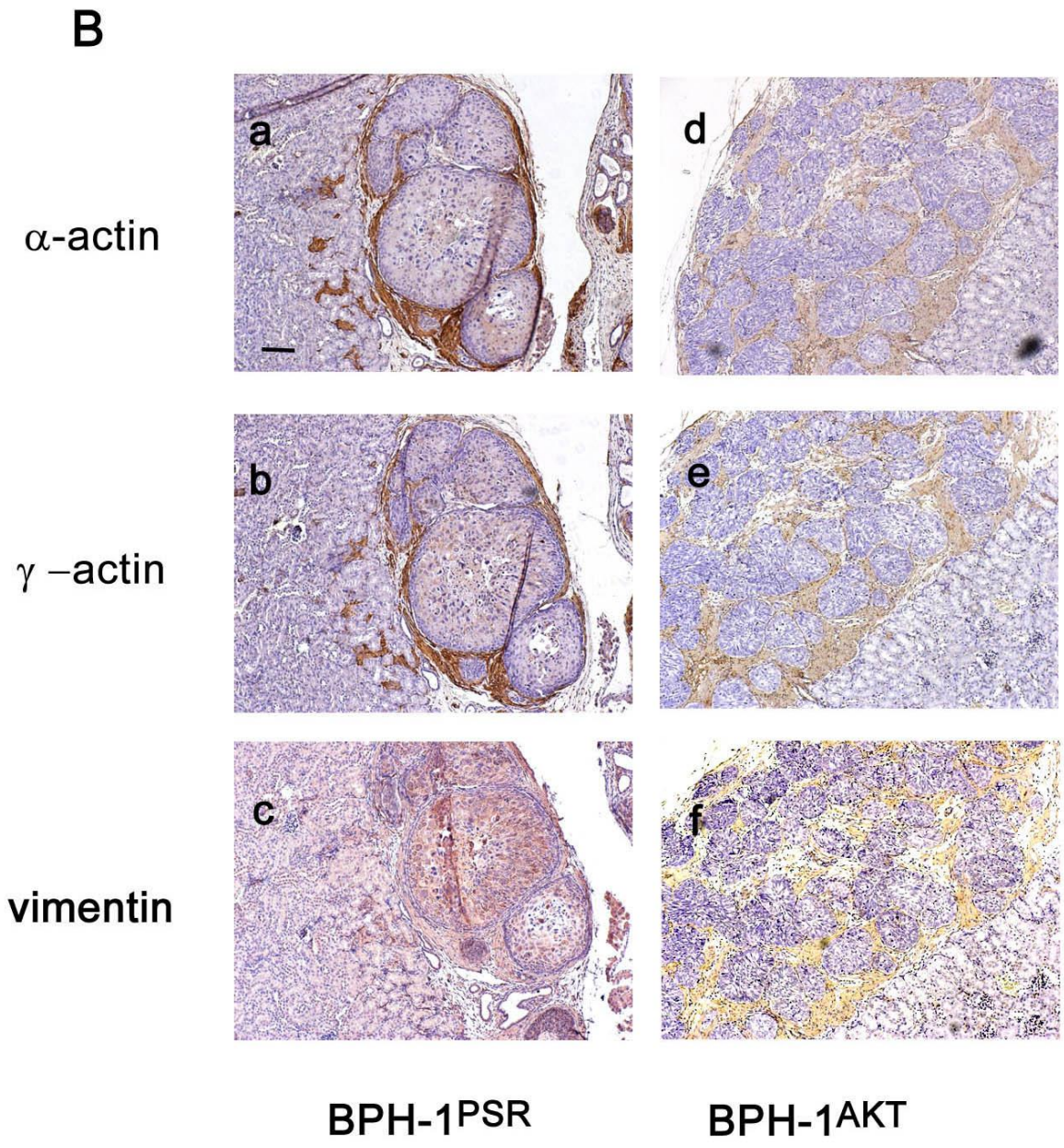

Figure 4-4 (B). Activation of Akt in BPH-1 cells caused a loss of stromal differentiation. The stromal cells in BPH-1 + rUGM tissue recombinants had abundant α-actin and γ-actin expression, but almost no vimentin expression (a, b and c). In stromal cells of BPH-1^{Akt} + rUGM tissue recombinants, there was suppression of α-actin expression (d) and induction of vimentin expression (f, arrow and I).

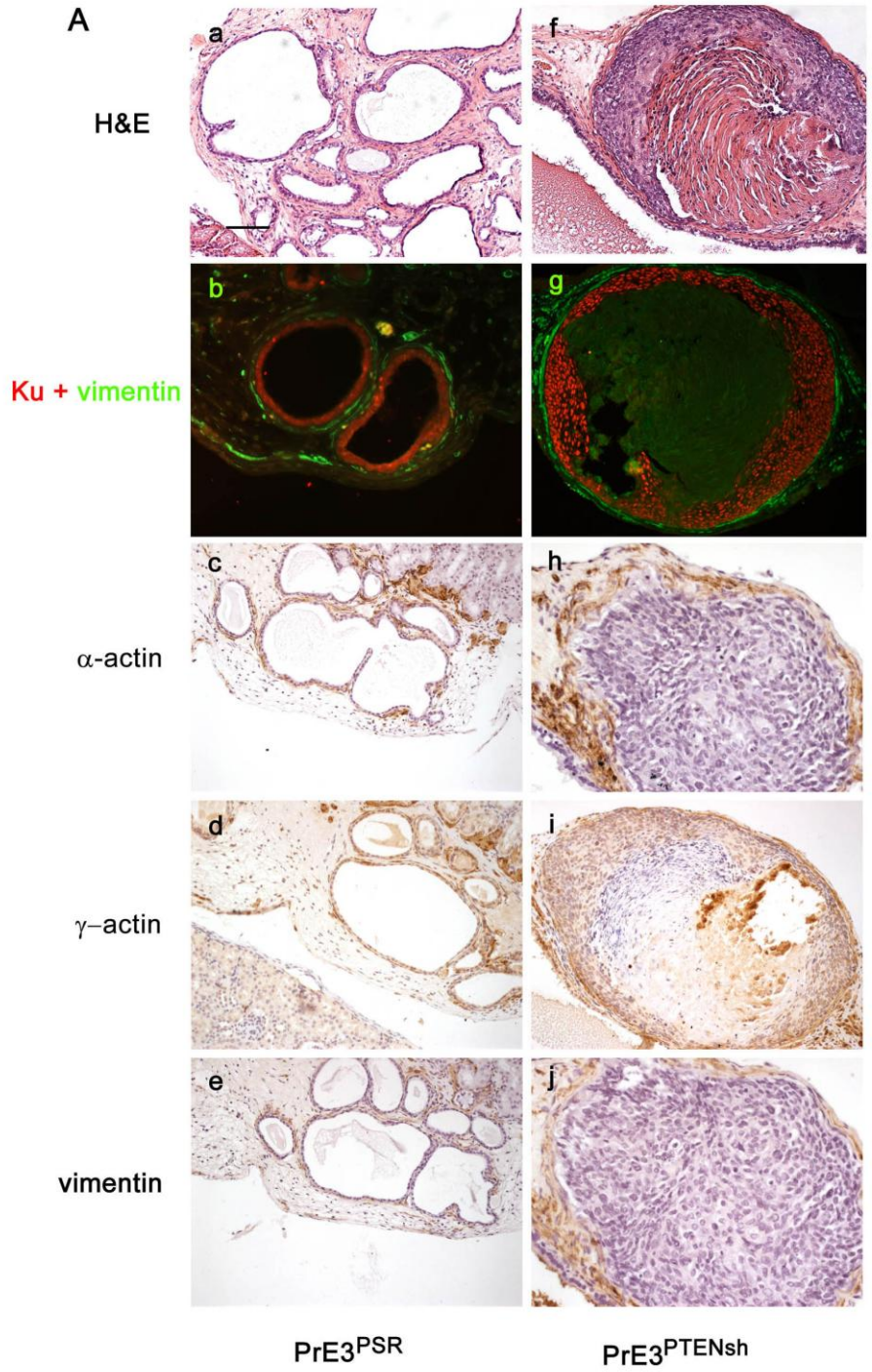

Figure 4-5. The effect of PTEN knock down is consistent by using a new human prostatic epithelial cells line. (A) $PrE3^{PSR}$ + rUGM tissue recombinants formed glandular structures after 5 months post grafting (a) with positive Ku 70 staining (b). $PrE3^{PTENsh}$ + rUGM tissue recombinants formed a PIN lesion (f). Cells continuously expressed Ku 70 (g) with induced vimentin expression (j). No obvious α–actin and γ-actin change was found in the PIN lesion (h and I) compared with control (c and d).

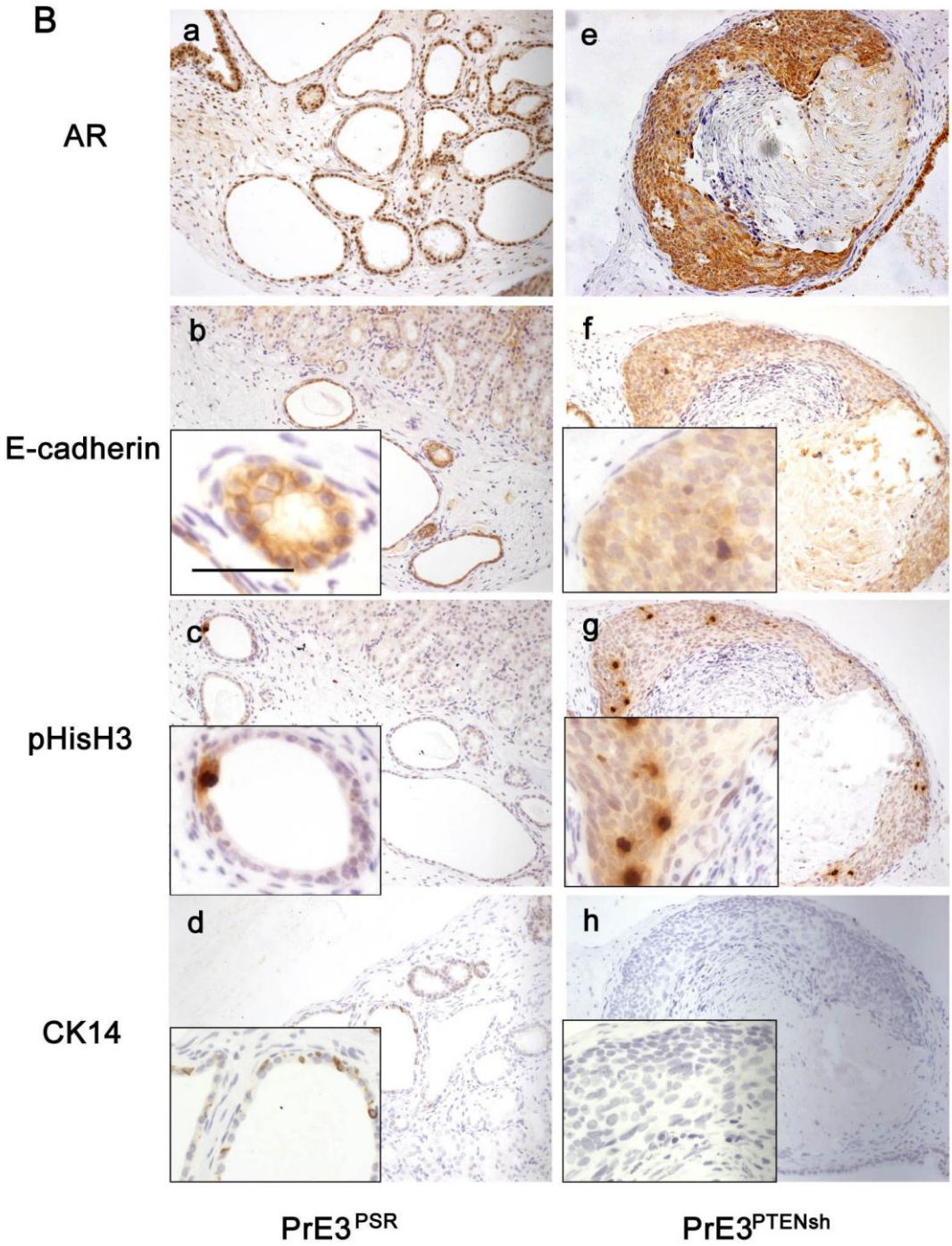

Figure 4-5 (B) Epithelial cells in both control and knock down recombinants continued to express AR (a and e). E-cadherin was positive in cell-cell junction of control recombinants (b), but E-cadherin expression was patchy in the PIN lesion (f). Increased pHisH3 positive cells in $PrE3^{PTENsh}$ cells ((g and inset (higher magnification)) than control $PrE3^{PSR}$ cells (c). CK 14 expression was negative in $PrE3^{PTENsh}$ cells (h), but the normal glands were CK14 expression in the basal layer (d).

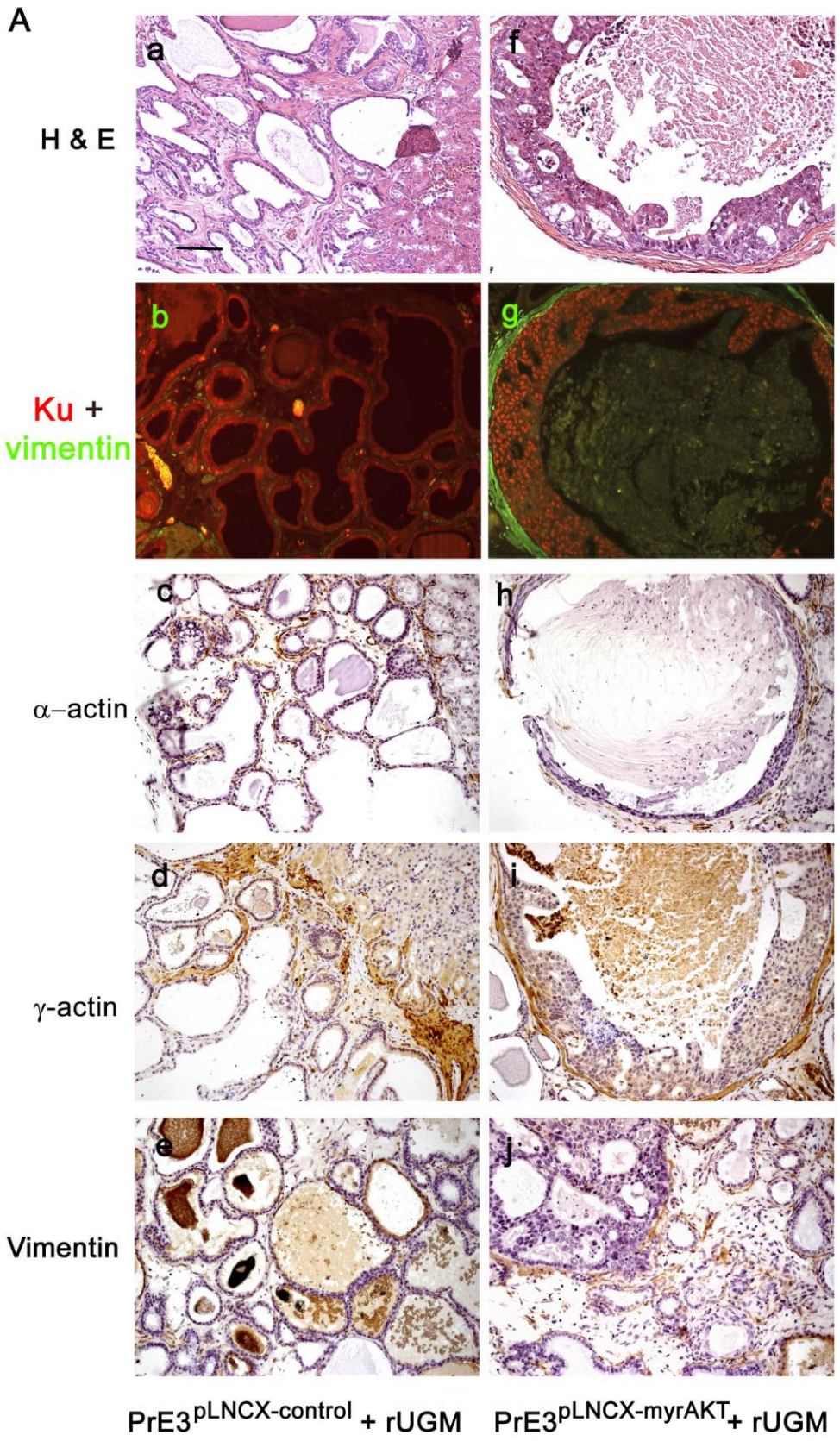

Figure 4-6. Constitutive expression of myrislated Akt in PrE3 cells caused a high grade cribriform PIN phenotype. (A) PrE3$^{pLNCX\text{-}control}$ + rUGM tissue recombinants formed glandular structures 5 months post grafting (a) with positive Ku 70 immunofluorescence

staining (b). In clear contrast, cells in PrE3$^{pLNCX\text{-}myr\text{-}Akt}$ + rUGM tissue recombinants formed a high grade PIN lesion in which cells fused into a big nest with enlarged nuclei (f). Cells continuously expressed Ku 70 (g) with induced vimentin expression (j). No obvious α–-actin and γ-actin change was found in the PIN lesion (h and i) compared with control (c and d).

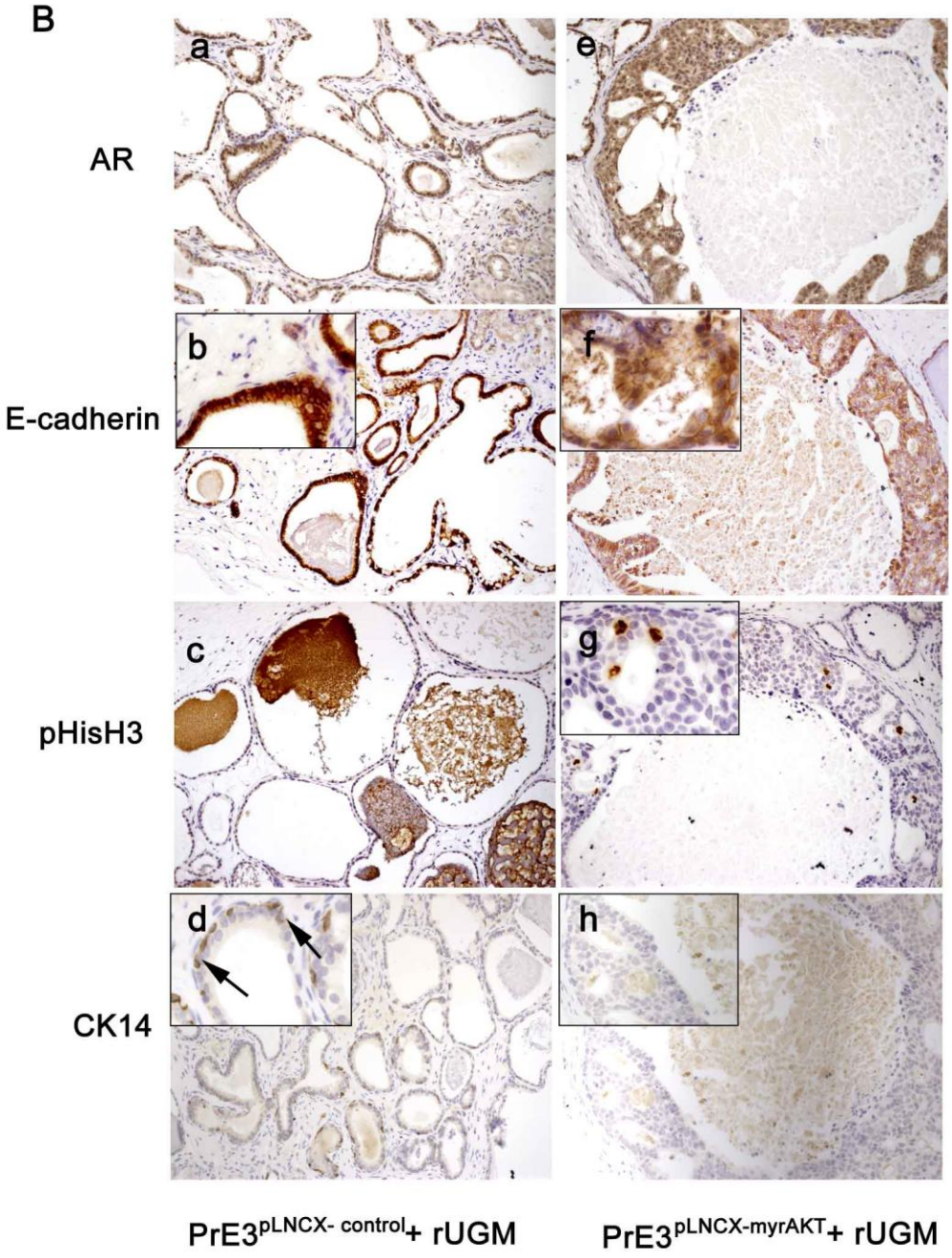

Figure 4-6 (B). Suppression of PTEN in less initiated prostate epithelial cells caused a hyperplasia phenotype. (B) Epithelial cells in both control and knock down recombinants continued to express AR (a and e). E-cadherin was positive at cell-cell junctions of control recombinants (b), but E-cadherin expression was lost in the PIN lesion (f). Increased pHisH3 positive cells in PrE3^{PTENsh} cells ((g and inset (higher magnification)) than control PrE3^{PSR} cells (c). CK 14 expression was negative in PrE3^{PTENsh} cells (h), but the normal glands retained CK14 expression in the basal layer (d).

Discussion

Loss of PTEN expression has been detected in many cancers including prostate (Di Cristofano et al., 2001; Di Cristofano et al., 1998). Elevation of Akt is a common response to the loss of the PTEN tumor suppressor gene (Cantley and Neel, 1999) and occurs frequently in human prostate cancer (Davies et al., 1999; Li et al., 1997). When PTEN activity was restored in PTEN null cells, Akt expression was suppressed, which directly links PTEN to Akt activity (Davies et al., 1999; Myers et al., 1998; Stambolic et al., 1998).

We determined that BPH-1 derived tumorigenic cell lines and a subset of prostate cancer cell lines had lower PTEN expression compared with parental BPH-1 and other non-malignant human prostatic epithelial cell lines. These molecular characteristics are consistent with differences between normal and malignant cells in primary prostate cancer, in which PTEN expression was downregulated in tumorigenic cells. Mutations, additions and deletions of PTEN genomic DNA were found in the noncoding 5'UTR of the PTEN gene in tumorigenic cells, but not in the benign parental BPH-1 cells. It has recently been reported that the long 5'UTR sequences of PTEN contains a promoter that is responsible for constitutive PTEN expression(Han et al., 2003). This promoter was mapped to the region between –551 and –220 bases upstream of the translation start site. The region where we found deletions contains multiple binding sites for transcription factors such as Sp1.Down-regulation of PTEN expression could be due to loss of this promoter activity (Ma et al., 2005a). Thus we speculate that PTEN downregulation in BPH-1^{CAFTD} cells may also due to loss of this second promoter activity. Deletions in this region my possibly affect

PTEN promoter activity in the 5'UTR. However, at this point it is not clear whether or not this area of the human 5'UTR contains the promoter and important transcription factor binding sites. In the future, a luciferase reporter assay should be performed to explore this hypothesis and to find candidate transcription factors which can constitutively activate the promoter in 5'UTR.

In this chapter, we made a PTEN knock down BPH-1 cell line to examine the consequences of loss of PTEN in benign prostate cells both *in vitro* and *in vivo.* BPH-1^{PTENsh} cells had enhanced proliferation, mobility, and invasion as compared with control cells. We were able to show that partial suppression of PTEN expression in the presence of SV40 was sufficient to drive human prostatic epithelium to form invasive tumors within the *in vivo* tissue recombination model. The BPH-1^{PTENsh} cells retained expression of SV-40 T antigen and proliferated faster than control cells *in vivo*. Retroviral infection of BPH-1 cells with the control plasmid resulted in a benign solid cord structure. Suppression of PTEN produces a cancer phenotype within our xenograft model that is progressive and invasive. The resulting tumors resemble a poorly differentiated invasive advanced carcinoma. A single addition of a dominant acting oncogene may be sufficient to convert a non-tumorigenetic cell to a fully tumorigenetic cell. Such as overexpression of c-MYC in benign prostate epithelium caused a cancer phenotype (Williams et al., 2005). This observation emphasized the importance of genetic changes as key determinants of malignancy. The BPH-1 cells were SV-40 T-antigen initiated, but this is insufficient *per se* to produce a tumor. The levels of PTEN suppression by a retroviral delivery system would

certainly constitute an additional molecular hit. The *in vitro* and *in vivo* data indicated the important role of PTEN in transformation of cells at early stages of tumor progression.

We went on to suppress PTEN in another initiated prostatic epithelial cell line (PrE3) and saw similar *in vivo* consequences to those seen in BPH-1 cells . However, PrE3 cells formed well differentiated glandular structures in the tissue recombination model. Knocking down PTEN in the PrE3 cells caused a PIN phenotype instead of an invasive tumor. To our knowledge, no data have been reported concerning the role of PTEN in initiating prostate cancer progression *in vivo* because of the lack of normal human prostatic cell lines. Our data provide new insights into the role of this lesion in prostate cancer progression.

Loss of PTEN expression can be a pivotal point in the cellular decision-making process that determines if a cell will undergo proliferation. PTEN suppression within the BPH-1 cells and PrE3 cells appeared to exhibit a proliferative effect which was demonstrated by elevation of pHisH3 positive cells. The lack of expression of the basal cell marker CK14 indicated that the PTEN knock down tumor, like human prostate adenocarcinoma, loses basal cells during tumor formation. The same phenomenon was also seen in PrE3^{PTENsh} PIN lesions. In the glands formed by PrE3 control cells, CK14 expressing cells clearly surrounded luminal cells, which confirmed the benign nature of these cells.

The hallmark of malignancy is the acquisition of an invasive phenotype. This process may

involve breakdown of cell-cell junctions, increased motility, and increased proliferation of the tumor cells. One of the cell-cell junction molecules, E-cadherin, exerts a critical role in the control of tumorigenicity. It is subjected to inactivation by multiple mechanisms including genetic and epigenetic events (Kotelevets et al., 2001). It was suggested that PTEN might participate in tumor cell invasion through stabilizing cell-cell junctions in kidney tumorigenic cell lines *in vitro* (Kotelevets et al., 2001). Transient reduction of PTEN expression by RNAi induces loss of cell adhesion (Mise-Omata et al., 2005). Our data suggested that when PTEN expression is partially lost in BPH-1 cells, they gained invasive ability and lost E-cadherin expression *in vivo*. The same phenomenon was seen in the PIN lesions formed by PrE3^{PTENsh} cells. Decreased or absent E-cadherin expression is a common occurrence in human prostate cancer (Rokhlin and Cohen, 1995; Umbas et al., 1992). Failure to detect E-cadherin expression may suggest cancer development in partial loss of PTEN model, which clearly correlates with the difference between normal and tumor cells in cancer patients.

Normal prostatic stroma predominantly expresses α-actin and γ–actin, but not vimentin, while tumor stroma expresses predominantly vimentin with some α–actin (Hayward et al., 1996). Our unpublished data demonstrated that LNCaP + rUGM tissue recombinants little α-actin expression and that most stromal cells had strong vimentin expression. This result correlated with the differences that we and others have seen in clinical samples. Our data suggested that partial loss of PTEN in epithelium resulted in a more fibroblastic/myofibroblastic stroma with a downregulation of α–actin and upregulation of

vimentin, consistent with a reactive stroma. These observations reflected the importance of PTEN in regulating stromal differentiation and thus stromal-epithelial interactions and in human prostate cancer progression. Homozygous deletion of PTEN is lethal, while heterozygote PTEN mice develop mPIN but only progress to an invasive phenotype after another genetic hit (Abate-Shen et al., 2003; Di Cristofano et al., 2001; Kim et al., 2002). In this human model we showed an accelerated progression after partial loss of PTEN in BPH-1 cells because the epithelium is already SV40 immortalized.

Akt is downstream PTEN signaling pathway and is constitutively activated in many cancers including prostate cancer (Nicholson and Anderson, 2002). We showed that the PTEN/Akt axis is important in human prostate cancer progression. Constitutive overexpression of Akt in both BPH-1 and PrE3 cells accelerated cell growth *in vivo*, demonstrated by increased numbers of pHisH3 positive cells. Out studies showed that loss of PTEN and constitutively activation of Akt protein can have dramatically different effects on tumor physiology. The recombinant of BPH-1^{Akt} + rUGM formed an atypical hyperplasia structure instead of an invasive tumor. A critical downstream effector of Akt, which contributes to tumorigenesis, is mTOR (Hay and Sonenberg, 2004). Constitutively Akt activation activates mTOR and at the same time mTOR activation inhibits Akt via an inhibitory feedback mechanism to controls cell proliferation and tumor progression. However, the loss of even one copy of PTEN may be sufficient to overcome this feedback mechanism, reactivate Akt, and dramatically enhance tumor severity and produce a different phenotype (Manning et al., 2005).

Since PrE3 cells formed benign glandular structures, which indicated a less initiated phenotype compared with BPH-1 cells, which loss the ability to form glandular structure. The more aggressive PIN structures in PrE3$^{myr\text{-}Akt}$ grafts suggested that Akt activation is a further downstream effect of PTEN loss in human prostate cancer. The phenotype of the tissue recombinants was similar to what was seen in PTEN knock down recombinants. The present study demonstrated the contribution of an individual gene to carcinogenesis. This is an approach which we have successfully applied to the overexpression of the c-myc proto-oncogene in human prostatic epithelial cells resulted in a new *in vivo* model in which benign human prostatic epithelial cells undergo malignant transformation to form metastatic tumors with continued expression of key markers such as PSA and AR.

In summary, our current work developed less aggressive models representing distinct grades of disease, with defined stage progression. Such models can be a target of molecular interrogation to determine how common genetic alterations affect prostate cancer phenotypes and lead to further genetic changes in response to common therapeutic strategies such as androgen ablation.

CHAPTER V

CONCLUSIONS AND FUTURE DIRECTIONS

The stromal microenvironment can either positively or negatively regulate tumor progression, however it is still unclear why the environment plays a dual role. The mechanistic basis for stromal programming is not completely understood. Many molecules and pathways play important roles in controlling proliferation, differentiation, and function of both epithelial and stromal cells. In adulthood, normal prostatic epithelial growth is regulated by reciprocal interactions between smooth muscle and epithelial cells. These interactions are mediated by the local synthesis and action of paracrine signaling molecules (Hayward et al., 1997). Signaling abnormalities between smooth muscle and epithelial cells may either actively promote carcinogenesis or permit the progression to anaplasia via loss of normal homeostatic controls (Hayward et al., 1998). Leland Chung's group reported that co-inoculation of tumorigenic Nbf-1 fibroblasts (an androgen-sensitive rat prostate fibroblast cell line) with human PC-3 cells accelerated tumor growth (Chung, 1995; Chung et al., 1981; Chung et al., 1991). The Cunha laboratory has indicated, using an *in vivo* model, that CAFs were capable of stimulating carcinogenesis and inducing the malignant progression of an initiated epithelium (BPH-1 cell line), while normal prostatic fibroblasts were incapable of stimulating such progression (Hayward et al., 2001; Olumi et al., 1999; Orimo et al., 2005)Other laboratories have made observations consistent with this result (Barclay et al., 2005; Hayward et al., 2001; Olumi et al., 1999; Orimo et al., 2005). Thus, the process of

prostatic carcinogenesis may include aberrations in the interactions of the prostatic epithelium, with its smooth muscle microenvironment resulting in reciprocal de-differentiation of both the emerging carcinoma cells and the prostatic smooth muscle. It is also possible that the stromal changes observed occur through the recruitment of other cell types such as macrophages or other bone marrow-derived cells. A detailed understanding of the signaling mechanisms between stroma and epithelium will allow design of therapies aimed at inhibiting prostate tumor growth. We have found that TGF-β expression is elevated in CAFs versus normal prostatic fibroblasts, which promotes invasion of tumorigenic but not non-tumorigenic cell lines (Ao et al., 2006). Crosstalk between a paracrine-acting cytokine (TGF-β) and chemokine pathways (SDF-1/CXCR4) promotes malignant progression of BPH-1 cells (Ao et al., 2007). Recently, it was shown that TGF-β is one of the fibroblast-supplied factors involved in suppression of epithelial transformation (Bhowmick et al., 2004a; Bhowmick et al., 2004b). Loss of TGF-β responsiveness in fibroblasts resulted in PIN through the activation of the paracrine hepatocyte growth factor (HGF) pathway (Bhowmick et al., 2004a; Bhowmick et al., 2004b). These data indicate that TGF-β inhibits cell growth in non-transformed prostatic cells, but functions in a pro-oncogenic manner in transformed prostatic cells. TGF-β is one important paracrine mediator of stromal-epithelial interactions, and is essential for stromal programming to promote adjacent epithelial tumor progression. However, the paracrine environment is complex and other important mediators of paracrine signaling and tumor progression that are waiting to be investigated. Changes in the epithelial and

stromal cells which modulate this signaling environments are not well understood and are a focus of this work.

In chapter II, I examined the consequences of manipulating cell proliferation in both epithelial and stromal cells by overexpressing cyclin D1. I observed that cyclin D1 overexpressing BPH-1 cells did not become tumorigenic under the influence of inductive rUGM in the tissue recombination model. However, the cyclin D1 overexpressing cells did have a higher proliferation rate *in vitro* and *in vivo*. These data underline the important point that increased proliferation *per se* is insufficient for malignant transformation of epithelial cells even in the face of SV-40 T-antigen expression. However, overexpression of cyclin D1 in NPF cells is sufficient to drive adjacent BPH-1 cells to become tumorigenic, an observation confirmed by the transformation of BPH-1$^{\text{NPF-cyclin D1}}$ cells. These observations indicate that upregulation of proliferation as well as changes in stromal gene expression can change the environment to promote carcinogenesis in less damaged epithelium. This underlines the idea that carcinoma is not solely a disease of epithelial cells but is a product of both the damaged epithelium and an altered microenvironment.

In chapter III, I proposed a possible mechanism for prostate cancer progression which involved stromal-epithelial interactions. Our data indicated that cathepsin D is a crucial mediator between BPH-1 and either NPF$^{\text{cyclin D1}}$ or CAFs *in vitro* and *in vivo*. Cathepsin D is upregulated in both NPF$^{\text{cyclin D1}}$ cells and CAFs as determined by microarray and western

blot analysis. My study demonstrated that cathepsin D plays a crucial role in prostatic fibroblast outgrowth and may favor prostate tumor progression acting via a paracrine loop. Cathepsin D is overexpressed and secreted by fibroblasts, and is captured *in vivo* by epithelial cells. The resultant cathepsin D overexpression in tumor epithelium promotes proliferation, motility, and invasion of epithelium and consequently enhances tumor-host homeostasis. The identification of factors such as cathepsin D that participate in the tumor-stroma communication might be crucial for the development of stromally-targeted therapy of prostate cancer.

In chapter IV, I defined the role of clinically observed genetic lesions in deregulating stromal differentiation. The ability of epithelial cells with defined alterations to establish and maintain smooth muscle differentiation in adjacent stromal cells was examined. Partial suppression of PTEN in the presence of SV40T expression is sufficient to initiate malignant transformation of human prostatic epithelium and caused high-grade PIN in benign PrEs. The ability of human prostatic epithelial cells to induce and maintain smooth muscle differentiation in adjacent stroma was shown to be negatively correlated to the level of genetic damage sustained by those epithelial cells.

The aim of this project was to examine how an oncogene (cyclin D1) and a tumor suppressor (PTEN) might affect stromal-epithelial interactions with the goal of building new models of human prostate cancer *in vivo*. A summary of this project is shown in Figure 5-1. Specifically, expression of cyclin D1 or PTEN are either positively or

negatively regulated in human prostatic epithelial or stromal cells. The effects of these changes are then assessed in tissue recombination models. This approach has been successfully applied to the overexpression of the c-myc proto-oncogene in human prostatic epithelial cells resulting in malignant transformation to form metastatic tumors with continued expression of key molecules such as PSA and the androgen receptor (Williams et al., 2005). In this project, we aimed to develop less aggressive models that represent distinct grades of disease. Such models can be a target of molecular interrogation to determine how these common genetic alterations affect prostate cancer phenotypes and lead to further genetic changes in response to common therapeutic strategies such as androgen ablation.

In summary, I found that by manipulating the proliferation of stromal fibroblasts by overexpressing cyclin D1 could alter the microenvironment resulting in the transformation of initiated BPH-1 cells through paracrine signaling. Cathepsin D was proposed to be an important mediator in these stromal-epithelial interactions. I also found that genetically modified epithelium (loss of PTEN) had reduced ability to induce and/or maintain smooth muscle differentiation in adjacent stromal cells, consistent with changes seen in the stromal cells adjacent to tumors in clinical samples.

Cyclin D1 degradation is mediated by phosphorylation and ubiquitin-dependent proteolysis (Diehl et al., 1997). Glycogen synthase kinase-3ß (GSK-3β) phosphorylates cyclin D1 leading to cyclin D1 ubiquitination and proteasomal degradation (Diehl et al., 1998). GSK-3β is phosphorylated and deactivated by Akt and GSK-3β activity is elevated

by overexpression of PTEN (Ohigashi et al., 2005). When PTEN expression is knocked down, GSK-3β activity is reduced and less cyclin D1 is degraded by phosphorylation. However, the accumulation of cyclin D1 in epithelial cells are not enough to drive cells to undergo malignant transformation. In addition to its role in regulating the AKT cell survival pathway, PTEN also suppresses the mitogen-activated protein (MAP) kinase signaling pathway and interact with integrin signaling pathways. Therefore, the phenotypes in PTEN knocked down cell in epithelial cells may be caused by cyclin D1-independent pathways. In the future, MAP kinase and integrin pathways will be examined if they are involved in the invasive phenotype in BPH-1^{PTENsh} cells. I examined the function of PTEN in epithelial cells in this project. However, the function of PTEN in stromal environment is waiting to be dissected and the link between PTEN and cyclin D1 in stroma can be studies in the future.

Prostate cancer research has been hindered by lack of well established, characterized, immortalized benign prostatic epithelial cells lines that express markers of normal prostatic epithelial cells. Such cells can be used to study multi-step carcinogenesis, cancer progression, and potential therapeutic agents to inhibit prostate cancer growth. The BPH-1 cell line is one such cell line that has been widely used in prostate cancer research. It is by far the only line which starts off benign an can be pushed to a malignant phenotype by either genetic modification or hormone treatment. The cells do not form tumors in SCID mice until 1 year post-grafting, which makes them an appropriate model to study tumor progression and stromal-epithelial interactions. However, BPH-1 cells are

SV-40 immortalized, and they do not form glandular structures *in vivo*. Dr. Ming Jiang in our laboratory developed a spontaneously immortalized prostate epithelial cell line, which is designated as PrE1. These cells give rise to normal glandular structure when recombined with rUGM. In the future, more genes and pathways which might be involved in stromal-epithelial interactions can be fully investigated using this new prostatic epithelial cell line.

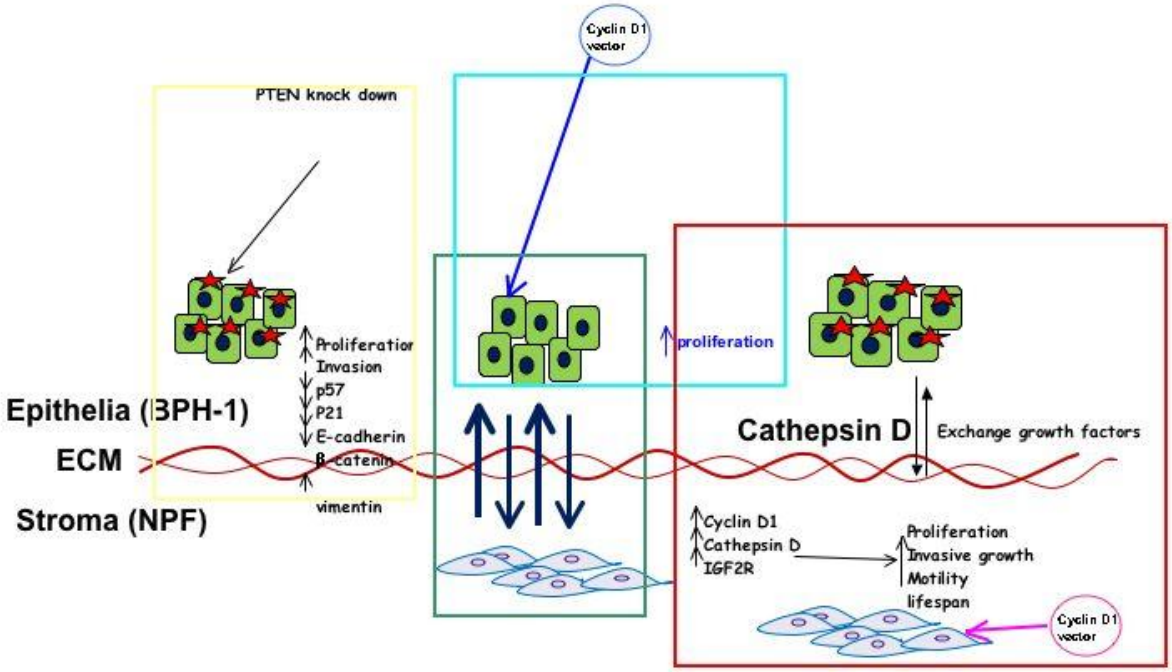

Figure 5-1. Working model of this project. Cyclin D1 overexpressing BPH-1 cells did not become tumorigenic under the influence of inductive rUGM in the tissue recombination model. However, overexpression of cyclin D1 in NPF cells is sufficient to drive adjacent BPH-1 cells to become tumorigenic possibly through upregulation of cathepsin D. Partial suppression of PTEN in the presence of SV40-T antigen expression is sufficient to initiate malignant transformation of human prostatic epithelium and caused high-grade PIN in benign PrE. The ability of human prostatic epithelial cells to induce and maintain smooth muscle differentiation in adjacent stroma was shown to be negatively correlated to the level of genetic damage sustained by those epithelial cells.

REFERENCES

Abate-Shen, C., Banach-Petrosky, W. A., Sun, X., Economides, K. D., Desai, N., Gregg, J. P., Borowsky, A. D., Cardiff, R. D., and Shen, M. M. (2003). Nkx3.1; Pten Mutant Mice Develop Invasive Prostate Adenocarcinoma and Lymph Node Metastases. Cancer Res *63*, 3886-3890.

Abate-Shen, C., and Shen, M. M. (2002). Mouse models of prostate carcinogenesis. Trends Genet *18*, S1-5.

Ablin, R. J. (1997). A retrospective and prospective overview of prostate-specific antigen. J Cancer Res Clin Oncol *123*, 583-594.

Amsellem-Ouazana, D., Younes, P., Conquy, S., Peyromaure, M., Flam, T., Debre, B., and Zerbib, M. (2005). Negative prostatic biopsies in patients with a high risk of prostate cancer. Is the combination of endorectal MRI and magnetic resonance spectroscopy imaging (MRSI) a useful tool? A preliminary study. Eur Urol *47*, 582-586.

Anderson, K. M., and Liao, S. (1968). Selective retention of dihydrotestosterone by prostatic nuclei. Nature *219*, 277-279.

Ao, M., Franco, O. E., Park, D., Raman, D., Williams, K., and Hayward, S. W. (2007). Cross-talk between paracrine-acting cytokine and chemokine pathways promotes malignancy in benign human prostatic epithelium. Cancer Res *67*, 4244-4253.

Ao, M., Williams, K., Bhowmick, N. A., and Hayward, S. W. (2006). Transforming growth factor-ß promotes invasion in tumorigenic but not in non-tumorigenic human prostatic epithelial cells. Cancer Research *66*, 8007-8016.

Arnold, A., and Papanikolaou, A. (2005). Cyclin D1 in breast cancer pathogenesis. J Clin Oncol *23*, 4215-4224.

Aumuller, G. (1989). [Functional morphology of the prostate]. Urologe A *28*, 306-310.

Aumuller, G., and Seitz, J. (1990). Protein secretion and secretory processes in male accessory sex glands. Int Rev Cytol *121*, 127-231.

Ayala, G., Tuxhorn, J. A., Wheeler, T. M., Frolov, A., Scardino, P. T., Ohori, M., Wheeler, M., Spitler, J., and Rowley, D. R. (2003). Reactive stroma as a predictor of biochemical-free recurrence in prostate cancer. Clin Cancer Res *9*, 4792-4801.

Bacac, M., Provero, P., Mayran, N., Stehle, J. C., Fusco, C., and Stamenkovic, I. (2006). A mouse stromal response to tumor invasion predicts prostate and breast cancer patient survival. PLoS ONE *1*, e32.

Barclay, W. W., Woodruff, R. D., Hall, M. C., and Cramer, S. D. (2005). A system for studying epithelial-stromal interactions reveals distinct inductive abilities of stromal cells from benign prostatic hyperplasia and prostate cancer. Endocrinology *146*, 13-18.

Bartkova, J., Lukas, J., Strauss, M., and Bartek, J. (1995). Cyclin D1 oncoprotein aberrantly accumulates in malignancies of diverse histogenesis. Oncogene *10*, 775-778.

Basset, P., Bellocq, J. P., Wolf, C., Stoll, I., Hutin, P., Limacher, J. M., Podhajcer, O. L., Chenard, M. P., Rio, M. C., and Chambon, P. (1990). A novel metalloproteinase gene specifically expressed in stromal cells of breast carcinomas. Nature *348*, 699-704.

Bautista, O. M., Kusek, J. W., Nyberg, L. M., McConnell, J. D., Bain, R. P., Miller, G., Crawford, E. D., Kaplan, S. A., Sihelnik, S. A., Brawer, M. K., and Lepor, H. (2003). Study design of the Medical Therapy of Prostatic Symptoms (MTOPS) trial. Control Clin Trials *24*, 224-243.

Bavik, C., Coleman, I., Dean, J. P., Knudsen, B., Plymate, S., and Nelson, P. S. (2006). The gene expression program of prostate fibroblast senescence modulates neoplastic epithelial cell proliferation through paracrine mechanisms. Cancer Res *66*, 794-802.

Bello, D., Webber, M. M., Kleinman, H. K., Wartinger, D. D., and Rhim, J. S. (1997). Androgen responsive adult human prostatic epithelial cell lines immortalized by human papillomavirus 18. Carcinogenesis *18*, 1215-1223.

Berchem, G., Glondu, M., Gleizes, M., Brouillet, J. P., Vignon, F., Garcia, M., and Liaudet-Coopman, E. (2002). Cathepsin-D affects multiple tumor progression steps in vivo: proliferation, angiogenesis and apoptosis. Oncogene *21*, 5951-5955.

Bergh, J., Marklund, I., Gustavsson, C., Wiklund, F., Gronberg, H., Allard, A., Alexeyev, O., and Elgh, F. (2007). No link between viral findings in the prostate and subsequent cancer development. Br J Cancer *96*, 137-139.

Berry, S. J., Coffey, D. S., Walsh, P. C., and Ewing, L. L. (1984). The development of human benign prostatic hyperplasia with age. J Urol *132*, 474-479.

Bhowmick, N. A., Chytil, A., Plieth, D., Gorska, A. E., Dumont, N., Shappell, S., Washington, M. K., Neilson, E. G., and Moses, H. L. (2004a). TGF-beta signaling in fibroblasts modulates the oncogenic potential of adjacent epithelia. Science *303*, 848-851.

Bhowmick, N. A., Neilson, E. G., and Moses, H. L. (2004b). Stromal fibroblasts in cancer initiation and progression. Nature *432*, 332-337.

Bloom, J. R., Stewart, S. L., Oakley-Girvans, I., Banks, P. J., and Chang, S. (2006). Family history, perceived risk, and prostate cancer screening among African American men. Cancer Epidemiol Biomarkers Prev *15*, 2167-2173.

Bosman, F. T., de Bruine, A., Flohil, C., van der Wurff, A., ten Kate, J., and Dinjens, W. W. (1993). Epithelial-stromal interactions in colon cancer. Int J Dev Biol *37*, 203-211.

Bostwick, D. G. (2000). Prostatic intraepithelial neoplasia. Curr Urol Rep *1*, 65-70.

Bostwick, D. G., and Brawer, M. K. (1987). Prostatic intra-epithelial neoplasia and early invasion in prostate cancer. Cancer *59*, 788-794.

Bostwick, D. G., Cooner, W. H., Denis, L., Jones, G. W., Scardino, P. T., and Murphy, G. P. (1992). The association of benign prostatic hyperplasia and cancer of the prostate. Cancer *70*, 291-301.

Bruchovsky, N., and Wilson, J. D. (1968). The conversion of testosterone to 5-α-androstan-17-beta-ol-3-one by rat prostate in vivo and in vitro. J Biol Chem *243*, 2012-2021.

Bubendorf, L., Kononen, J., Koivisto, P., Schraml, P., Moch, H., Gasser, T. C., Willi, N., Mihatsch, M. J., Sauter, G., and Kallioniemi, O. P. (1999). Survey of gene amplifications during prostate cancer progression by high-throughout fluorescence in situ hybridization on tissue microarrays. Cancer Res *59*, 803-806.

Caldon, C. E., Daly, R. J., Sutherland, R. L., and Musgrove, E. A. (2006). Cell cycle control in breast cancer cells. J Cell Biochem *97*, 261-274.

Cantley, L. C., and Neel, B. G. (1999). New insights into tumor suppression: PTEN suppresses tumor formation by restraining the phosphoinositide 3-kinase/AKT pathway. Proc Natl Acad Sci U S A *96*, 4240-4245.

Chen, Y., Martinez, L. A., LaCava, M., Coghlan, L., and Conti, C. J. (1998). Increased cell growth and tumorigenicity in human prostate LNCaP cells by overexpression to cyclin D1. Oncogene *16*, 1913-1920.

Cherry, J. P., Mordente, J. A., Chapman, J. R., Choudhury, M. S., Tazaki, H., Mallouh, C., and Konno, S. (1998). Analysis of cathepsin D forms and their clinical implications in human prostate cancer. J Urol *160*, 2223-2228.

Chiquet-Ehrismann, R., Mackie, E. J., Pearson, C. A., and Sakakura, T. (1986). Tenascin: an extracellular matrix protein involved in tissue interactions during fetal development and oncogenesis. Cell *47*, 131-139.

Chung, L. W. (1991). Fibroblasts are critical determinants in prostatic cancer growth and dissemination. Cancer Metastasis Rev *10*, 263-274.

Chung, L. W. (1995). The role of stromal-epithelial interaction in normal and malignant growth. Cancer Surv *23*, 33-42.

Chung, L. W. K., Anderson, N. G., Neubauer, B. L., Cunha, G. R., Thompson, T. C., and Rocco, A. K. (1981). Tissue interactions in prostate development: roles of sex steroids. In The Prostatic Cell: Structure and Function Part A., G. P. Murphy, A. A. Sandberg, and J. P. Karr, eds. (New York, A. R. Liss.), pp. 177-203,.

Chung, L. W. K., and Cunha, G. R. (1983). Stromal-epithelial interactions. II. Regulation of prostatic growth by embryonic urogenital sinus mesenchyme. Prostate *4*, 503-511.

Chung, L. W. K., Gleave, M. E., Hsieh, J.-T., Hong, S.-J., and Zhau, H. E. (1991). Reciprocal mesenchymal-epithelial interaction affecting prostate tumour growth and hormonal responsiveness. In Prostate Cancer: Cell and Molecular Mechanisms in Diagnosis and Treatment, J. T. Isaacs, ed. (Cold Spring Harbor, Cold Spring Harbor Laboratory Press), pp. 91-122.

Coffey, D. S., and Pienta, K. J. (1987). New concepts in studying the control of normal and cancer growth of the prostate. In Current Concepts and Approaches to the Study of Prostate Cancer, D. S. Coffey, N. Bruchovsky, W. A. Gardner, J. Resnick, and J. P. Karr, eds. (New York, A.R. Liss), pp. 1-73.

Cunha, G. R. (1975). Age-dependent loss of sensitivity of female urogenital sinus to androgenic conditions as a function of the epithelia-stromal interaction in mice. Endocrinology *97*, 665-673.

Cunha, G. R., Alarid, E. T., Turner, T., Donjacour, A. A., Boutin, E. L., and Foster, B. A. (1992). Normal and abnormal development of the male urogenital tract: Role of androgens, mesenchymal-epithelial interactions and growth factors. J Androl *13*, 465-475.

Cunha, G. R., Donjacour, A. A., Cooke, P. S., Mee, S., Bigsby, R. M., Higgins, S. J., and Sugimura, Y. (1987). The endocrinology and developmental biology of the prostate. Endocr Rev *8*, 338-362.

Cunha, G. R., Fujii, H., Neubauer, B. L., Shannon, J. M., Sawyer, L., and Reese, B. A. (1983). Epithelial-mesenchymal interactions in prostatic development. I. morphological observations of prostatic induction by urogenital sinus mesenchyme in epithelium of the adult rodent urinary bladder. J Cell Biol *96*, 1662-1670.

Cunha, G. R., Hayward, S. W., and Wang, Y. Z. (2002). Role of stroma in carcinogenesis of the prostate. Differentiation *70*, 473-485.

Cunha, G. R., Hayward, S. W., Wang, Y. Z., and Ricke, W. A. (2003). Role of the stromal microenvironment in carcinogenesis of the prostate. Int J Cancer *107*, 1-10.

Cunha, G. R., Reese, B. A., and Sekkingstad, M. (1980). Induction of nuclear androgen-binding sites in epithelium of the embryonic urinary bladder by mesenchyme of the urogenital sinus of embryonic mice. Endocrinology *107*, 1767-1770.

Cunha, G. R., Ricke, W., Thomson, A., Marker, P. C., Risbridger, G., Hayward, S. W., Wang, Y. Z., Donjacour, A. A., and Kurita, T. (2004). Hormonal, cellular, and molecular regulation of normal and neoplastic prostatic development. J Steroid Biochem Mol Biol *92*, 221-236.

Cunha, G. R., and Young, P. (1992). Role of stroma in oestrogen-induced epithelial proliferation. Epithelial Cell Biol *1*, 18-31.

Dai, W. S., Gutai, J. P., Kuller, L. H., and Cauley, J. A. (1988). Cigarette smoking and serum sex hormones in men. Am J Epidemiol *128*, 796-805.

Dalrymple, S., Antony, L., Xu, Y., Uzgare, A. R., Arnold, J. T., Savaugeot, J., Sokoll, L. J., De Marzo, A. M., and Isaacs, J. T. (2005). Role of notch-1 and E-cadherin in the differential response to calcium in culturing normal versus malignant prostate cells. Cancer Res *65*, 9269-9279.

Damber, J. E. (1998). Prostate cancer: epidemiology and risk factors. Curr Opin Urol *8*, 375-380.

Davies, M. A., Koul, D., Dhesi, H., Berman, R., McDonnell, T. J., McConkey, D., Yung, W. K., and Steck, P. A. (1999). Regulation of Akt/PKB activity, cellular growth, and apoptosis in prostate carcinoma cells by MMAC/PTEN. Cancer Res *59*, 2551-2556.

Day, K. C., McCabe, M. T., Zhao, X., Wang, Y., Davis, J. N., Phillips, J., Von Geldern, M., Ried, T., KuKuruga, M. A., Cunha, G. R., *et al.* (2002). Rescue of embryonic epithelium reveals that the homozygous deletion of the retinoblastoma gene confers growth factor independence and immortality but does not influence epithelial differentiation or tissue morphogenesis. J Biol Chem *277*, 44475-44484.

De Cosse, J., Gossens, C. L., and Kuzma, J. F. (1973). Breast Cancer: Induction of differentiation by embryonic tissue. Science *181*, 1057-1058.

De Marzo, A. M., Platz, E. A., Sutcliffe, S., Xu, J., Gronberg, H., Drake, C. G., Nakai, Y., Isaacs, W. B., and Nelson, W. G. (2007). Inflammation in prostate carcinogenesis. Nat Rev Cancer *7*, 256-269.

DeMarzo, A. M., Nelson, W. G., Isaacs, W. B., and Epstein, J. I. (2003). Pathological and molecular aspects of prostate cancer. Lancet *361*, 955-964.

Dennis, L. K., Lynch, C. F., and Torner, J. C. (2002). Epidemiologic association between prostatitis and prostate cancer. Urology *60*, 78-83.

Di Cristofano, A., De Acetis, M., Koff, A., Cordon-Cardo, C., and Pandolfi, P. P. (2001). Pten and p27KIP1 cooperate in prostate cancer tumor suppression in the mouse. Nat Genet *27*, 222-224.

Di Cristofano, A., Pesce, B., Cordon-Cardo, C., and Pandolfi, P. P. (1998). Pten is essential for embryonic development and tumour suppression. Nat Genet *19*, 348-355.

Diehl, J. A., Cheng, M., Roussel, M. F., and Sherr, C. J. (1998). Glycogen synthase kinase-3beta regulates cyclin D1 proteolysis and subcellular localization. Genes Dev *12*, 3499-3511.

Diehl, J. A., Zindy, F., and Sherr, C. J. (1997). Inhibition of cyclin D1 phosphorylation on threonine-286 prevents its rapid degradation via the ubiquitin-proteasome pathway. Genes Dev *11*, 957-972.

Dunning, W. F. (1963). Prostate cancer in the rat. Nat'l Cancer Inst Monogr *12*, 351-370.

Ellwood-Yen, K., Graeber, T. G., Wongvipat, J., Iruela-Arispe, M. L., Zhang, J., Matusik, R., Thomas, G. V., and Sawyers, C. L. (2003). Myc-driven murine prostate cancer shares molecular features with human prostate tumors. Cancer Cell *4*, 223-238.

Feng, P., Li, T. L., Guan, Z. X., Franklin, R. B., and Costello, L. C. (2002). Direct effect of zinc on mitochondrial apoptogenesis in prostate cells. Prostate *52*, 311-318.

Ferrandina, G., Scambia, G., Bardelli, F., Benedetti Panici, P., Mancuso, S., and Messori, A. (1997). Relationship between cathepsin-D content and disease-free survival in node-negative breast cancer patients: a meta-analysis. Br J Cancer *76*, 661-666.

Ferrini, R. L., and Barrett-Connor, E. (1998). Sex hormones and age: a cross-sectional study of testosterone and estradiol and their bioavailable fractions in community-dwelling men. Am J Epidemiol *147*, 750-754.

Foekens, J. A., Look, M. P., Bolt-de Vries, J., Meijer-van Gelder, M. E., van Putten, W. L., and Klijn, J. G. (1999). Cathepsin-D in primary breast cancer: prognostic evaluation involving 2810 patients. Br J Cancer *79*, 300-307.

Franco, O. E., Arima, K., Yanagawa, M., and Kawamura, J. (2000). The usefulness of power Doppler ultrasonography for diagnosing prostate cancer: histological correlation of each biopsy site. BJU Int *85*, 1049-1052.

Frank, S. J., Pisters, L. L., Davis, J., Lee, A. K., Bassett, R., and Kuban, D. A. (2007). An assessment of quality of life following radical prostatectomy, high dose external beam radiation therapy and brachytherapy iodine implantation as monotherapies for localized prostate cancer. J Urol *177*, 2151-2156.

Franks, L. M. (1954a). Benign nodular hyperplasia of the prostate: A review. Ann R Coll Surg *14*, 92-106.

Franks, L. M. (1954b). Latent carcinoma of the prostate. J Pathol Bacteriol *68*, 603-616.

Franks, L. M. (1976). The natural history of prostatic cancer. Prog Clin Biol Res *6*, 103-109.
Fu, M., Wang, C., Li, Z., Sakamaki, T., and Pestell, R. G. (2004). Minireview: Cyclin D1: normal and abnormal functions. Endocrinology *145*, 5439-5447.

Fujiwara, Y., Hoon, D. S., Yamada, T., Umeshita, K., Gotoh, M., Sakon, M., Nishisho, I., and Monden, M. (2000). PTEN / MMAC1 mutation and frequent loss of heterozygosity identified in chromosome 10q in a subset of hepatocellular carcinomas. Jpn J Cancer Res *91*, 287-292.

Fukamachi, H., Mizuno, T., and Kim, Y. S. (1986). Morphogenesis of human colon cancer cells with fetal rat mesenchymes in organ culture. Experientia *42*, 312-315.

Gann, P. H. (2002). Risk factors for prostate cancer. Rev Urol *4 Suppl 5*, S3-S10.

Garcia, J. M., Silva, J. M., Dominguez, G., Gonzalez, R., Navarro, A., Carretero, L., Provencio, M., Espana, P., and Bonilla, F. (1999). Allelic loss of the PTEN region (10q23) in breast carcinomas of poor pathophenotype. Breast Cancer Res Treat *57*, 237-243.

Garcia, M., Derocq, D., Pujol, P., and Rochefort, H. (1990). Overexpression of transfected cathepsin D in transformed cells increases their malignant phenotype and metastatic potency. Oncogene *5*, 1809-1814.

Givan, A. L. (2001). Cells from Within: DNA in Life and Death. In Flow Cytometry: First Principles (Second Edition), pp. chapter 8 (p 123-158).

Gleason D, M. G. (1974). The Veterans Administration Cooperative Urological Research Group: Prediction of prognosis for prostatic adenocarcinoma by combined histologic grading and clinical staging. Journal of Urology 1974 *111*, 58-64.

Gleason, D. F. (1977). Histologic grading and clinical staging of prostatic carcinoma. In Urologic Pathology, M. Tannenbaum, ed. (Lea and Febiger), pp. 171-198.

Gocheva, V., Zeng, W., Ke, D., Klimstra, D., Reinheckel, T., Peters, C., Hanahan, D., and Joyce, J. A. (2006). Distinct roles for cysteine cathepsin genes in multistage tumorigenesis. Genes Dev *20*, 543-556.

Goldstraw, M. A., Fitzpatrick, J. M., and Kirby, R. S. (2007). What is the role of inflammation in the pathogenesis of prostate cancer? BJU Int.

Golimbu, M., Morales, P., Al-Askari, S., and Shulman, Y. (1981). CAT scanning in staging of prostatic cancer. Urology *18*, 305-308.

Greenlee, R. T., Hill-Harmon, M. B., Murray, T., and Thun, M. (2001). Cancer statistics, 2001. CA Cancer J Clin *51*, 15-36.

Grinnell, F. (1994). Fibroblasts, myofibroblasts, and wound contraction. J Cell Biol *124*, 401-404.
Grossfeld, G., Hayward, S., Tlsty, T., and Cunha, G. (1998). The role of stroma in prostatic carcinogenesis. Endocrine-related cancer *5*, 253-270.

Gu, Y., Kim, K. H., Ko, D., Srivastava, S., Moul, J. W., McLeod, D. G., and Rhim, J. S. (2005). Androgen and androgen receptor antagonist responsive primary African-American benign prostate epithelial cell line. Anticancer Res *25*, 1-8.

Gu, Y., Li, H., Miki, J., Kim, K. H., Furusato, B., Sesterhenn, I. A., Chu, W. S., McLeod, D. G., Srivastava, S., Ewing, C. M., *et al.* (2006). Phenotypic characterization of telomerase-immortalized primary non-malignant and malignant tumor-derived human prostate epithelial cell lines. Exp Cell Res *312*, 831-843.

Gumbiner, L. M., Gumerlock, P. H., Mack, P. C., Chi, S. G., deVere White, R. W., Mohler, J. L., Pretlow, T. G., and Tricoli, J. V. (1999). Overexpression of cyclin D1 is rare in human prostate carcinoma. Prostate *38*, 40-45.

Hamilton, W., Sharp, D. J., Peters, T. J., and Round, A. P. (2006). Clinical features of prostate cancer before diagnosis: a population-based, case-control study. Br J Gen Pract *56*, 756-762.

Han, B., Dong, Z., Liu, Y., Chen, Q., Hashimoto, K., and Zhang, J. T. (2003). Regulation of constitutive expression of mouse PTEN by the 5'-untranslated region. Oncogene *22*, 5325-5337.

Hay, N., and Sonenberg, N. (2004). Upstream and downstream of mTOR. Genes Dev *18*, 1926-1945.

Hayashi, N., and Cunha, G. R. (1991). Mesenchyme-induced changes in the neoplastic characteristics of the Dunning prostatic adenocarcinoma. Cancer Res *51*, 4924-4930.

Hayashi, N., Cunha, G. R., and Parker, M. (1993). Permissive and instructive induction of adult rodent prostatic epithelium by heterotypic urogenital sinus mesenchyme. Epithelial Cell Biol *2*, 66-78.

Hayashi, N., Cunha, G. R., and Wong, Y. C. (1990). Influence of male genital tract mesenchymes on differentiation of Dunning prostatic adenocarcinoma. Cancer Res *50*, 4747-4754.

Hayward, S. W. (2002). Approaches to modeling stromal-epithelial interactions. J Urol *168*, 1165-1172.

Hayward, S. W., Baskin, L. S., Haughney, P. C., Foster, B. A., Cunha, A. R., Dahiya, R., Prins, G. S., and Cunha, G. R. (1996). Stromal development in the ventral prostate, anterior prostate and seminal vesicle of the rat. Acta Anatomica *155*, 94-103.

Hayward, S. W., and Cunha, G. R. (2000). The prostate: development and physiology. Radiol Clin North Am *38*, 1-14.

Hayward, S. W., Dahiya, R., Cunha, G. R., Bartek, J., Despande, N., and Narayan, P. (1995). Establishment and characterization of an immortalized but non-tumorigenic human prostate epithelial cell Line: BPH-1. In Vitro *31A*, 14-24.

Hayward, S. W., Haughney, P. C., Lopes, E. S., Danielpour, D., and Cunha, G. R. (1999). The rat prostatic epithelial cell line NRP-152 can differentiate in vivo in response to its stromal environment. Prostate *39*, 205-212.

Hayward, S. W., Haughney, P. C., Rosen, M. A., Greulich, K. M., Weier, H. U., Dahiya, R., and Cunha, G. R. (1998). Interactions between adult human prostatic epithelium and rat urogenital sinus mesenchyme in a tissue recombination model. Differentiation *63*, 131-140.

Hayward, S. W., Rosen, M. A., and Cunha, G. R. (1997). Stromal-epithelial interactions in the normal and neoplastic prostate. Br J Urol *79 Suppl 2*, 18-26.

Hayward, S. W., Wang, Y., Cao, M., Hom, Y. K., Zhang, B., Grossfeld, G. D., Sudilovsky, D., and Cunha, G. R. (2001). Malignant transformation in a nontumorigenic human prostatic epithelial cell line. Cancer Res *61*, 8135-8142.

He, Y., Franco, O. E., Jiang, M., Williams, K., Love, H. D., Coleman, I. M., Nelson, P. S., and Hayward, S. W. (2007). Tissue-Specific Consequences of Cyclin D1 Overexpression in Prostate Cancer Progression. Cancer Res *67*, 8188-8197.

Hori, J., Okuyama, M., Azumi, M., Kato, Y., Saga, Y., Hashimoto, H., Tokumitsu, M., and Kakizaki, H. (2006). [Indication of repeat prostate biopsy for the diagnosis of prostate cancer]. Hinyokika Kiyo *52*, 835-838; discussion 838-839.

Hsieh-Li, H. M., Witte, D. P., Weinstein, M., Branford, W., Li, H., Small, K., and Potter, S. S. (1995). Hoxa-11 structure, extensive antisense transcription, and function in male and female fertility. Development *121*, 1373-1385.

Hua, V. N., and Schaeffer, A. J. (2004). Acute and chronic prostatitis. Med Clin North Am *88*, 483-494.

Hunter, T., and Pines, J. (1994). Cyclins and cancer. II: Cyclin D and CDK inhibitors come of age. Cell *79*, 573-582.

Imperato-McGinley, J., Binienda, Z., Arthur, A., Minenberg, D. T., Vaughan, E. D., and Quimby, F. W. (1985). The development of a male pseudohermaphroditic rat using an inhibitor of the enzyme 5α-reductase. Endocrinology *116*, 807-812.

Imperato-McGinley, J., Guerrero, L., Gautier, T., and Peterson, R. E. (1974). Steroid 5α-reductase deficiency in man: An inherited form of pseudohermaphroditism. Science *186*, 1213-1215.

Isaacs, J. T., and Coffey, D. S. (1989). Etiology and disease process of benign prostatic hyperplasia. Prostate Suppl *2*, 33-50.

Joesting, M. S., Perrin, S., Elenbaas, B., Fawell, S. E., Rubin, J. S., Franco, O. E., Hayward, S. W., Cunha, G. R., and Marker, P. C. (2005). Identification of SFRP1 as a candidate mediator of stromal-to-epithelial signaling in prostate cancer. Cancer Res *65*, 10423-10430.

Josso, N. (1981). Differentiation of the genital tract: stimulators and inhibitors. In Mechanisms of Sex Differentiation in Animals and Man, C. R. Austin, and R. G. Edwards, eds. (New York, Academic Press), pp. 165-204.

Jost, A. (1947). Recherche sur la différenciation de l'embryon de lapin. III. Rôle des gonades Foetales dans la différenciation sexuelle somatique. Arch Anat Microc Morphol Exp *36*, 272-315.

Joyce, J. A. (2005). Therapeutic targeting of the tumor microenvironment. Cancer Cell *7*, 513-520.

Joyce, J. A., Baruch, A., Chehade, K., Meyer-Morse, N., Giraudo, E., Tsai, F. Y., Greenbaum, D. C., Hager, J. H., Bogyo, M., and Hanahan, D. (2004). Cathepsin cysteine proteases are effectors of invasive growth and angiogenesis during multistage tumorigenesis. Cancer Cell *5*, 443-453.

Joyce, J. A., and Hanahan, D. (2004). Multiple roles for cysteine cathepsins in cancer. Cell Cycle *3*, 1516-1619.

Kallakury, B. V., Sheehan, C. E., Ambros, R. A., Fisher, H. A., Kaufman, R. P., Jr., and Ross, J. S. (1997). The prognostic significance of p34cdc2 and cyclin D1 protein expression in prostate adenocarcinoma. Cancer *80*, 753-763.

Kassen, A., Sutkowski, D. M., Ahn, H., Sensibar, J. A., Kozlowski, J. M., and Lee, C. (1996). Stromal cells of the human prostate: initial isolation and characterization. Prostate *28*, 89-97.

Kim, M. J., Cardiff, R. D., Desai, N., Banach-Petrosky, W. A., Parsons, R., Shen, M. M., and Abate-Shen, C. (2002). Cooperativity of Nkx3.1 and Pten loss of function in a mouse model of prostate carcinogenesis. Proc Natl Acad Sci U S A *99*, 2884-2889.

Knudson, C. B., and Knudson, W. (1993). Hyaluronan-binding proteins in development, tissue homeostasis, and disease. Faseb J *7*, 1233-1241.

Kobayashi, N., Barnard, R. J., Henning, S. M., Elashoff, D., Reddy, S. T., Cohen, P., Leung, P., Hong-Gonzalez, J., Freedland, S. J., Said, J., *et al.* (2006). Effect of altering dietary omega-6/omega-3 fatty acid ratios on prostate cancer membrane composition, cyclooxygenase-2, and prostaglandin E2. Clin Cancer Res *12*, 4662-4670.

Koivisto, P. (1997). Aneuploidy and rapid cell proliferation in recurrent prostate cancers with androgen receptor gene amplification. Prostate Cancer Prostatic Dis *1*, 21-25.

Kotelevets, L., van Hengel, J., Bruyneel, E., Mareel, M., van Roy, F., and Chastre, E. (2001). The lipid phosphatase activity of PTEN is critical for stabilizing intercellular junctions and reverting invasiveness. J Cell Biol *155*, 1129-1135.

Krongrad, A., and Drollen, M. (1993). Prostatic diseases, W. B. Sanders Publishing).

Kumar, V. L., and Majumder, P. K. (1995). Prostate gland: structure, functions and regulation. Int Urol Nephrol *27*, 231-243.

Lang, S. H., Sharrard, R. M., Stark, M., Villette, J. M., and Maitland, N. J. (2001a). Prostate epithelial cell lines form spheroids with evidence of glandular differentiation in three-dimensional Matrigel cultures. Br J Cancer *85*, 590-599.

Lang, S. H., Stark, M., Collins, A., Paul, A. B., Stower, M. J., and Maitland, N. J. (2001b). Experimental prostate epithelial morphogenesis in response to stroma and three-dimensional matrigel culture. Cell Growth Differ *12*, 631-640.

Lau, K. M., LaSpina, M., Long, J., and Ho, S. M. (2000). Expression of estrogen receptor (ER)-alpha and ER-beta in normal and malignant prostatic epithelial cells: regulation by methylation and involvement in growth regulation. Cancer Res *60*, 3175-3182.

Laurent-Matha, V., Maruani-Herrmann, S., Prebois, C., Beaujouin, M., Glondu, M., Noel, A., Alvarez-Gonzalez, M. L., Blacher, S., Coopman, P., Baghdiguian, S., *et al.* (2005). Catalytically inactive human cathepsin D triggers fibroblast invasive growth. J Cell Biol *168*, 489-499.

Lee, J., Demissie, K., Lu, S. E., and Rhoads, G. G. (2007). Cancer incidence among Korean-American immigrants in the United States and native Koreans in South Korea. Cancer Control *14*, 78-85.

Lei, Q., Jiao, J., Xin, L., Chang, C. J., Wang, S., Gao, J., Gleave, M. E., Witte, O. N., Liu, X., and Wu, H. (2006). NKX3.1 stabilizes p53, inhibits AKT activation, and blocks prostate cancer initiation caused by PTEN loss. Cancer Cell *9*, 367-378.

Lesko, S. M., Rosenberg, L., and Shapiro, S. (1996). Family history and prostate cancer risk. Am J Epidemiol *144*, 1041-1047.

Li, J., Yen, C., Liaw, D., Podsypanina, K., Bose, S., Wang, S. I., Puc, J., Miliaresis, C., Rodgers, L., McCombie, R., *et al.* (1997). PTEN, a putative protein tyrosine phosphatase gene mutated in human brain, breast, and prostate cancer. Science *275*, 1943-1947.

Li, L. C., Carroll, P. R., and Dahiya, R. (2005). Epigenetic changes in prostate cancer: implication for diagnosis and treatment. J Natl Cancer Inst *97*, 103-115.

Liaw, D., Marsh, D. J., Li, J., Dahia, P. L., Wang, S. I., Zheng, Z., Bose, S., Call, K. M., Tsou, H. C., Peacocke, M., *et al.* (1997). Germline mutations of the PTEN gene in Cowden disease, an inherited breast and thyroid cancer syndrome. Nat Genet *16*, 64-67.

Liotta, L. A., and Kohn, E. C. (2001). The microenvironment of the tumour-host interface. Nature *411*, 375-379.

Liu, W., James, C. D., Frederick, L., Alderete, B. E., and Jenkins, R. B. (1997). PTEN/MMAC1 mutations and EGFR amplification in glioblastomas. Cancer Res *57*, 5254-5257.

Lowsley, O. S. (1912). The development of the human prostate gland with reference to the development of other structures at the neck of the urinary bladder. Am J Anat *13*, 299-349.

Ma, D. Z., Xu, Z., Liang, Y. L., Su, J. M., Li, Z. X., Zhang, W., Wang, L. Y., and Zha, X. L. (2005a). Down-regulation of PTEN expression due to loss of promoter activity in human hepatocellular carcinoma cell lines. World J Gastroenterol *11*, 4472-4477.

Ma, X., Ziel-van der Made, A. C., Autar, B., van der Korput, H. A., Vermeij, M., van Duijn, P., Cleutjens, K. B., de Krijger, R., Krimpenfort, P., Berns, A., *et al.* (2005b). Targeted biallelic inactivation of Pten in the mouse prostate leads to prostate cancer accompanied by increased epithelial cell proliferation but not by reduced apoptosis. Cancer Res *65*, 5730-5739.

Maehama, T., and Dixon, J. E. (1998). The tumor suppressor, PTEN/MMAC1, dephosphorylates the lipid second messenger, phosphatidylinositol 3,4,5-trisphosphate. J Biol Chem *273*, 13375-13378.

Maffini, M. V., Soto, A. M., Calabro, J. M., Ucci, A. A., and Sonnenschein, C. (2004). The stroma as a crucial target in rat mammary gland carcinogenesis. J Cell Sci *117*, 1495-1502.

Makar, R., Mason, A., Kittelson, J. M., Bowden, G. T., Cress, A. E., and Nagle, R. B. (1994). Immunohistochemical analysis of cathepsin D in prostate carcinoma. Mod Pathol *7*, 747-751.

Manning, B. D., Logsdon, M. N., Lipovsky, A. I., Abbott, D., Kwiatkowski, D. J., and Cantley, L. C. (2005). Feedback inhibition of Akt signaling limits the growth of tumors lacking Tsc2. Genes Dev *19*, 1773-1778.

Masuda, A., and Takahashi, T. (2002). Chromosome instability in human lung cancers: possible underlying mechanisms and potential consequences in the pathogenesis. Oncogene *21*, 6884-6897.

Masumori, N., Thomas, T. Z., Chaurand, P., Case, T., Paul, M., Kasper, S., Caprioli, R. M., Tsukamoto, T., Shappell, S. B., and Matusik, R. J. (2001). A probasin-large T antigen transgenic mouse line develops prostate adenocarcinoma and neuroendocrine carcinoma with metastatic potential. Cancer Res *61*, 2239-2249.

Matusik, R. J., Masumori, N., Thomas, T., Case, T., Paul, M., Kasper, S., and Shappell, S. B. (2001). Transgenic mouse models of prostate cancer. In Contemporary endocrinology: Transgenics in endocrinology, M. Matzuk, C. W. Brown, and T. R. Kumar, eds. (Totowa, NJ, Humana Press Inc.), pp. 401-425.

Maurizi, M., Almadori, G., Cadoni, G., Scambia, G., Ottaviani, F., Ferrandina, G., Paludetti, G., D'Abramo, G., and Mancuso, S. (1996). Cathepsin D concentration in primary laryngeal cancer: correlation with clinico-pathological parameters, EGFR status and prognosis. Int J Cancer *69*, 105-109.

McNeal, J. (1980). The anatomic heterogeneity of the prostate. In Progress in clinical and biological research, G. P. Murphy, ed. (New York, Alan R. Liss), pp. 149-160.

McNeal, J. E. (1969). Origin and development of carcinoma of the prostate. Cancer *23*, 24-34.

McNeal, J. E. (1978). Origin and evolution of benign prostatic enlargement. Invest Urol *15*, 340-345.

McNeal, J. E. (1983). The prostate gland: morphology and pathobiology. Monogr Urology *4*, 3-37.

McNeal, J. E. (1984). Prostate Anatomy and BPH Morphogenisis. Prog Clin Biol Res *145*, 27-54.

Mhawech-Fauceglia, P., Zhang, S., Terracciano, L., Sauter, G., Chadhuri, A., Herrmann, F. R., and Penetrante, R. (2007). Prostate-specific membrane antigen (PSMA) protein expression in normal and neoplastic tissues and its sensitivity and specificity in prostate adenocarcinoma: an immunohistochemical study using mutiple tumour tissue microarray technique. Histopathology *50*, 472-483.

Mikuz, G. (1997). Pathology of prostate cancer. Old problems and new facts. Adv Clin Path *1*, 21-34.

Mintz, B. (1978). Genetic Mosaicism and In Vivo Analyses of Neoplasia and Differentiation. In Cell Differentiation and Neoplasia, G. Saunders, ed. (New York, Raven Press), pp. 27-56.

Mise-Omata, S., Obata, Y., Iwase, S., Mise, N., and Doi, T. S. (2005). Transient strong reduction of PTEN expression by specific RNAi induces loss of adhesion of the cells. Biochem Biophys Res Commun *328*, 1034-1042.

Mordente, J. A., Choudhury, M. S., Tazaki, H., Mallouh, C., and Konno, S. (1998). Hydrolysis of androgen receptor by cathepsin D: its biological significance in human prostate cancer. Br J Urol *82*, 431-435.

Mori, H., Maki, M., Oishi, K., Jaye, M., Igarashi, K., Yoshida, O., and Hatanaka, M. (1990). Increased expression of genes for basic fibroblast growth factor and transforming growth factor type beta 2 in human benign prostatic hyperplasia. Prostate *16*, 71-80.

Mueller, M. M., and Fusenig, N. E. (2004). Friends or foes - bipolar effects of the tumour stroma in cancer. Nat Rev Cancer *4*, 839-849.

Myers, M. P., Pass, I., Batty, I. H., Van der Kaay, J., Stolarov, J. P., Hemmings, B. A., Wigler, M. H., Downes, C. P., and Tonks, N. K. (1998). The lipid phosphatase activity of PTEN is critical for its tumor supressor function. Proc Natl Acad Sci U S A *95*, 13513-13518.

Nelson, W. G., De Marzo, A. M., DeWeese, T. L., and Isaacs, W. B. (2004). The role of inflammation in the pathogenesis of prostate cancer. J Urol *172*, S6-11; discussion S11-12.

Neubauer, B. L., Chung, L. W. K., McCormick, K. A., Taguchi, O., Thompson, T. C., and Cunha, G. R. (1983). Epithelial-mesenchymal interactions in prostatic development. II. Biochemical observations of prostatic induction by urogenital sinus mesenchyme in epithelium of the adult rodent urinary bladder. J Cell Biol *96*, 1671-1676.

Nicholson, K. M., and Anderson, N. G. (2002). The protein kinase B/Akt signalling pathway in human malignancy. Cell Signal *14*, 381-395.

Nomura, T., and Katunuma, N. (2005). Involvement of cathepsins in the invasion, metastasis and proliferation of cancer cells. J Med Invest *52*, 1-9.

O'Berg, M. T., Chen, J. L., Burke, C. A., Walrath, J., and Pell, S. (1985). Epidemiologic study of workers exposed to acrylonitrile: an update. J Occup Med *27*, 835-840.

Ohigashi, T., Mizuno, R., Nakashima, J., Marumo, K., and Murai, M. (2005). Inhibition of Wnt signaling downregulates Akt activity and induces chemosensitivity in PTEN-mutated prostate cancer cells. Prostate *62*, 61-68.

Olumi, A. F., Grossfeld, G. D., Hayward, S. W., Carroll, P. R., Tlsty, T. D., and Cunha, G. R. (1999). Carcinoma-associated fibroblasts direct tumor progression of initiated human prostatic epithelium. Cancer Res *59*, 5002-5011.

Orimo, A., Gupta, P. B., Sgroi, D. C., Arenzana-Seisdedos, F., Delaunay, T., Naeem, R., Carey, V. J., Richardson, A. L., and Weinberg, R. A. (2005). Stromal Fibroblasts Present in Invasive Human Breast Carcinomas Promote Tumor Growth and Angiogenesis through Elevated SDF-1/CXCL12 Secretion. Cell *121*, 335-348.

Paramio, J. M., Navarro, M., Segrelles, C., Gomez-Casero, E., and Jorcano, J. L. (1999). PTEN tumour suppressor is linked to the cell cycle control through the retinoblastoma protein. Oncogene *18*, 7462-7468.

Parker, A. S., Cerhan, J. R., Putnam, S. D., Cantor, K. P., and Lynch, C. F. (1999). A cohort study of farming and risk of prostate cancer in Iowa. Epidemiology *10*, 452-455.

Peehl, D. M., Wong, S. T., Sellers, R. G., Jin, S., and Rhim, J. S. (1997). Loss of response to epidermal growth factor and retinoic acid accompanies the transformation of human prostatic epithelial cells to tumorigenicity with v-Ki-ras. Carcinogenesis *18*, 1643-1650.

Pera, M., Fernandez, P. L., Palacin, A., Cardesa, A., Dasenbrock, C., Tillman, T., and Mohr, U. (2001). Expression of cyclin D1 and p53 and its correlation with proliferative activity in the spectrum of esophageal carcinomas induced after duodenal content reflux and 2,6-dimethylnitrosomorpholine administration in rats. Carcinogenesis *22*, 271-277.

Petty, W. J., Dragnev, K. H., and Dmitrovsky, E. (2003). Cyclin D1 as a target for chemoprevention. Lung Cancer *41 Suppl 1*, S155-161.

Pierce, G. (1974). The Benign Cells of Malignant Tumors. In Developmental Aspects of Carcinogenesis and Immunity, T. King, ed. (New York, Academic Press, Inc.), pp. 3-22.

Plaskon, L. A., Penson, D. F., Vaughan, T. L., and Stanford, J. L. (2003). Cigarette smoking and risk of prostate cancer in middle-aged men. Cancer Epidemiol Biomarkers Prev *12*, 604-609.

Pollard, M. (1992). The Lobund-Wistar rat model of prostate cancer. J Cell Biochem Suppl *16H*, 84-88.

Pollard, M. (1998). Lobund-Wistar rat model of prostate cancer in man. Prostate *37*, 1-4.
Polsky, D., and Cordon-Cardo, C. (2003). Oncogenes in melanoma. Oncogene *22*, 3087-3091.

Powell, I. J. (2007). Epidemiology and pathophysiology of prostate cancer in African-American men. J Urol *177*, 444-449.

Ricke, W. A., Ishii, K., Ricke, E. A., Simko, J., Wang, Y., Hayward, S. W., and Cunha, G. R. (2006). Steroid hormones stimulate human prostate cancer progression and metastasis. Int J Cancer *118*, 2123-2131.

Rivero, V. E., Motrich, R. D., Maccioni, M., and Riera, C. M. (2007). Autoimmune etiology in chronic prostatitis syndrome: an advance in the understanding of this pathology. Crit Rev Immunol *27*, 33-46.

Roberts, R. O., Jacobson, D. J., Rhodes, T., Klee, G. G., Leiber, M. M., and Jacobsen, S. J. (2004). Serum sex hormones and measures of benign prostatic hyperplasia. Prostate *61*, 124-131.

Rochefort, H. (1992). Cathepsin D in breast cancer: a tissue marker associated with metastasis. Eur J Cancer *28A*, 1780-1783.

Rokhlin, O. W., and Cohen, M. B. (1995). Expression of cellular adhesion molecules on human prostate tumor cell lines. Prostate *26*, 205-212.

Ropiquet, F., Giri, D., Kwabi-Addo, B., Schmidt, K., and Ittmann, M. (2000). FGF-10 is expressed at low levels in the human prostate. Prostate *44*, 334-338.

Rosol, T. J., Tannehill-Gregg, S. H., LeRoy, B. E., Mandl, S., and Contag, C. H. (2003). Animal models of bone metastasis. Cancer *97*, 748-757.

Rossi, D. (2006). [Localized prostate cancer. Local treatment and what place for lymphadenectomy]. Ann Urol (Paris) *40 Suppl 2*, S24-28.

Roy, P. G., and Thompson, A. M. (2006). Cyclin D1 and breast cancer. Breast *15*, 718-727.

Royuela, M., de Miguel, M. P., Bethencourt, F. R., Sanchez-Chapado, M., Fraile, B., Arenas, M. I., and Paniagua, R. (2001). Estrogen receptors alpha and beta in the normal, hyperplastic and carcinomatous human prostate. J Endocrinol *168*, 447-454.

Sandhu, J. S., and Te, A. E. (2004). The role of 5-alpha-reductase inhibition as monotherapy in view of the MTOPS data. Curr Urol Rep *5*, 274-279.

Schmitt-Graff, A., Desmouliere, A., and Gabbiani, G. (1994). Heterogeneity of myofibroblast phenotypic features: an example of fibroblastic cell plasticity. Virchows Arch *425*, 3-24.

Seidman, J. D., Berman, J. J., Moore, G. W., and Yetter, R. A. (1992). Multiparameter DNA flow cytometry of keratoacanthoma. Anal Quant Cytol Histol *14*, 113-119.

Sharma, P., and Schreiber-Agus, N. (1999). Mouse models of prostate cancer. Oncogene *18*, 5349-5355.

Sherr, C. J., Matsushime, H., and Roussel, M. F. (1992). Regulation of CYL/cyclin D genes by colony-stimulating factor 1. Ciba Found Symp *170*, 209-219; discussion 219-226.

Shibata, Y., Ito, K., Suzuki, K., Nakano, K., Fukabori, Y., Suzuki, R., Kawabe, Y., Honma, S., and Yamanaka, H. (2000). Changes in the endocrine environment of the human prostate transition zone with aging: simultaneous quantitative analysis of prostatic sex steroids and comparison with human prostatic histological composition. Prostate *42*, 45-55.

Silver, R. I., Wiley, E. L., Davis, D. L., Thigpen, A. E., Russell, D. W., and McConnell, J. D. (1994). Expression and regulation of steroid 5 alpha-reductase 2 in prostate disease. J Urol *152*, 433-437.

Simardi, L. H., Tobias-MacHado, M., Kappaz, G. T., Taschner Goldenstein, P., Potts, J. M., and Wroclawski, E. R. (2004). Influence of asymptomatic histologic prostatitis on serum prostate-specific antigen: a prospective study. Urology *64*, 1098-1101.

Singer, C., Rasmussen, A., Smith, H. S., Lippman, M. E., Lynch, H. T., and Cullen, K. J. (1995). Malignant breast epithelium selects for insulin-like growth factor II expression in breast stroma: evidence for paracrine function. Cancer Res *55*, 2448-2454.

Sneyd, M. J., Cox, B., Paul, C., and Skegg, D. C. (2003). PSA testing and digital rectal examination in New Zealand. Aust N Z J Public Health *27*, 502-506.

Song, Z., Wu, X., Powell, W. C., Cardiff, R. D., Cohen, M. B., Tin, R. T., Matusik, R. J., Miller, G. J., and Roy-Burman, P. (2002). Fibroblast growth factor 8 isoform B overexpression in prostate epithelium: a new mouse model for prostatic intraepithelial neoplasia. Cancer Res *62*, 5096-5105.

Stambolic, V., Suzuki, A., de la Pompa, J. L., Brothers, G. M., Mirtsos, C., Sasaki, T., Ruland, J., Penninger, J. M., Siderovski, D. P., and Mak, T. W. (1998). Negative regulation of PKB/Akt-dependent cell survival by the tumor suppressor PTEN. Cell *95*, 29-39.

Sugimura, Y., Cunha, G. R., and Bigsby, R. M. (1986a). Androgenic induction of deoxyribonucleic acid synthesis in prostatic glands induced in the urothelium of testicular feminized (Tfm/y) mice. Prostate *9*, 217-225.

Sugimura, Y., Cunha, G. R., and Donjacour, A. A. (1986b). Morphogenesis of ductal networks in the mouse prostate. Biol Reprod *34*, 961-971.

Suzuki, H., Freije, D., Nusskern, D. R., Okami, K., Cairns, P., Sidransky, D., Isaacs, W. B., and Bova, G. S. (1998). Interfocal heterogeneity of PTEN/MMAC1 gene alterations in multiple metastatic prostate cancer tissues. Cancer Res *58*, 204-209.

Takeda, H., Suematsu, N., and Mizuno, T. (1990). Transcription of prostatic steroid binding protein (PSBP) gene is induced by epithelial-mesenchymal interaction. Development *110*, 273-282.

Tang, D., Liu, J. J., Rundle, A., Neslund-Dudas, C., Savera, A. T., Bock, C. H., Nock, N. L., Yang, J. J., and Rybicki, B. A. (2007). Grilled meat consumption and PhIP-DNA adducts in prostate carcinogenesis. Cancer Epidemiol Biomarkers Prev *16*, 803-808.

Tetu, B., Brisson, J., Lapointe, H., Wang, C. S., Bernard, P., and Blanchette, C. (1999). Cathepsin D expression by cancer and stromal cells in breast cancer: an immunohistochemical study of 1348 cases. Breast Cancer Res Treat *55*, 137-147.

Thompson, I. M., Ankerst, D. P., Chi, C., Lucia, M. S., Goodman, P. J., Crowley, J. J., Parnes, H. L., and Coltman, C. A., Jr. (2005). Operating characteristics of prostate-specific antigen in men with an initial PSA level of 3.0 ng/ml or lower. Jama *294*, 66-70.

Thomson, A. A., and Cunha, G. R. (1999). Prostatic growth and development are regulated by FGF10. Development *126*, 3693-3701.

Thomson, A. A., Foster, B. A., and Cunha, G. R. (1997). Analysis of growth factor and receptor mRNA levels during development of the rat seminal vesicle and prostate. Development *124*, 2431-2439.

True, L., Coleman, I., Hawley, S., Huang, C. Y., Gifford, D., Coleman, R., Beer, T. M., Gelmann, E., Datta, M., Mostaghel, E., *et al.* (2006). A molecular correlate to the Gleason grading system for prostate adenocarcinoma. Proc Natl Acad Sci U S A *103*, 10991-10996.

Tuxhorn, J. A., Ayala, G. E., and Rowley, D. R. (2001). Reactive stroma in prostate cancer progression. J Urol *166*, 2472-2483.

Tuxhorn, J. A., Ayala, G. E., Smith, M. J., Smith, V. C., Dang, T. D., and Rowley, D. R. (2002). Reactive stroma in human prostate cancer: induction of myofibroblast phenotype and extracellular matrix remodeling. Clin Cancer Res *8*, 2912-2923.

Umbas, R., Schalken, J. A., Aalders, T. W., Carter, B. S., Karthaus, H. F., Schaafsma, H. E., Debruyne, F. M., and Isaacs, W. B. (1992). Expression of the cellular adhesion molecule E-cadherin is reduced or absent in high-grade prostate cancer. Cancer Res *52*, 5104-5109.

Untergasser, G., Gander, R., Lilg, C., Lepperdinger, G., Plas, E., and Berger, P. (2005). Profiling molecular targets of TGF-beta1 in prostate fibroblast-to-myofibroblast transdifferentiation. Mech Ageing Dev *126*, 59-69.

van Weerden, W. M., and Romijn, J. C. (2000). Use of nude mouse xenograft models in prostate cancer research. Prostate *43*, 263-271.

Vilanova, J. C., and Barcelo, J. (2007). Prostate cancer detection: magnetic resonance (MR) spectroscopic imaging. Abdom Imaging.

Villers, A., Rebillard, X., Soulie, M., Davin, J. L., Coloby, P., Moreau, J. L., Mejean, A., Irani, J., Coulange, C., and Mangin, P. (2003). [Prostate cancer screening]. Prog Urol *13*, 209-214.

Visakorpi, T. (1999). Molecular genetics of prostate cancer. Ann Chir Gynaecol *88*, 11-16.
Visakorpi, T. (2003). The molecular genetics of prostate cancer. Urology *62*, 3-10.

Walrath, J., Fayerweather, W. E., Gilby, P. G., and Pell, S. (1989). A case-control study of cancer among du pont employees with potential for exposure to dimethylformamide. J Occup Med *31*, 432-438.

Walsh, P. C., Hutchins, G. M., and Ewing, L. L. (1983). Tissue content of dihydrotestosterone in human prostatic hyperplasia is not supranormal. J Clin Invest *72*, 1772-1777.

Walsh, P. C., Madden, J. D., Harrod, M. J., Goldstein, J. L., MacDonald, P. C., and Wilson, J. D. (1974). Familial incomplete male pseudohermaphroditism, Type 2: Decreased dihydrotestosterone formation in pseudovaginal perineoscrotal hypospadias. N Engl J Med *291*, 944-949.

Wang, S., Gao, J., Lei, Q., Rozengurt, N., Pritchard, C., Jiao, J., Thomas, G. V., Li, G., Roy-Burman, P., Nelson, P. S., *et al.* (2003). Prostate-specific deletion of the murine Pten tumor suppressor gene leads to metastatic prostate cancer. Cancer Cell *4*, 209-221.

Wang, Y., Sudilovsky, D., Zhang, B., Haughney, P. C., Rosen, M. A., Wu, D. S., Cunha, T. J., Dahiya, R., Cunha, G. R., and Hayward, S. W. (2001). A human prostatic epithelial model of hormonal carcinogenesis. Cancer Res *61*, 6064-6072.

Wang, Y. Z., and Wong, Y. C. (1998). Sex hormone-induced prostatic carcinogenesis in the noble rat: the role of insulin-like growth factor-I (IGF-I) and vascular endothelial growth factor (VEGF) in the development of prostate cancer. Prostate *35*, 165-177.

Waters, D. J., and Bostwick, D. G. (1997). Prostatic intraepithelial neoplasia occurs spontaneously in the canine prostate. J Urol *157*, 713-716.

Waters, D. J., Hayden, D. W., Bell, F. W., Klausner, J. S., Qian, J., and Bostwick, D. G. (1997). Prostatic intraepithelial neoplasia in dogs with spontaneous prostate cancer. Prostate *30*, 92-97.

Waters, D. J., Sakr, W. A., Hayden, D. W., Lang, C. M., McKinney, L., Murphy, G. P., Radinsky, R., Ramoner, R., Richardson, R. C., and Tindall, D. J. (1998). Workgroup 4: spontaneous prostate carcinoma in dogs and nonhuman primates. Prostate *36*, 64-67.

Weaver, V. M., Petersen, O. W., Wang, F., Larabell, C. A., Briand, P., Damsky, C., and Bissell, M. J. (1997). Reversion of the malignant phenotype of human breast cells in three-dimensional culture and in vivo by integrin blocking antibodies. J Cell Biol *137*, 231-245.

Webber, M. M., Waghray, A., and Bello, D. (1995). Prostate-specific antigen, a serine protease, facilitates human prostate cancer cell invasion. Clin Cancer Res *1*, 1089-1094.

Westley, B. R., and May, F. E. (1999). Prognostic value of cathepsin D in breast cancer. Br J Cancer *79*, 189-190.

Williams, K., Fernandez, S., Stien, X., Ishii, K., Love, H. D., Lau, Y. F., Roberts, R. L., and Hayward, S. W. (2005). Unopposed c-MYC expression in benign prostatic epithelium causes a cancer phenotype. Prostate *63*, 369-384.

Wright, J. H., McDonnell, S., Portella, G., Bowden, G. T., Balmain, A., and Matrisian, L. M. (1994). A switch from stromal to tumor cell expression of stromelysin-1 mRNA associated with the conversion of squamous to spindle carcinomas during mouse skin tumor progression. Mol Carcinog *10*, 207-215.

Wymann, M. P., and Pirola, L. (1998). Structure and function of phosphoinositide 3-kinases. Biochim Biophys Acta *1436*, 127-150.

Yasunaga, Y., Nakamura, K., Ewing, C. M., Isaacs, W. B., Hukku, B., and Rhim, J. S. (2001). A novel human cell culture model for the study of familial prostate cancer. Cancer Res *61*, 5969-5973.

Zagars, G. K., and Pollack, A. (1995). Radiation therapy for T1 and T2 prostate cancer: prostate-specific antigen and disease outcome. Urology *45*, 476-483.

Zhang, J., Hess, M. W., Thurnher, M., Hobisch, A., Radmayr, C., Cronauer, M. V., Hittmair, A., Culig, Z., Bartsch, G., and Klocker, H. (1997). Human prostatic smooth muscle cells in culture: estradiol enhances expression of smooth muscle cell-specific markers. Prostate *30*, 117-129.

Zhang, X., Lee, C., Ng, P. Y., Rubin, M., Shabsigh, A., and Buttyan, R. (2000). Prostatic neoplasia in transgenic mice with prostate-directed overexpression of the c-myc oncoprotein. Prostate *43*, 278-285.

Zhao, G., Bai, X. F., Luo, D. W., and Gao, D. Y. (2006). Modeling the heat transfer problem for the novel combined cryosurgery and hyperthermia system. Cryo Letters *27*, 115-126.